Harmonic decomposition of two particle angular correlations in Pb–Pb collisions at $\sqrt{s_{NN}} = 2.76$ TeV

Andrew Adare
Yale University
for the
ALICE Collaboration

October 20, 2011

Based on arXiv:1109.2501
(Submitted 12 Sep 2011)

ALICE

Yale University

LUX ET VERITAS

Harmonics of Big and Little Bangs

Temperature anisotropy from CMB radiation

Power spectra hold a wealth of info from early epochs

WMAP

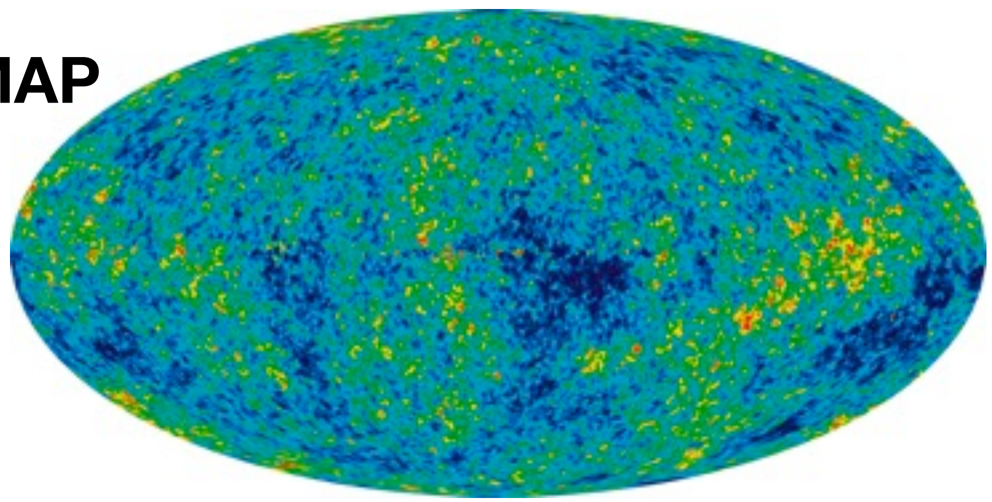

The Astrophysical Journal Supplement Series, 192:14 (15pp), 2011 February

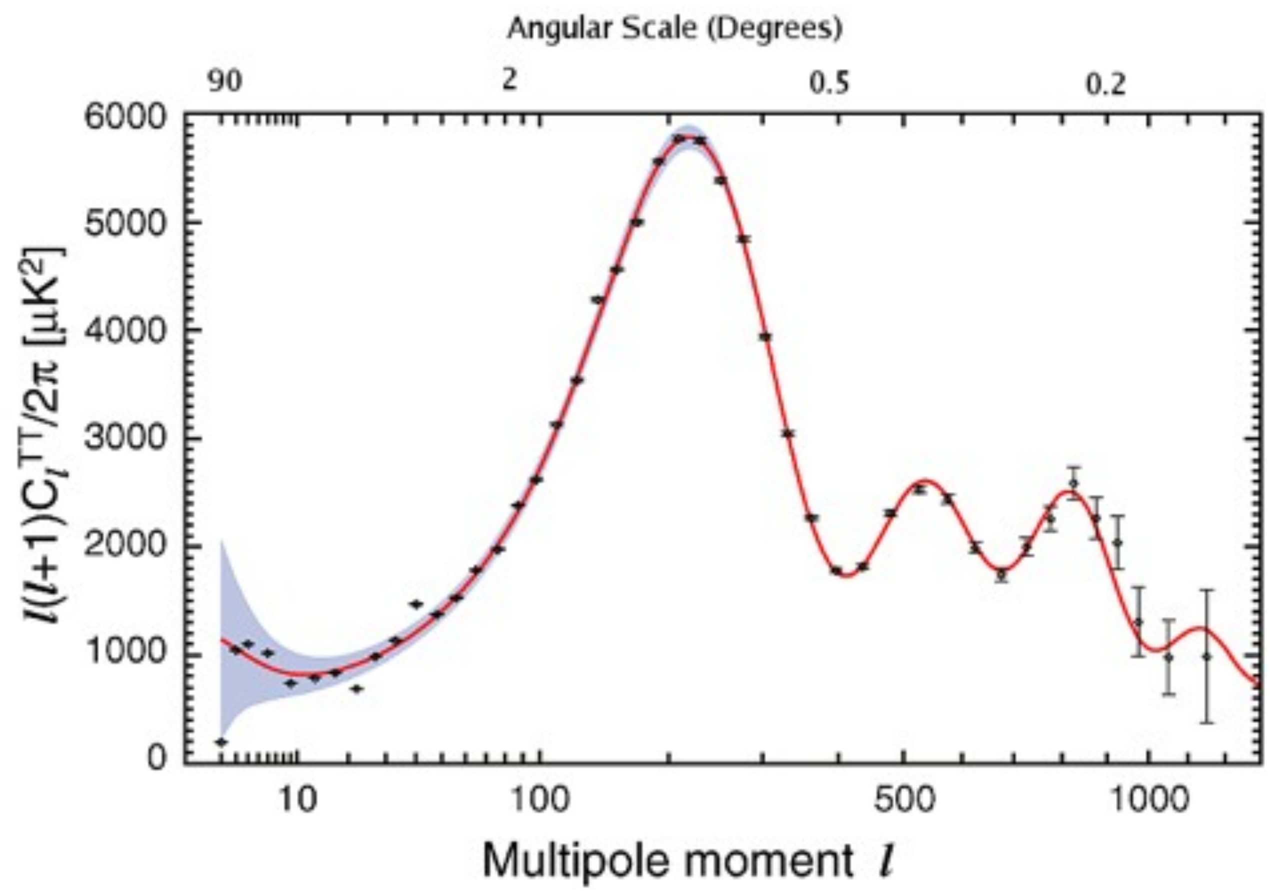

TeV-scale Pb-Pb collisions

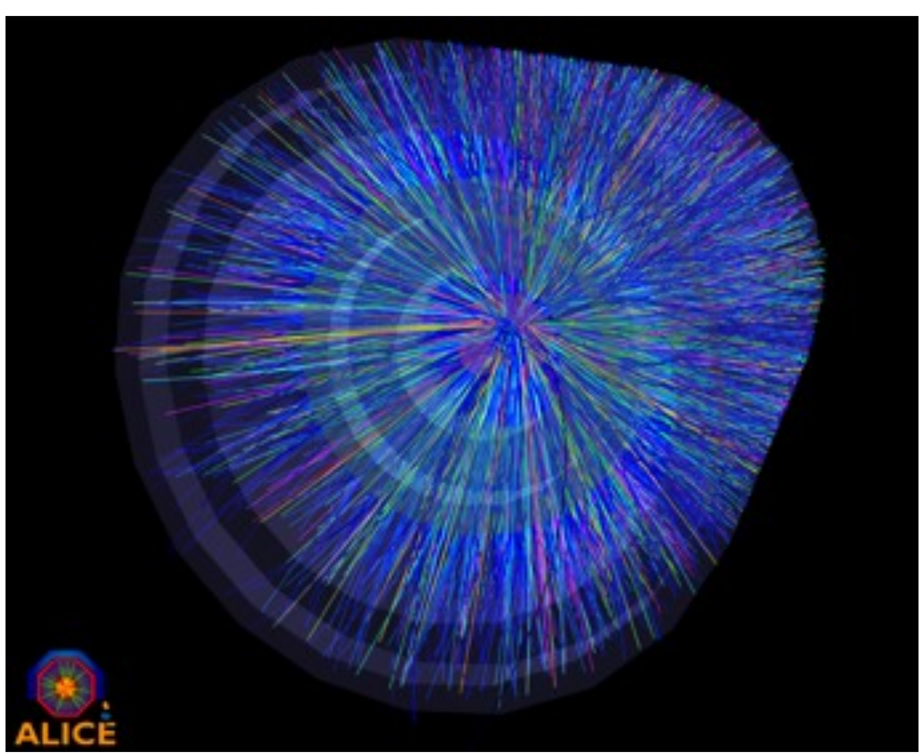

Can we similarly make "power spectra" from A+A collisions?

What can be learned?

A. Adare (ALICE)

Same and mixed event pair distributions

$$\Delta\phi = \phi_A - \phi_B \qquad \Delta\eta = \eta_A - \eta_B$$

$N_{same}^{AB}(\Delta\phi, \Delta\eta)$

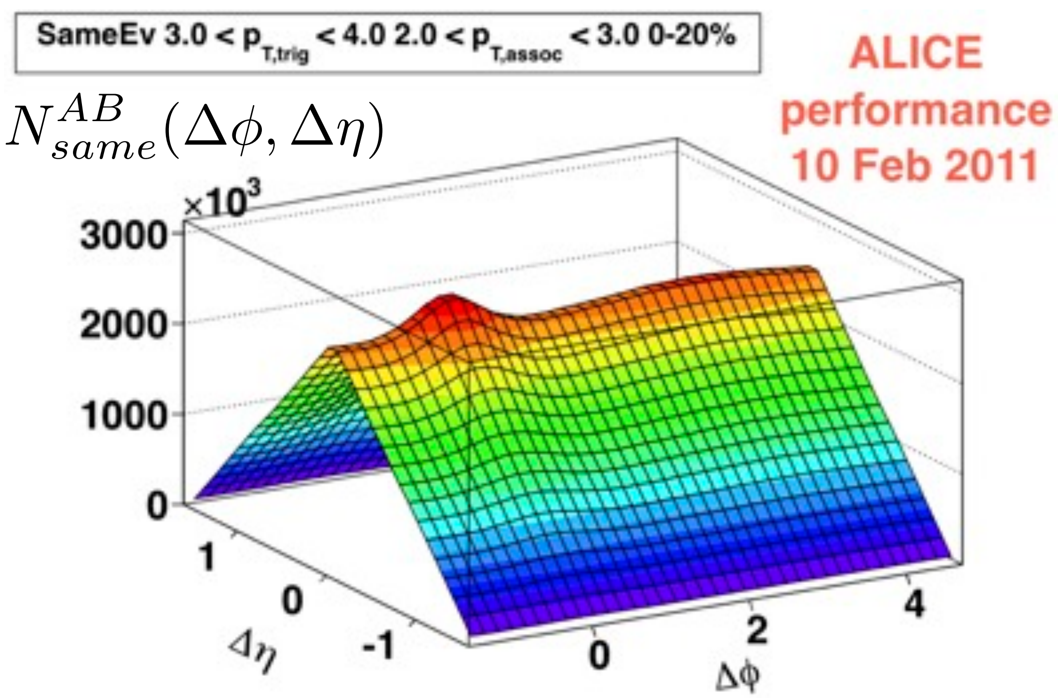

$N_{mixed}^{AB}(\Delta\phi, \Delta\eta)$

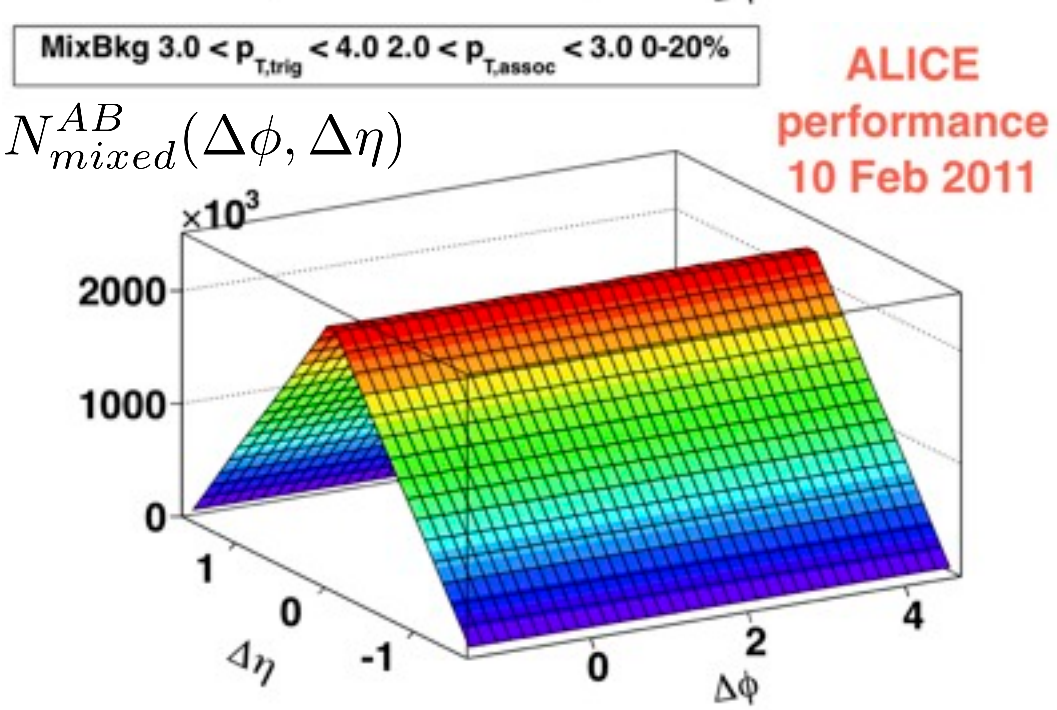

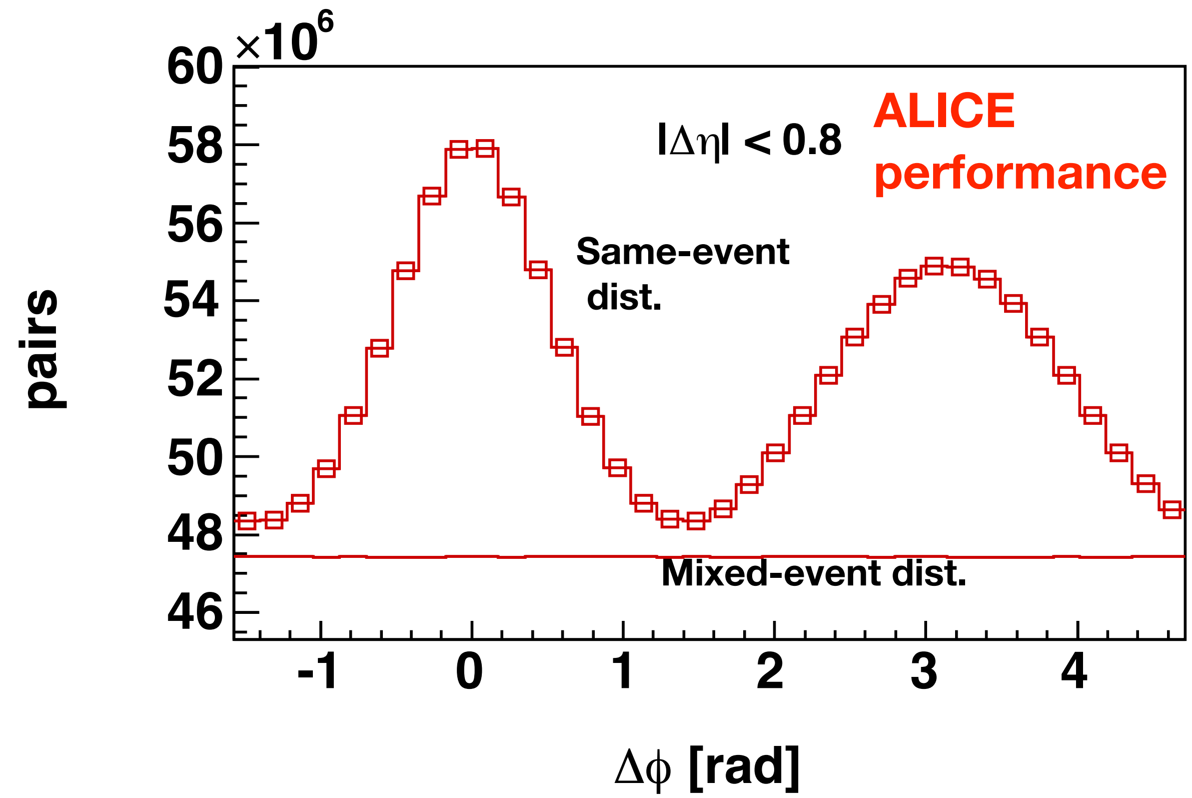

Azimuthal correlation function:

$$C(\Delta\phi) \equiv \frac{N_{mixed}^{AB}}{N_{same}^{AB}} \cdot \frac{dN_{same}^{AB}/d\Delta\phi}{dN_{mixed}^{AB}/d\Delta\phi}$$

Analysis and dataset

Pb-Pb at 2.76 TeV

13.5 M events in 0-90% after event selection

Centrality

VZERO detectors

resolution < 1%

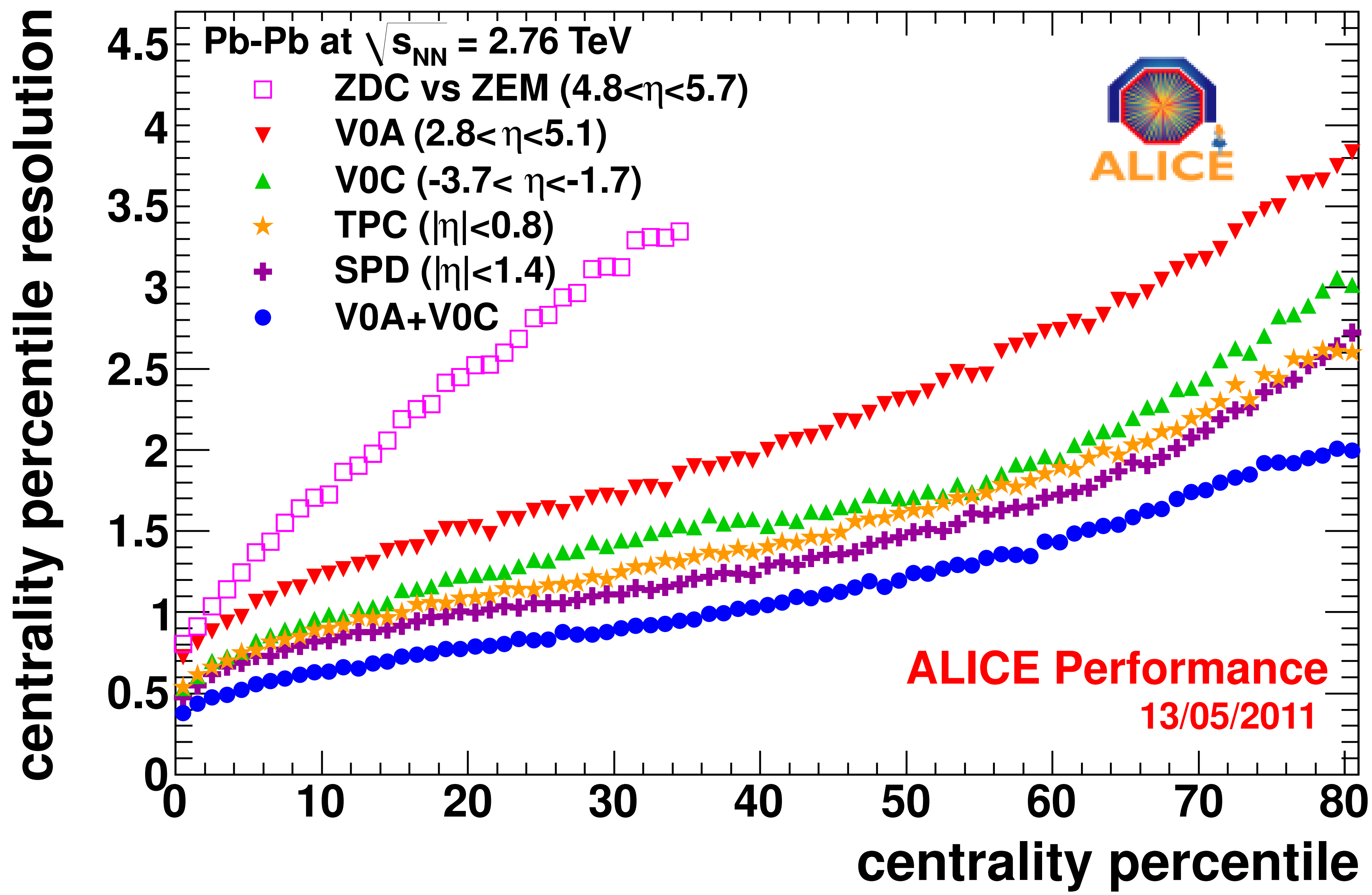

Tracking

TPC points + ITS vertex

optimum acceptance + precision for correlations

In central and low-p_T "bulk-dominated" long-range correlations

A near side ridge is observed

A very broad away side is observed, even doubly-peaked for 0-2% central

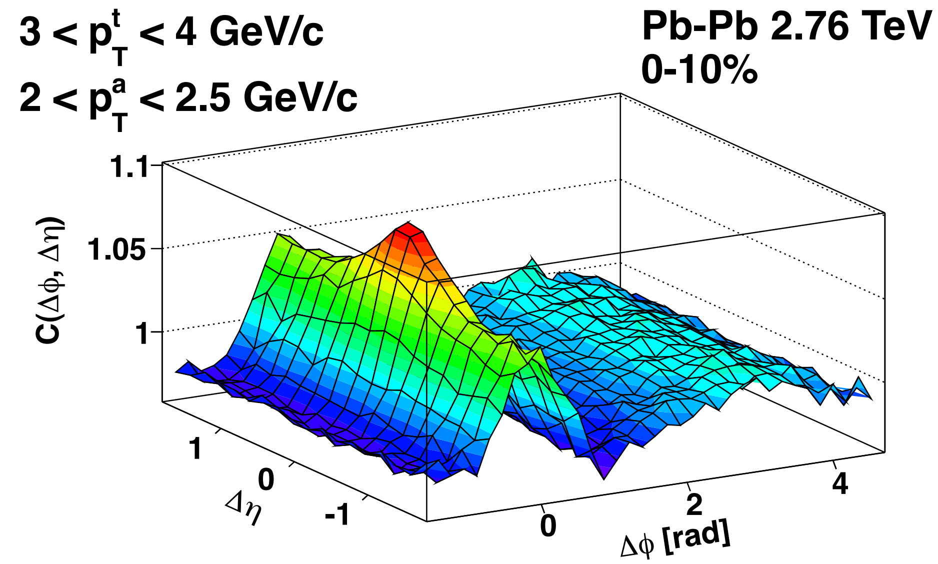

In high-p_T "jet-dominated" correlations

The near-side ridge is not visible

The away-side jet is very strong; sharp like proton-proton case

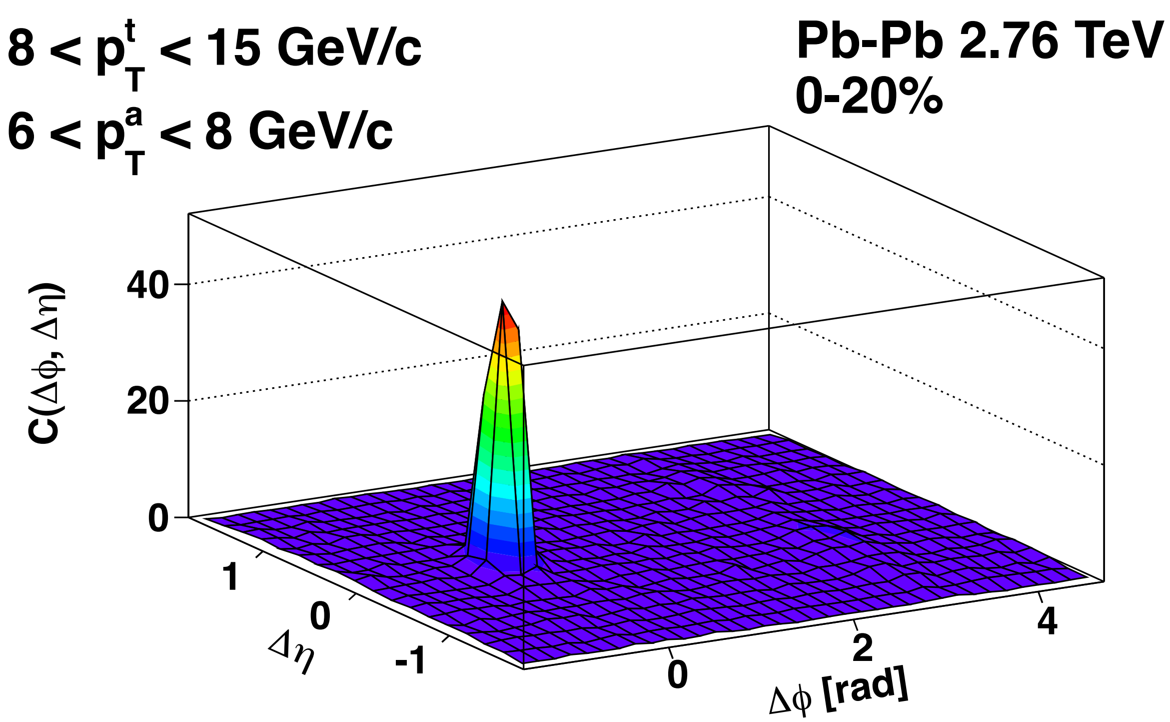

Event structure and shape evolution

In central and low-p_T "bulk-dominated" long-range correlations

A near side ridge is observed

A very broad away side is observed, even doubly-peaked for 0-2% central

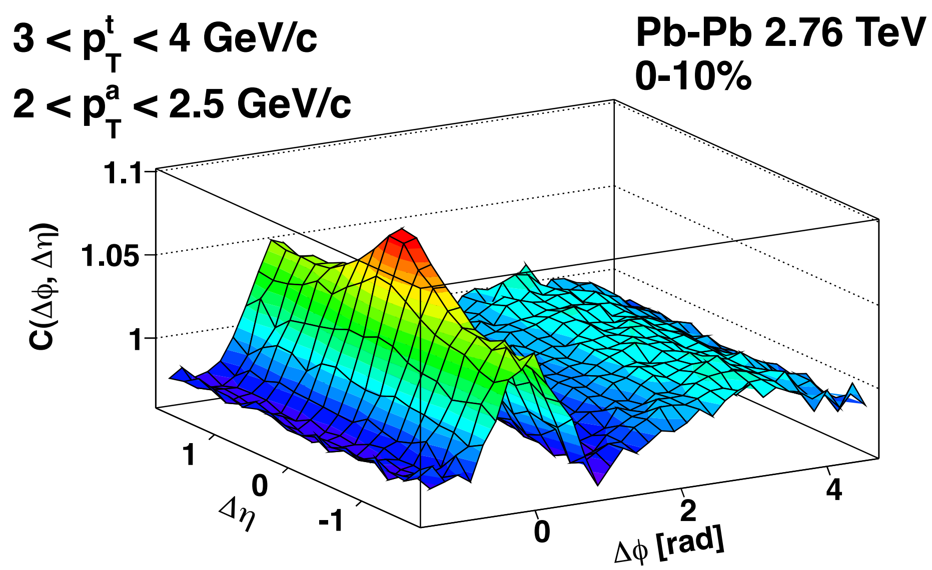

In high-p_T "jet-dominated" long-range correlations

The near-side ridge is not visible

The away-side jet is very strong; sharp like proton-proton case

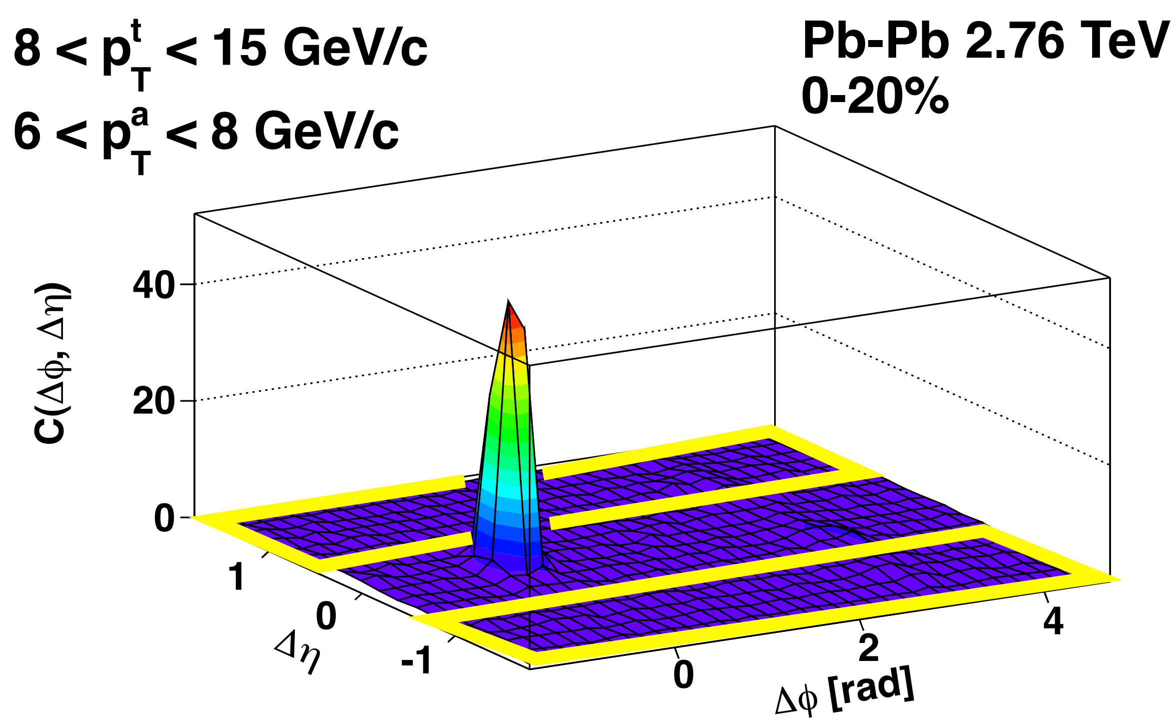

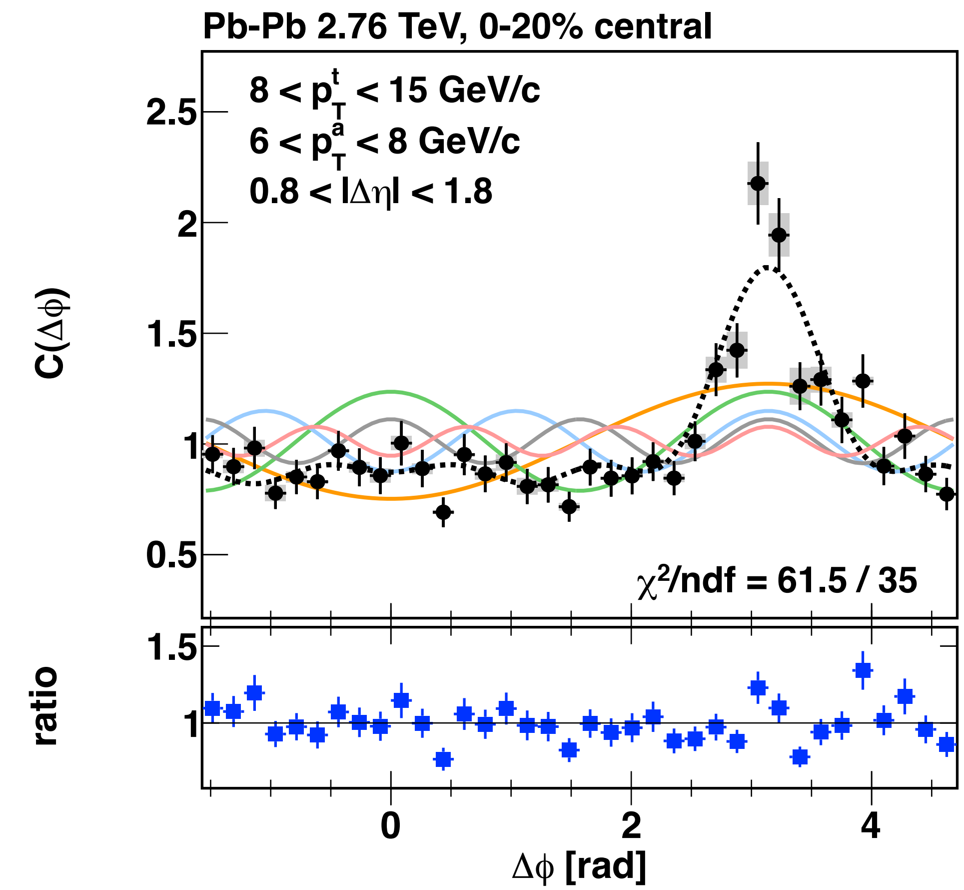

Event structure and shape evolution

In central and low-p_T "bulk-dominated" long-range correlations

- A near side ridge is observed
- A very broad away side is observed, even doubly-peaked for 0-2% central

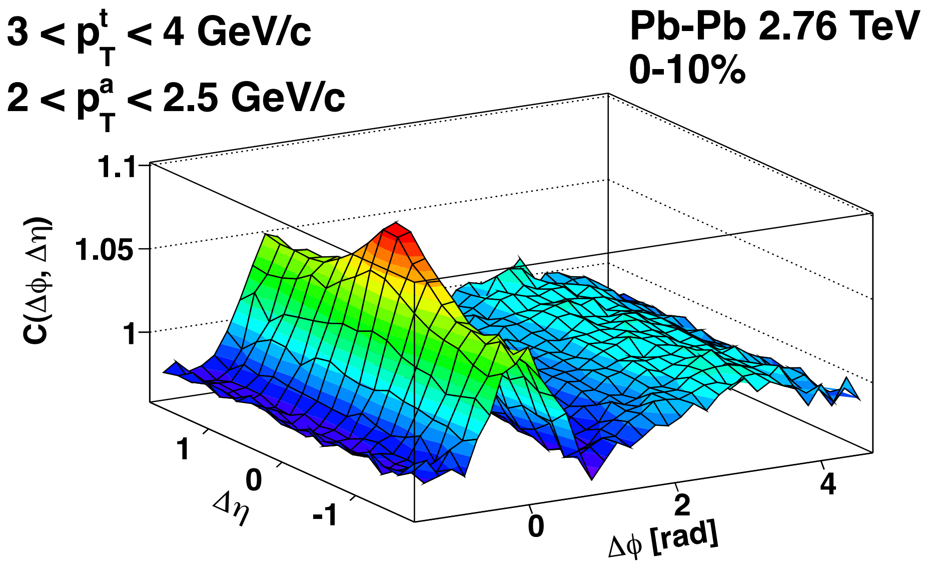

In high-p_T "jet-dominated" long-range correlations

- The near-side ridge is not visible
- The away-side jet is very strong; sharp like proton-proton case

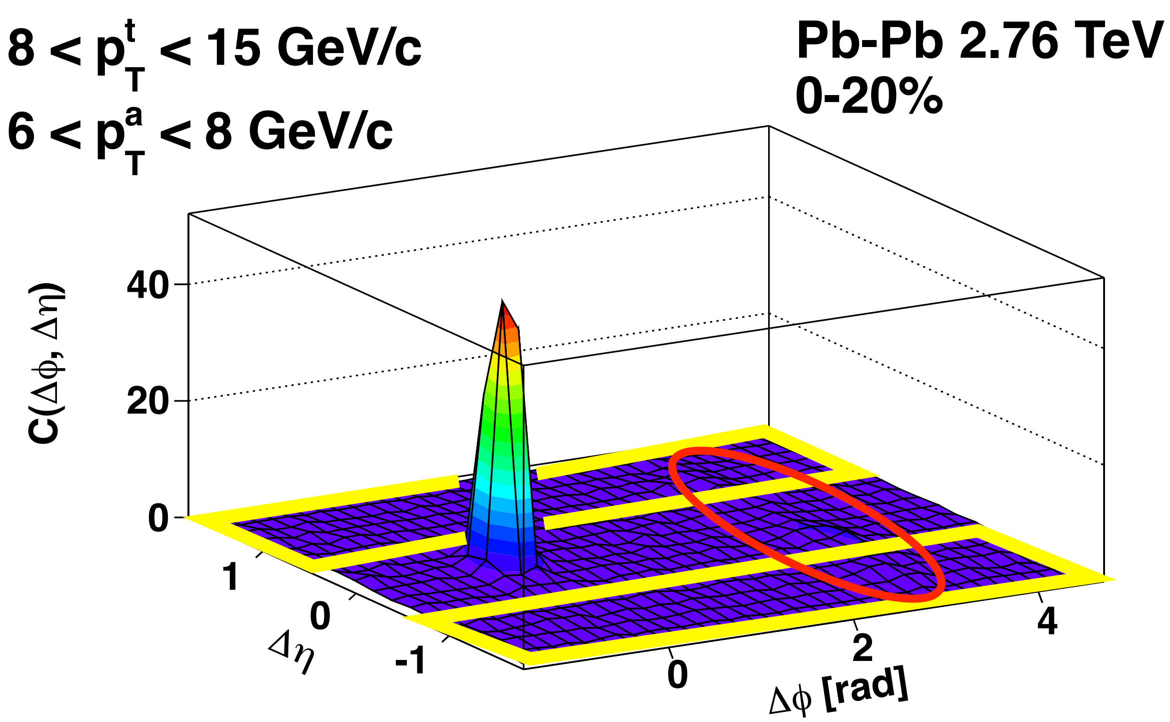

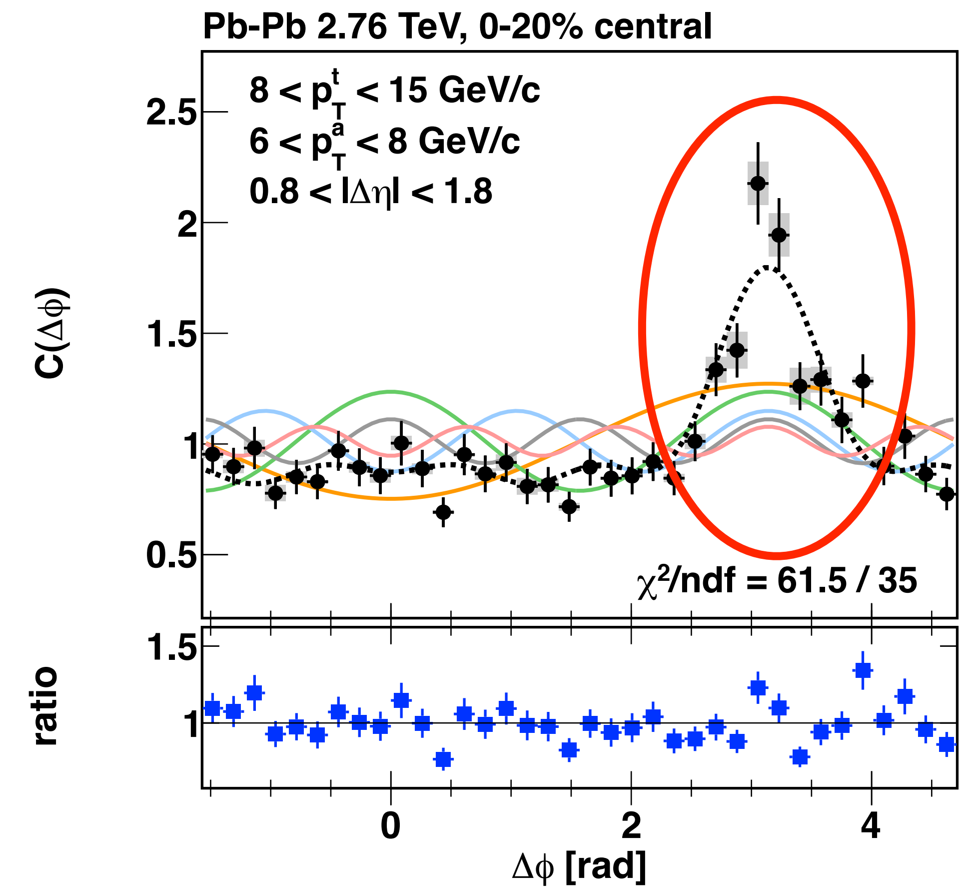

Single vs. pair Fourier decomposition

Single-particle anisotropy

(the familiar v_n coefficients)

$$\frac{dN}{d\phi} \propto 1 + \sum_{n=1}^{\infty} 2v_n(p_T)\cos(n(\phi - \Psi_n))$$

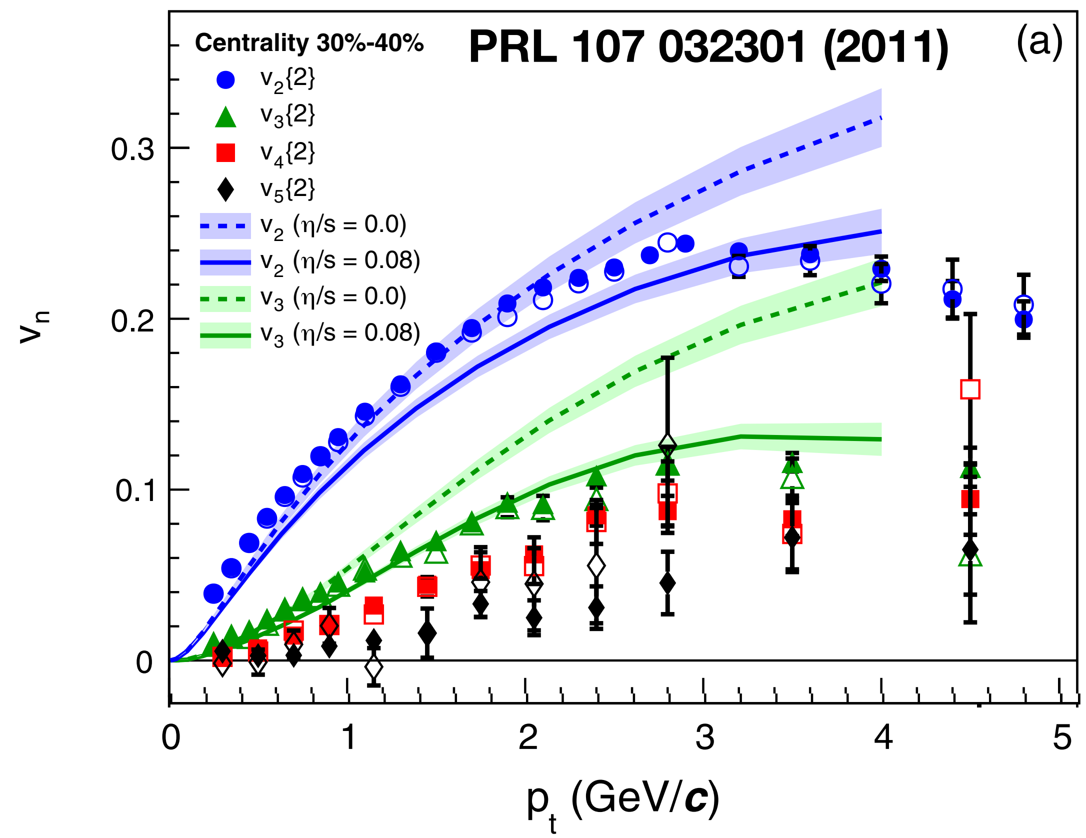

Pair anisotropy

Similar form, but indep. of Ψ_n

$$\frac{dN^{\text{pairs}}}{d\Delta\phi} \propto 1 + \sum_{n=1}^{\infty} 2V_{n\Delta}(p_T^t, p_T^a)\cos(n\Delta\phi)$$

Extract directly from 2-particle azimuthal correlations!

$$V_{n\Delta} \equiv \langle \cos(n\Delta\phi) \rangle = \sum_i C_i \cos(n\Delta\phi_i) \Big/ \sum_i C_i \,.$$

Single vs. pair Fourier decomposition

Single-particle anisotropy

(the familiar v_n coefficients)

$$\frac{dN}{d\phi} \propto 1 + \sum_{n=1}^{\infty} 2v_n(p_T)\cos(n(\phi - \Psi_n))$$

Pair anisotropy

Similar form, but indep. of Ψ_n

$$\frac{dN^{pairs}}{d\Delta\phi} \propto 1 + \sum_{n=1}^{\infty} 2V_{n\Delta}(p_T^t, p_T^a)\cos(n\Delta\phi)$$

Extract directly from 2-particle azimuthal correlations!

$$V_{n\Delta} \equiv \langle\cos(n\Delta\phi)\rangle = \sum_i C_i \cos(n\Delta\phi_i) \Big/ \sum_i C_i .$$

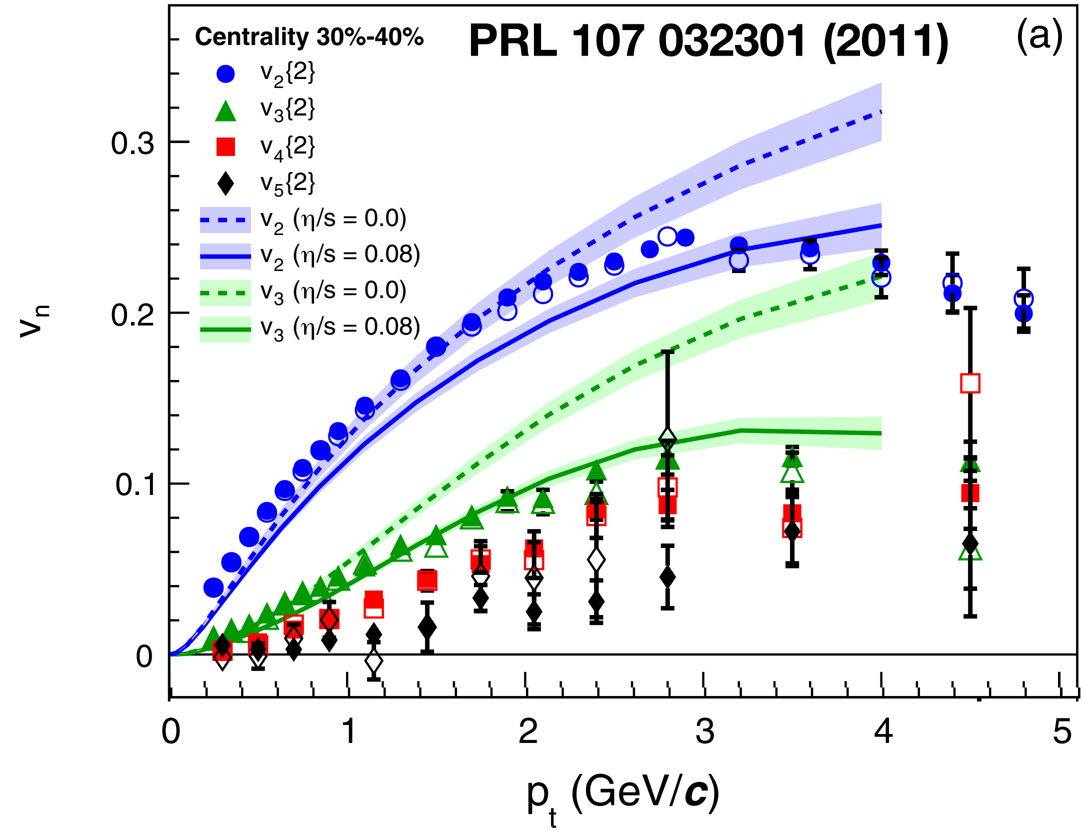

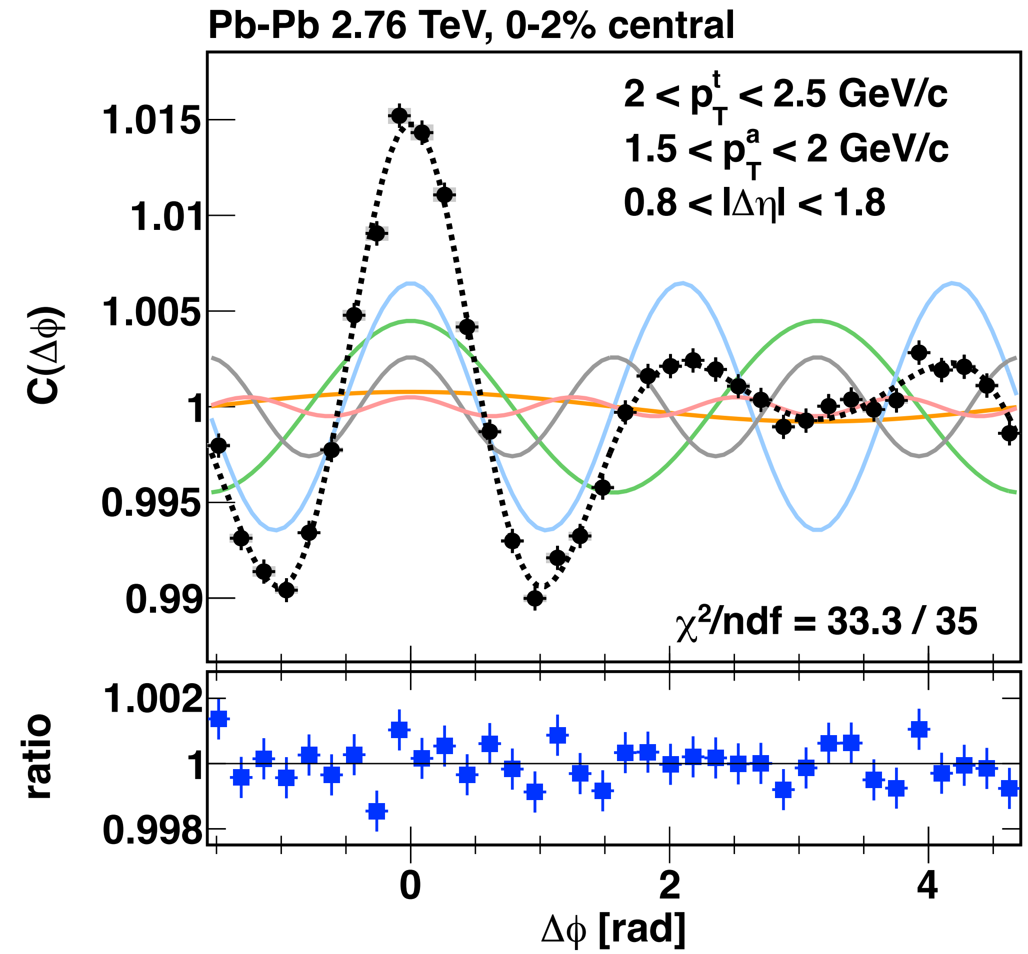

A. Adare (ALICE)

Decomposition in bulk region

“Power spectrum” of pair Fourier components $V_{n\Delta}$

For ultra-central collisions, n = 3 dominates.

In bulk-dominated correlations, the n > 5 harmonics are weak.

(But not necessarily zero...work in progress.)

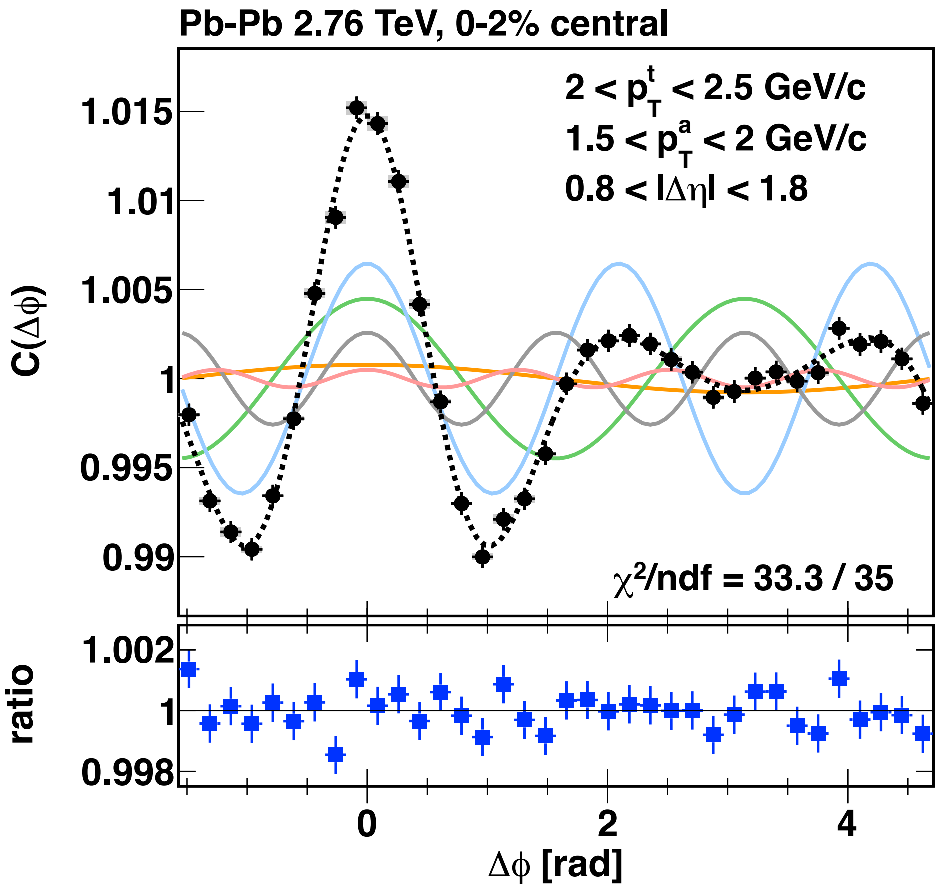

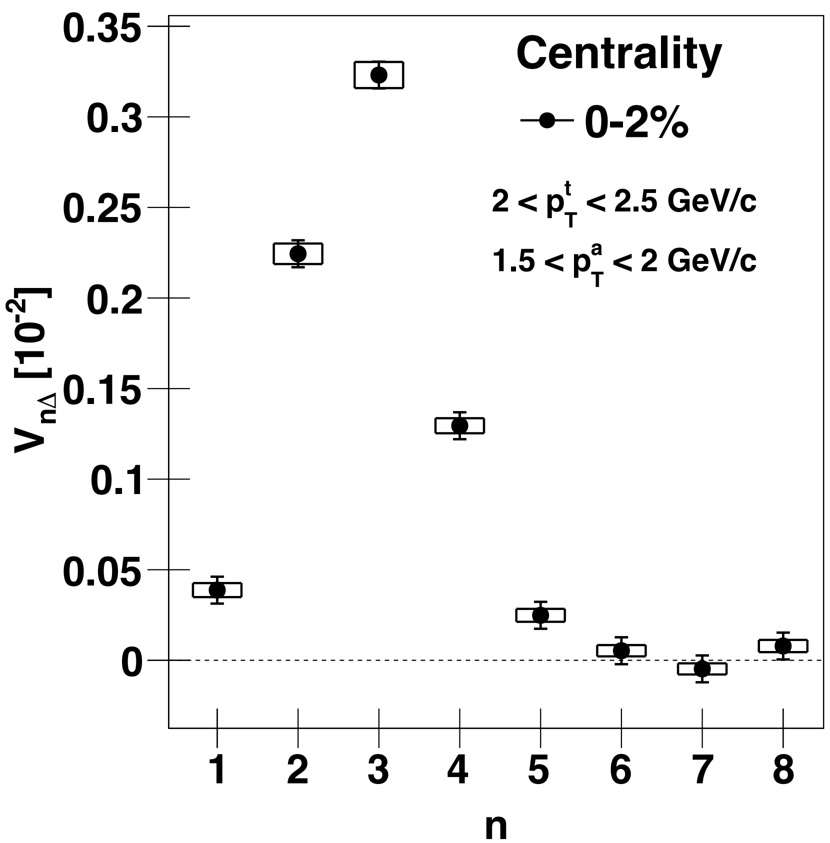

$V_{2\Delta}$ dominates as collisions become less central.

Collision geometry, rather than fluctuations, becomes primary effect

Decomposition in bulk region

"Power spectrum" of pair Fourier components $V_{n\Delta}$

For ultra-central collisions, n = 3 dominates.

In bulk-dominated correlations, the n > 5 harmonics are weak.

(But not necessarily zero...work in progress.)

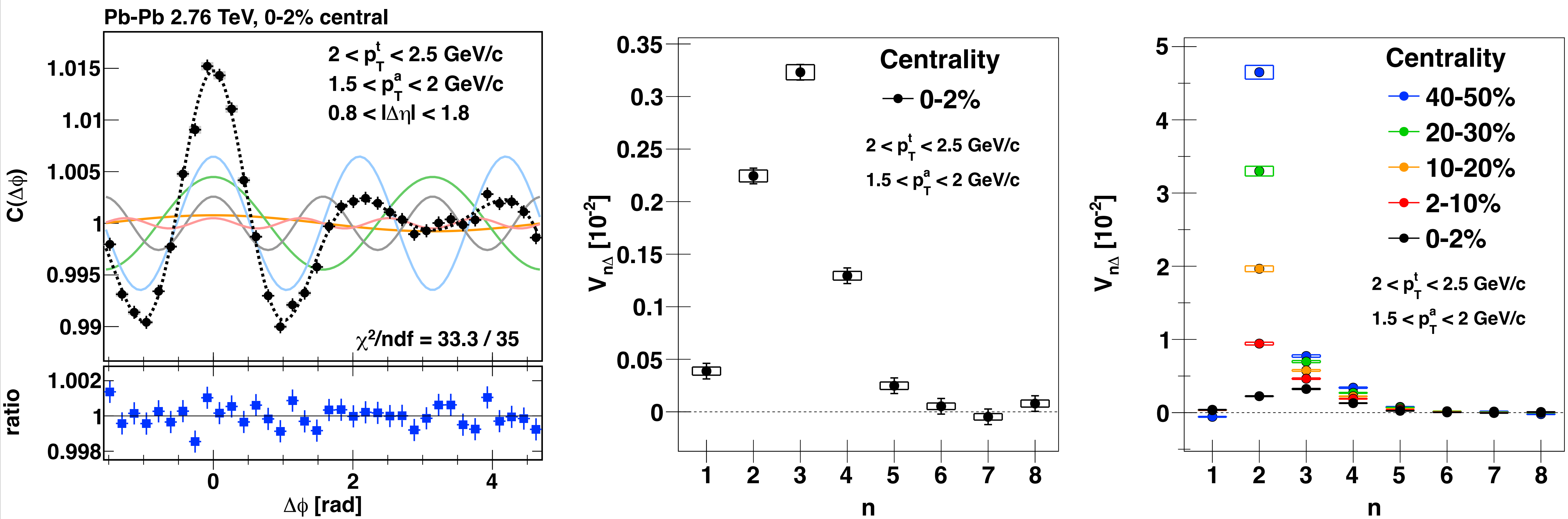

$V_{2\Delta}$ dominates as collisions become less central.

Collision geometry, rather than fluctuations, becomes primary effect

Decomposition in bulk region

"Power spectrum" of pair Fourier components $V_{n\Delta}$

For ultra-central collisions, n = 3 dominates.

In bulk-dominated correlations, the n > 5 harmonics are weak.

(But not necessarily zero...work in progress.)

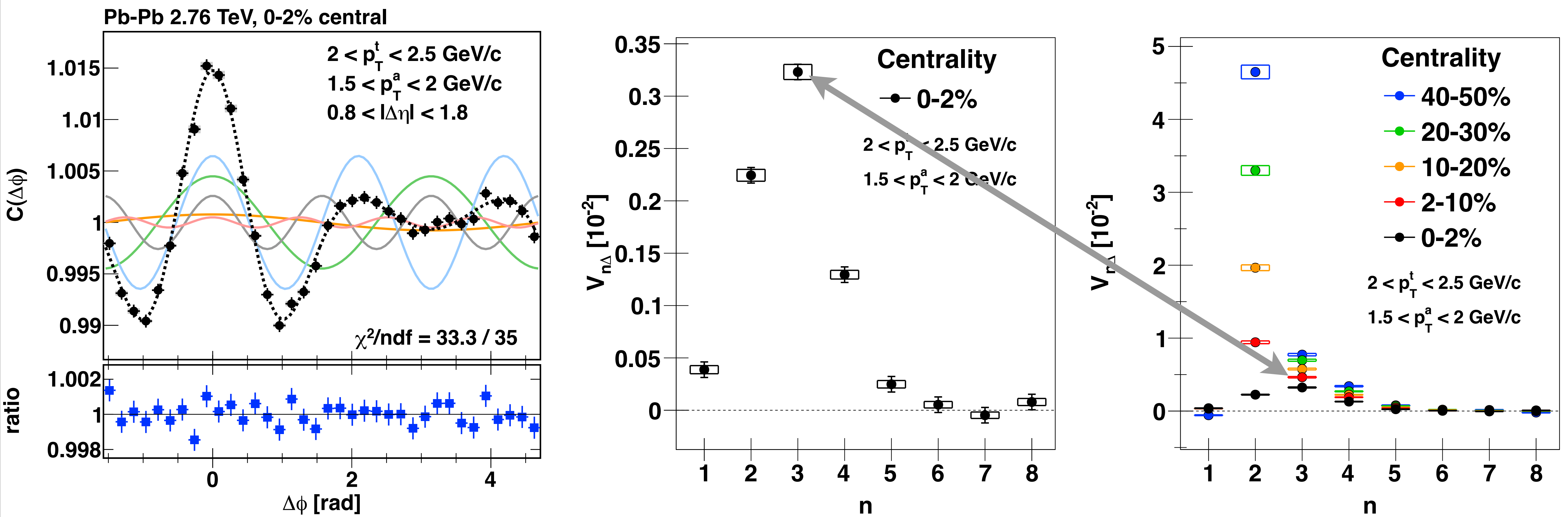

$V_{2\Delta}$ dominates as collisions become less central.

Collision geometry, rather than fluctuations, becomes primary effect

A. Adare (ALICE)

Decomposition in jet region

Di-jet Fourier components $V_{n\Delta}$

Very different spectral signature than bulk correlations!

- All odd harmonics < 0, and finite to large n

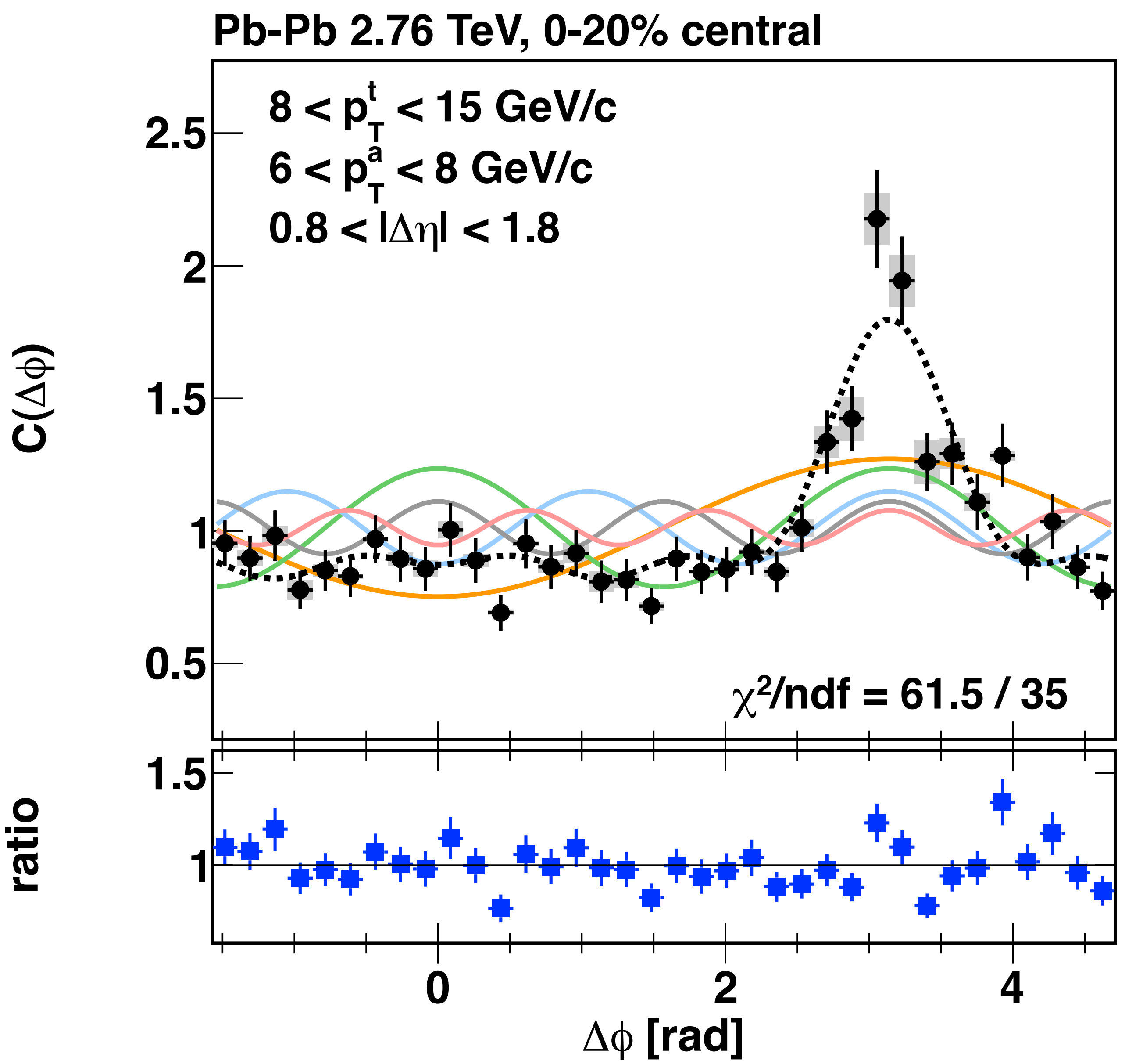

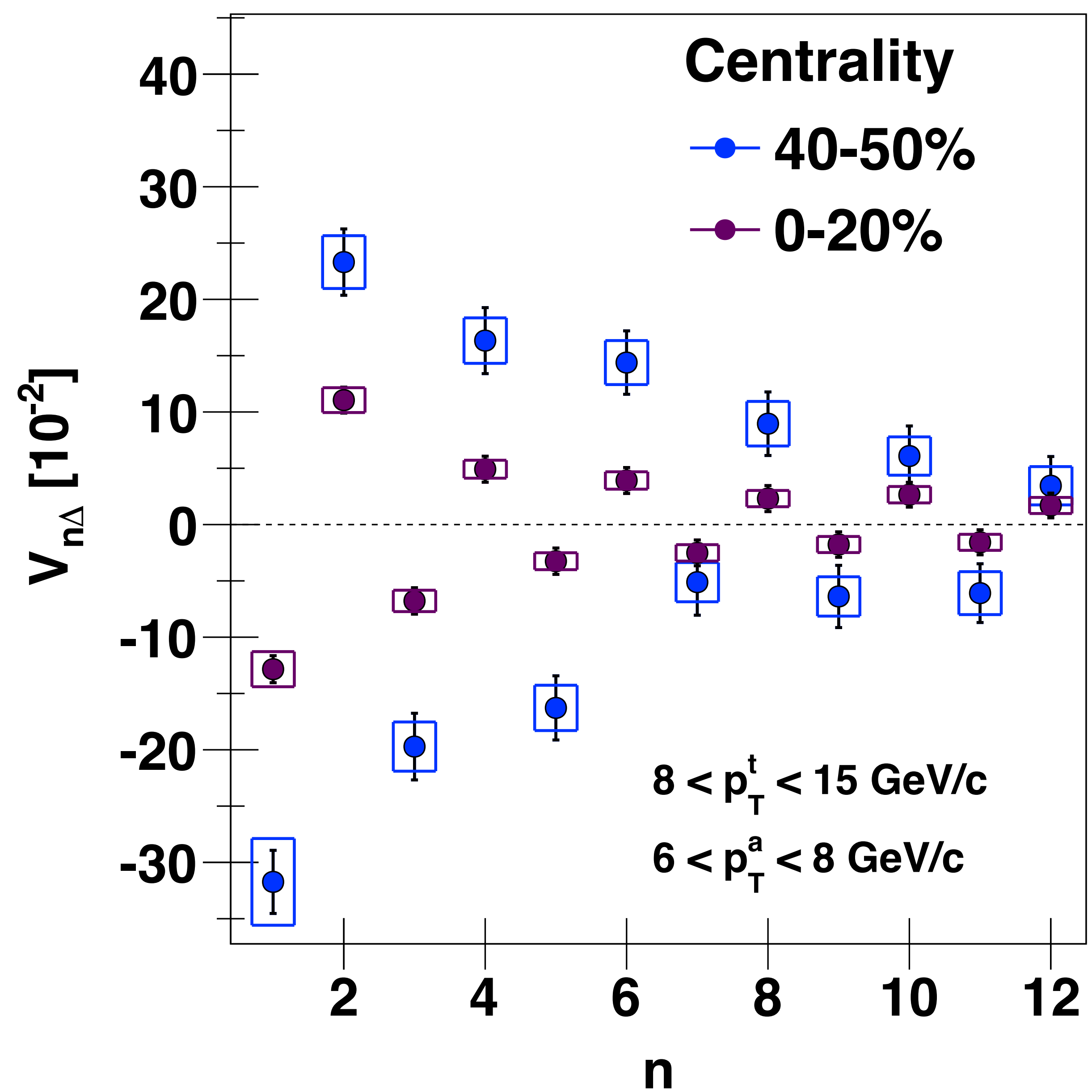

A. Adare (ALICE)

Aside: Gaussian Fourier transform

Away-side peak is (sort of) Gaussian:

The F.T. of a Gaussian($\mu=\pi$, $\sigma_{\Delta\varphi}$) is ±Gaussian($\mu=0$, $\sigma_n = 1/\sigma_{\Delta\varphi}$).

Fit demonstration: when $\mu=\pi$, odd $V_{n\Delta}$ coefficients are negative.

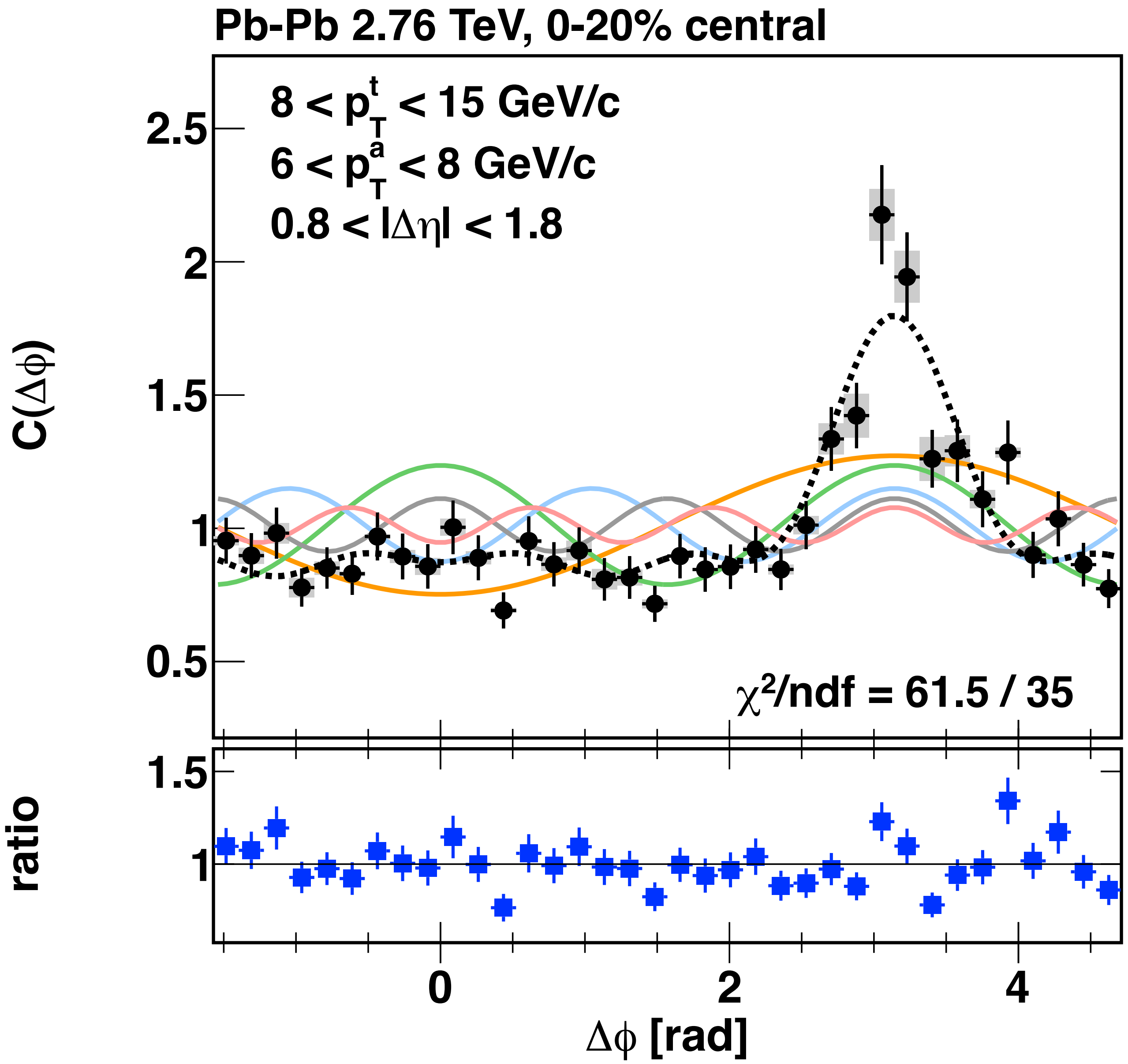

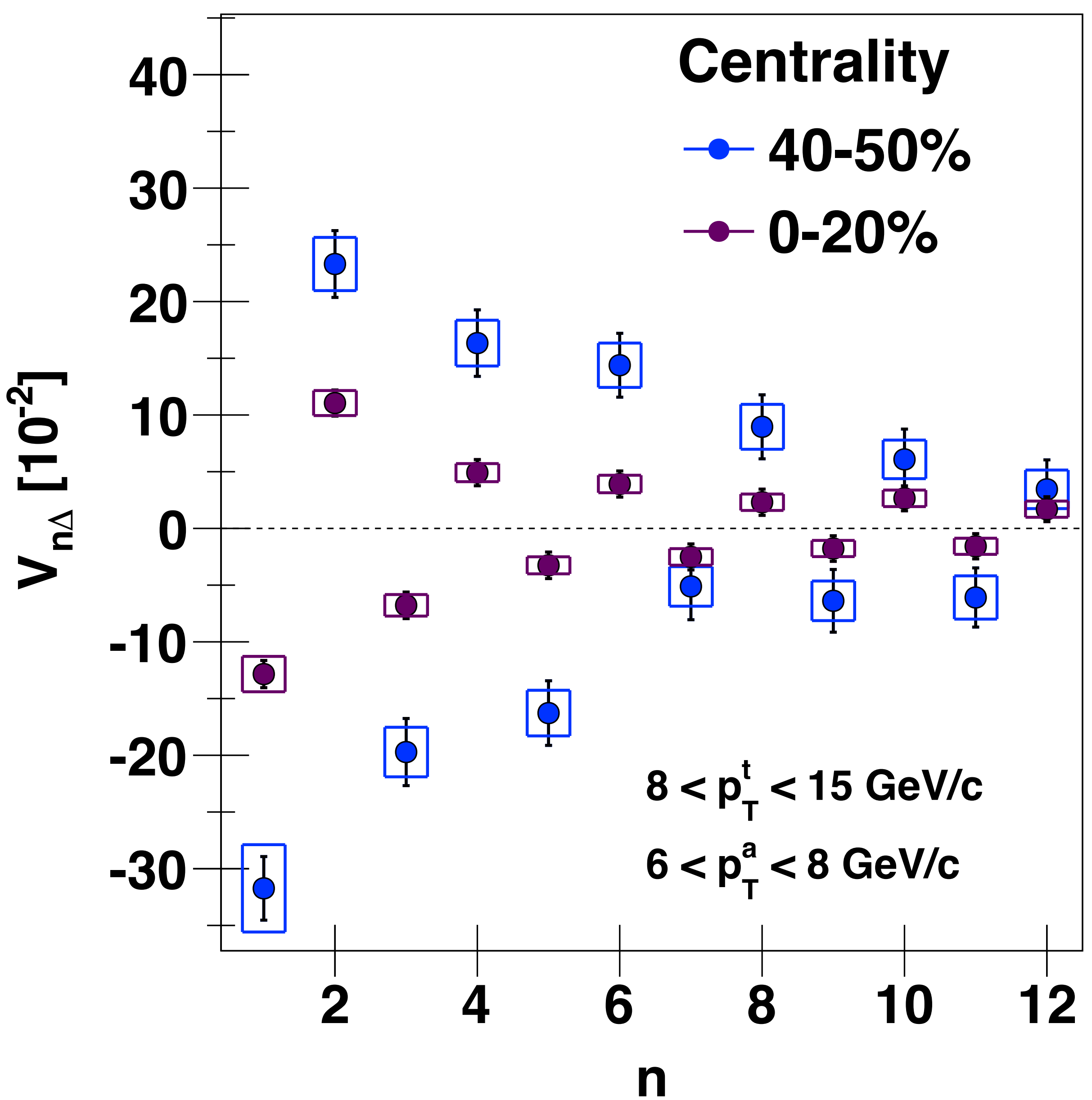

A. Adare (ALICE)

Away-side peak is (sort of) Gaussian:

The F.T. of a Gaussian($\mu=\pi$, $\sigma_{\Delta\varphi}$) is ±Gaussian($\mu=0$, $\sigma_n = 1/\sigma_{\Delta\varphi}$).

Fit demonstration: when $\mu=\pi$, odd $V_{n\Delta}$ coefficients are negative.

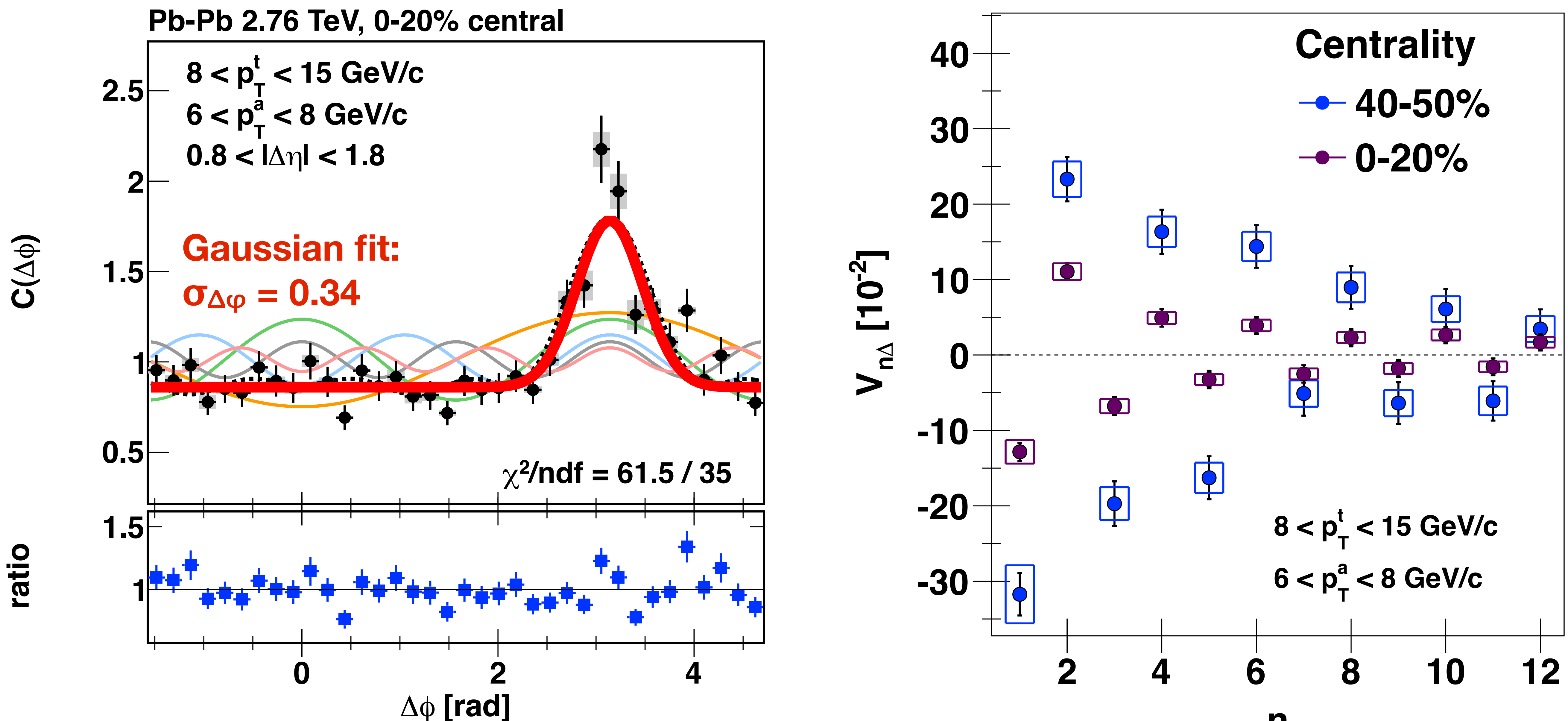

A. Adare (ALICE)

Aside: Gaussian Fourier transform

Away-side peak is (sort of) Gaussian:

The F.T. of a Gaussian($\mu=\pi$, $\sigma_{\Delta\varphi}$) is ±Gaussian($\mu=0$, $\sigma_n = 1/\sigma_{\Delta\varphi}$).

Fit demonstration: when $\mu=\pi$, odd $V_{n\Delta}$ coefficients are negative.

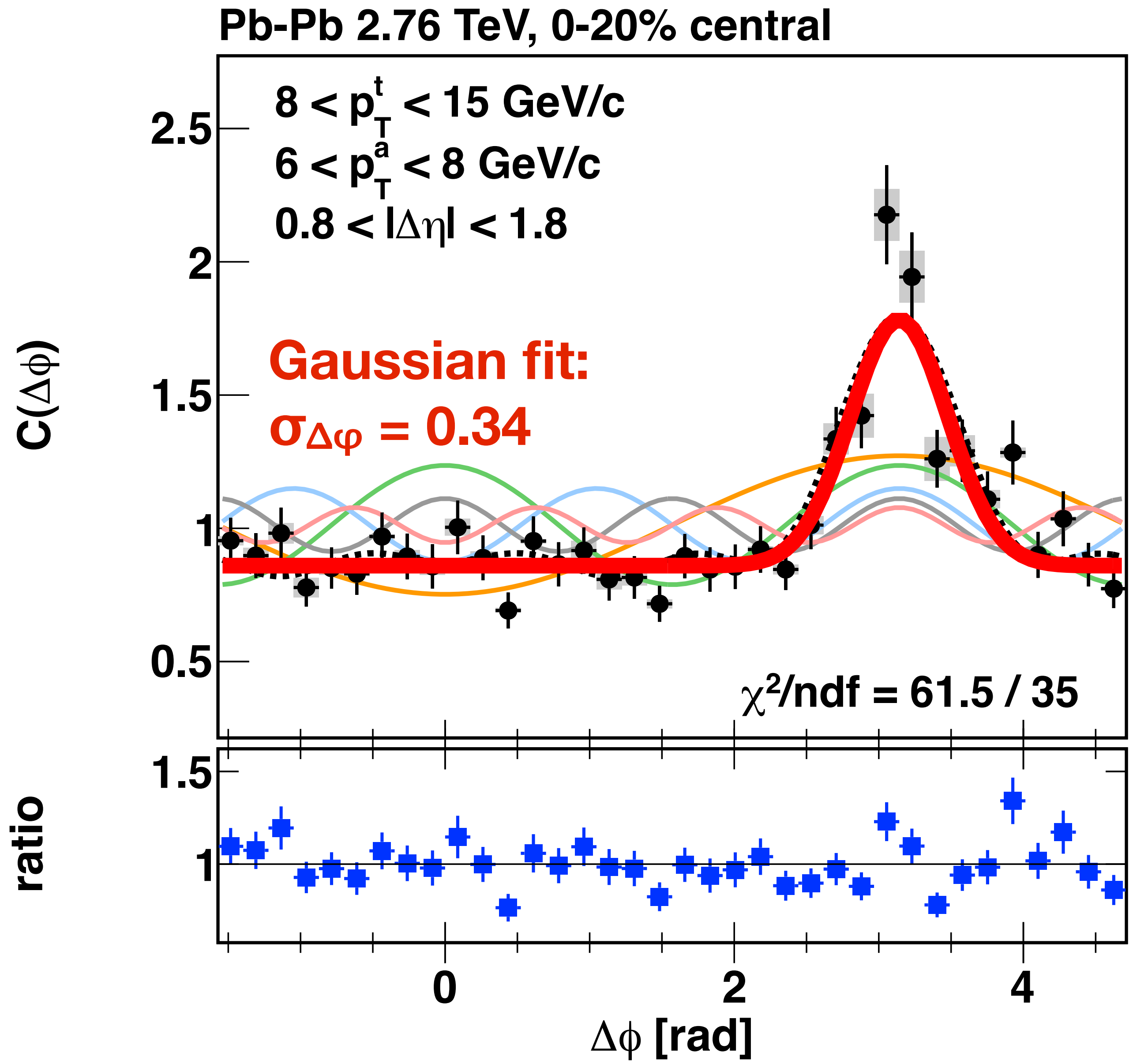

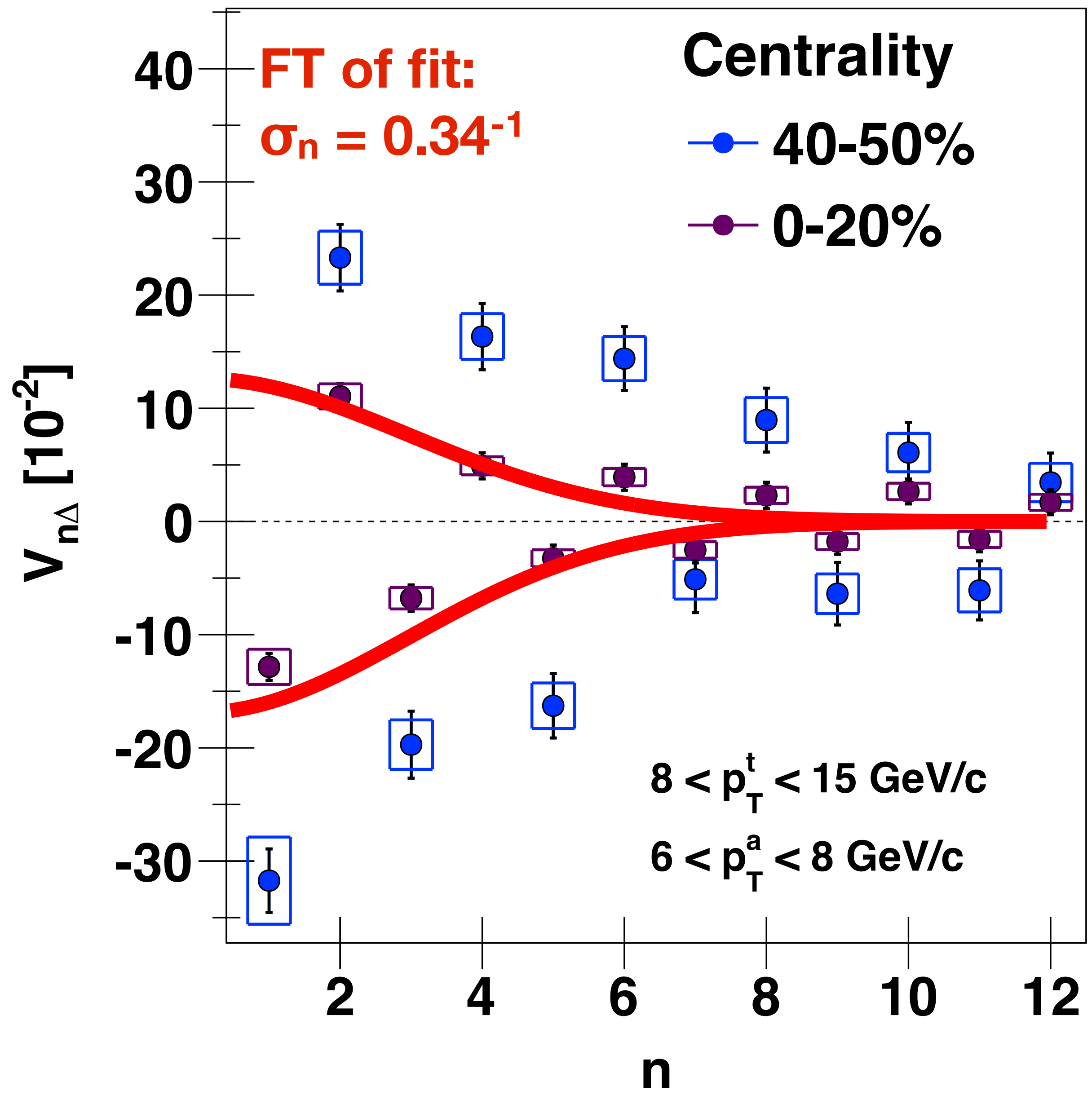

A. Adare (ALICE)

Trigger p_T^t dependence of $V_{n\Delta}$

Similar trends as for v_n

Rises with p_T^t to maximum near 3-4 GeV, then declines

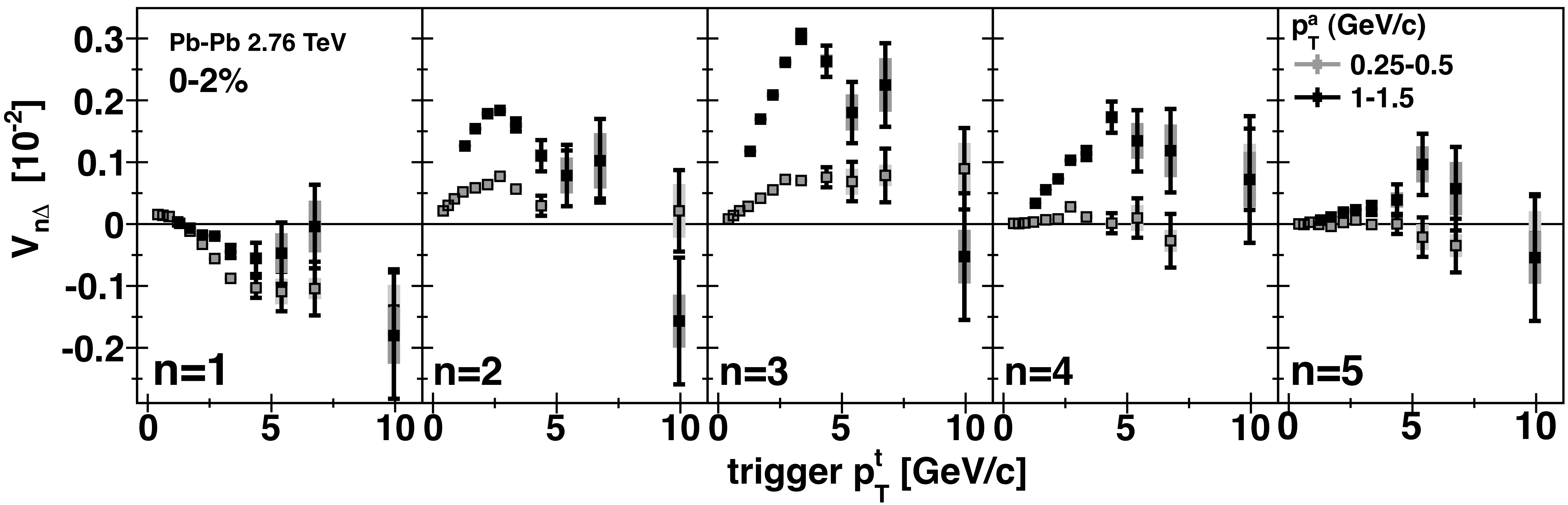

Centrality dependence:

$V_{2\Delta}$ dominates as collisions become less central

Trigger p_T^t dependence of $V_{n\Delta}$

Similar trends as for v_n

Rises with p_T^t to maximum near 3-4 GeV, then declines

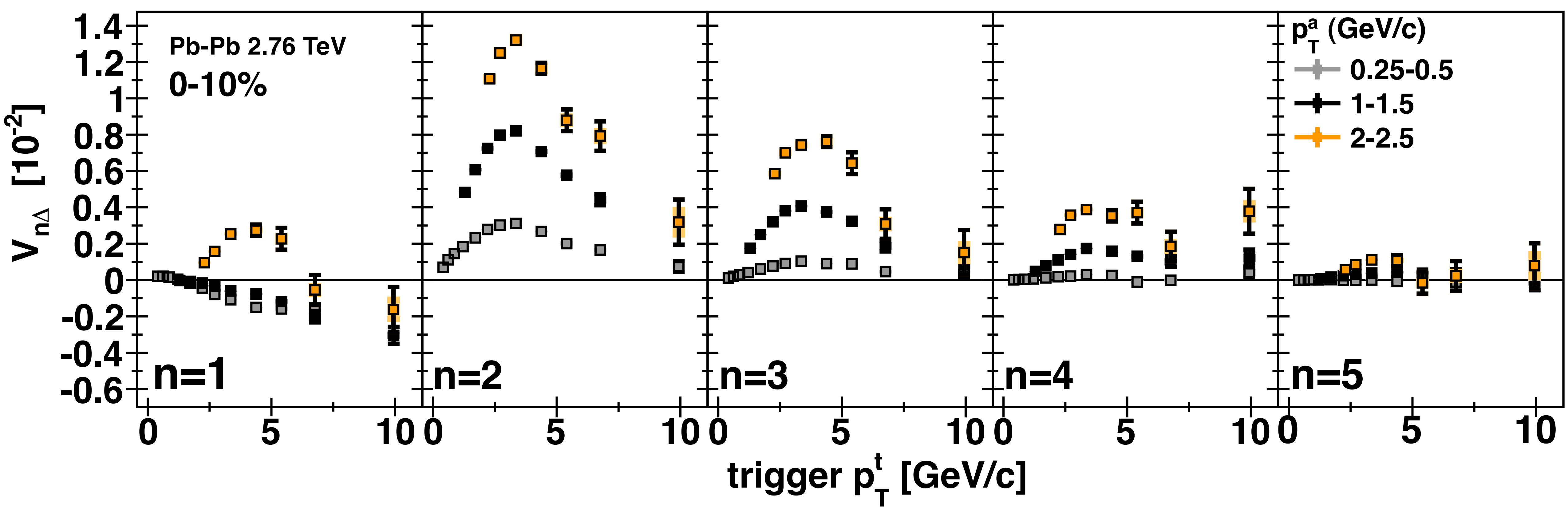

Centrality dependence:

$V_{2\Delta}$ dominates as collisions become less central

Trigger p_T^t dependence of $V_{n\Delta}$

Similar trends as for v_n

Rises with p_T^t to maximum near 3-4 GeV, then declines

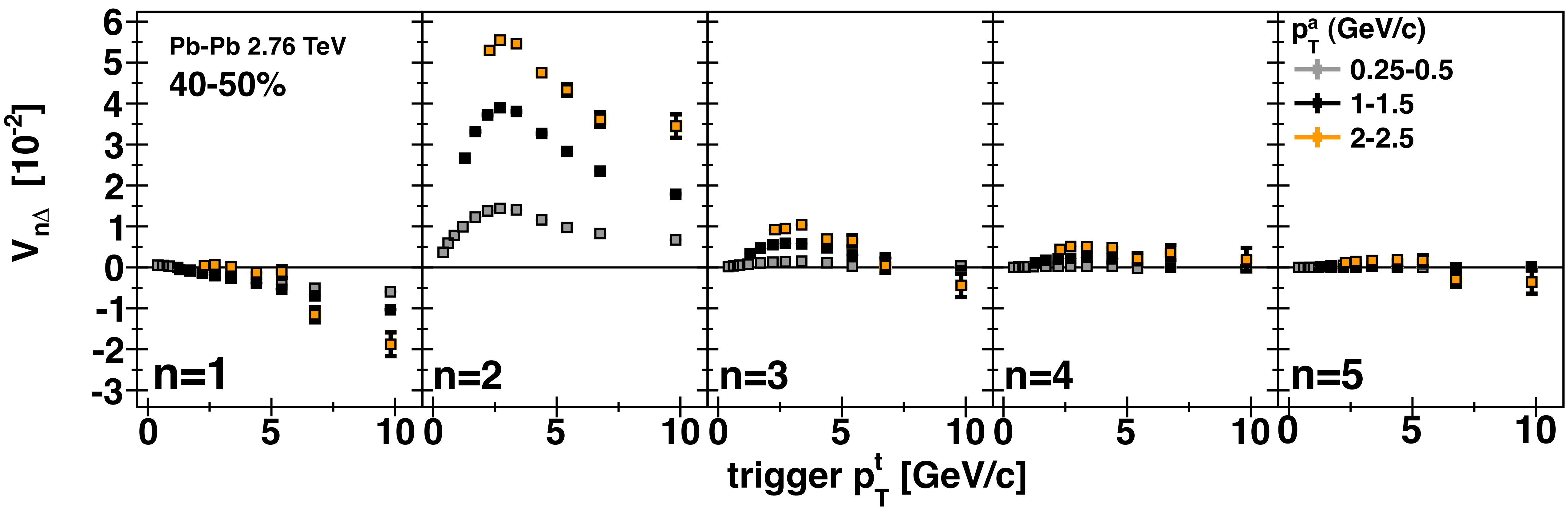

Centrality dependence:

$V_{2\Delta}$ dominates as collisions become less central

The factorization hypothesis

Factorization of two-particle anisotropy

For pairs correlated to one another through a common symmetry plane Ψ_n, their correlation is dictated by bulk anisotropy:

$$\begin{aligned} V_{n\Delta}(p_T^t, p_T^a) &= \langle\langle e^{in(\phi_a - \phi_t)} \rangle\rangle \\ &= \langle\langle e^{in(\phi_a - \Psi_n)} \rangle\rangle \langle\langle e^{-in(\phi_t - \Psi_n)} \rangle\rangle \\ &= \langle v_n\{2\}(p_T^t)\, v_n\{2\}(p_T^a) \rangle. \end{aligned}$$

$V_{n\Delta}$ would be generated from one $v_n(p_T)$ curve, evaluated at p_T^t and p_T^a.

Factorization expected:

✔ **For correlations from collective flow.**

Flow is global and affects all particles in the event.

✘ **Not for pairs from fragmenting di-jets.**

Di-jet shapes are “local”, not strongly connected to Ψ_n.

The factorization hypothesis

Factorization of two-particle anisotropy

For pairs correlated to one another through a common symmetry plane Ψ_n, their correlation is dictated by bulk anisotropy:

$$
\begin{aligned}
V_{n\Delta}(p_T^t, p_T^a) &= \langle\langle e^{in(\phi_a - \phi_t)}\rangle\rangle \\
&= \langle\langle e^{in(\phi_a - \Psi_n)}\rangle\rangle\langle\langle e^{-in(\phi_t - \Psi_n)}\rangle\rangle \\
&= \langle v_n\{2\}(p_T^t)\, v_n\{2\}(p_T^a)\rangle .
\end{aligned}
$$

$V_{n\Delta}$ would be generated from one $v_n(p_T)$ curve, evaluated at p_T^t and p_T^a.

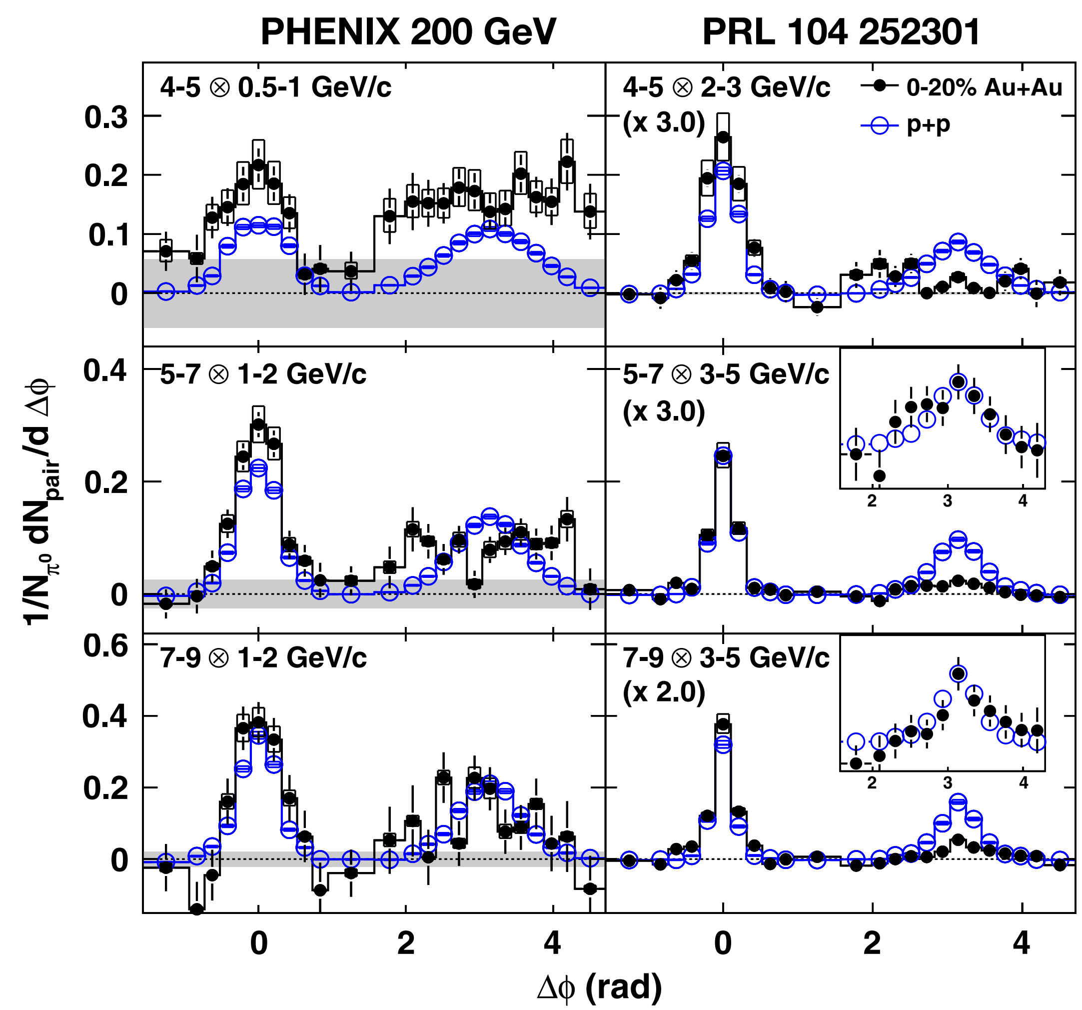

Factorization expected:

✔ **For correlations from collective flow.**

Flow is global and affects all particles in the event.

✘ **Not for pairs from fragmenting di-jets.**

Di-jet shapes are “local”, not strongly connected to Ψ_n.

A. Adare (ALICE)

Testing factorization with a global fit

Improving on $V_{n\Delta} = v_n(p_T)^2$ with triggered correlations...

12 p_T^t bins, 12 p_T^a bins; $p_T^t \geq p_T^a$ ⇒ 78 $V_{n\Delta}$ points.

Fit all simultaneously to find $v_n(p_T)$ curve with best-fit $v_n(p_T^t)$ x $v_n(p_T^a)$ product.

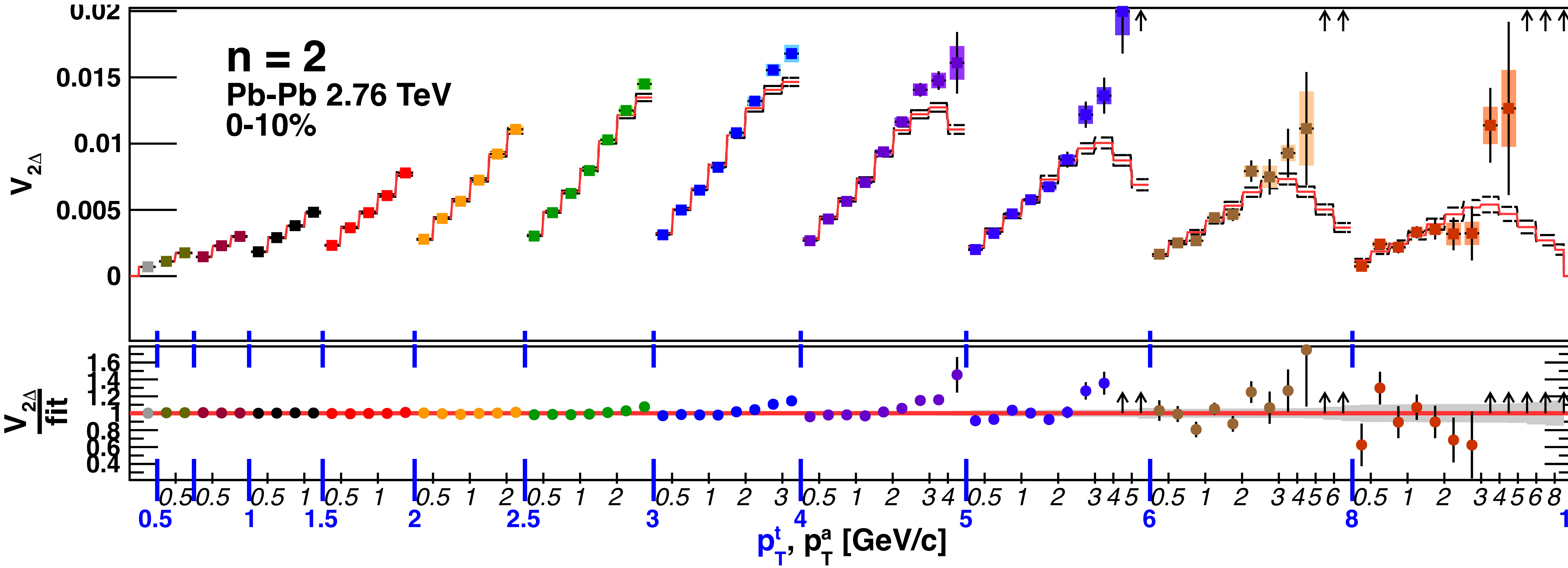

At each n:

- **Fit supports factorization at low p_T^a**

⇒ suggests flow correlations.

- **Fit deviates from data in jet-dominated high p_T^a region**

⇒ collective description less appropriate.

A. Adare (ALICE)

Testing factorization with a global fit

Improving on $V_{n\Delta} = v_n(p_T)^2$ with triggered correlations...

12 p_T^t bins, 12 p_T^a bins; $p_T^t \geq p_T^a$ ⇒ 78 $V_{n\Delta}$ points.

Fit all simultaneously to find $v_n(p_T)$ curve with best-fit $v_n(p_T^t)$ x $v_n(p_T^a)$ product.

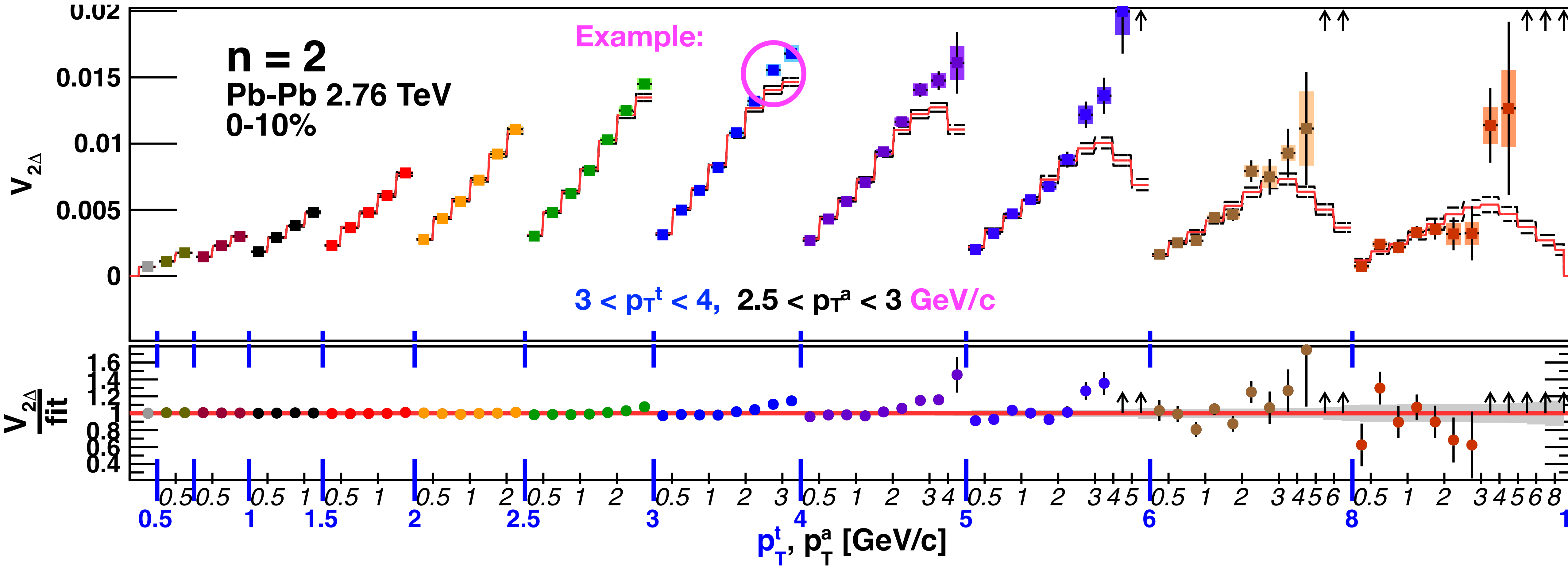

At each n:

- **Fit supports factorization at low p_T^a**

⇒ suggests flow correlations.

- **Fit deviates from data in jet-dominated high p_T^a region**

⇒ collective description less appropriate.

A. Adare (ALICE)

Testing factorization with a global fit

Improving on $V_{n\Delta} = v_n(p_T)^2$ with triggered correlations...

12 p_T^t bins, 12 p_T^a bins; $p_T^t \geq p_T^a$ ⇒ 78 $V_{n\Delta}$ points.

Fit all simultaneously to find $v_n(p_T)$ curve with best-fit $v_n(p_T^t)$ x $v_n(p_T^a)$ product.

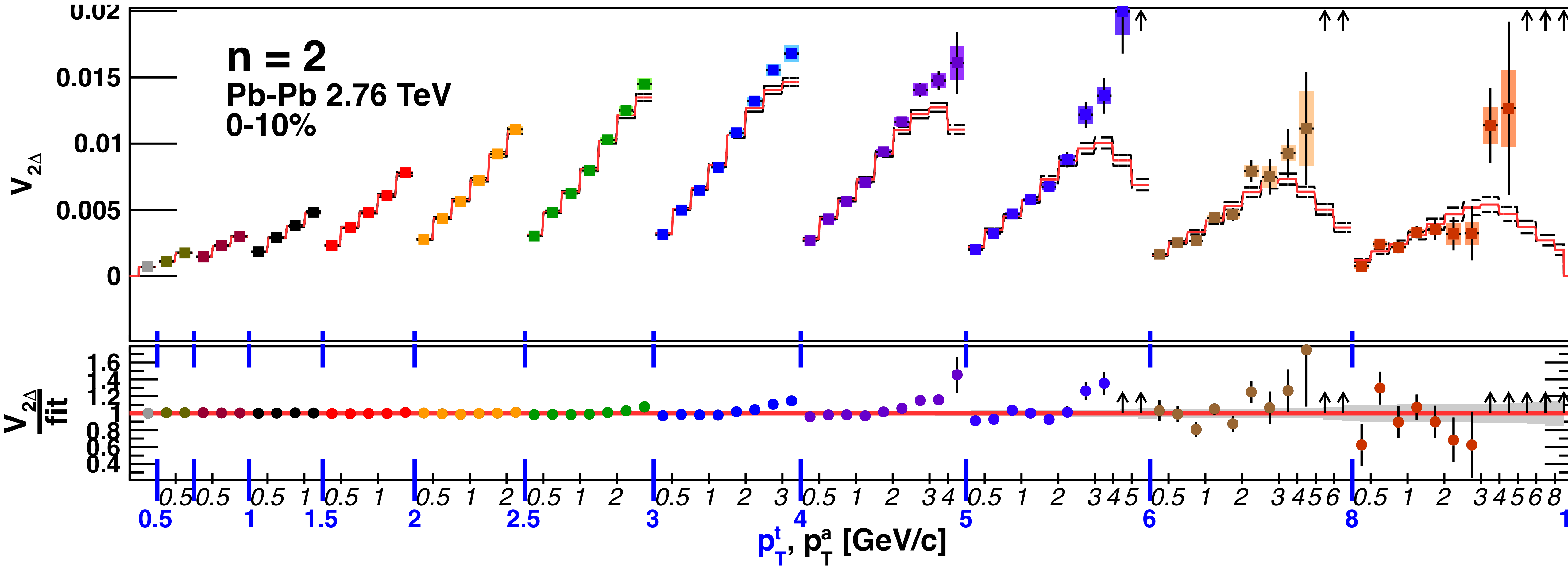

At each n:

- **Fit supports factorization at low p_T^a**

⇒ suggests flow correlations.

- **Fit deviates from data in jet-dominated high p_T^a region**

⇒ collective description less appropriate.

A. Adare (ALICE)

Testing factorization with a global fit

Improving on $V_{n\Delta} = v_n(p_T)^2$ with triggered correlations...

12 p_T^t bins, 12 p_T^a bins; $p_T^t \geq p_T^a$ ⇒ 78 $V_{n\Delta}$ points.

Fit all simultaneously to find $v_n(p_T)$ curve with best-fit $v_n(p_T^t) \times v_n(p_T^a)$ product.

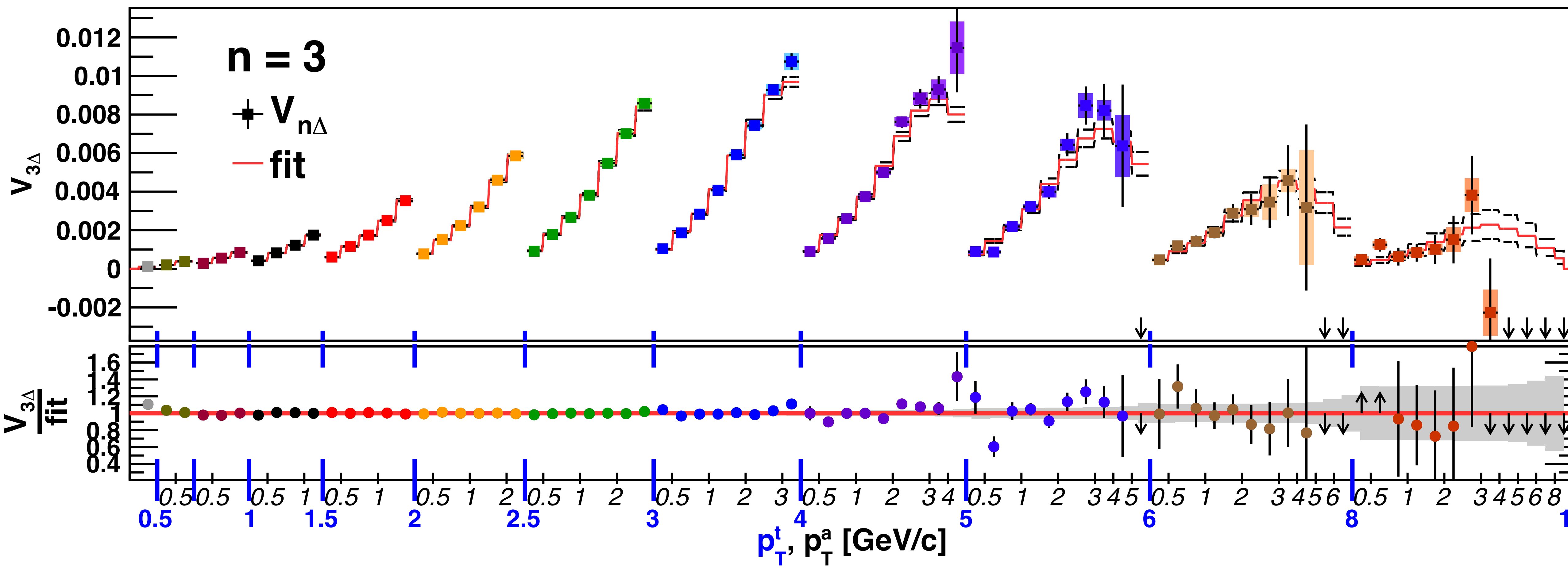

At each n:

- **Fit supports factorization at low p_T^a**

⇒ suggests flow correlations.

- **Fit deviates from data in jet-dominated high p_T^a region**

⇒ collective description less appropriate.

Testing factorization with a global fit

Improving on $V_{n\Delta} = v_n(p_T)^2$ with triggered correlations...

12 p_T^t bins, 12 p_T^a bins; $p_T^t \geq p_T^a$ $\Rightarrow$ 78 $V_{n\Delta}$ points.

Fit all simultaneously to find $v_n(p_T)$ curve with best-fit $v_n(p_T^t)$ x $v_n(p_T^a)$ product.

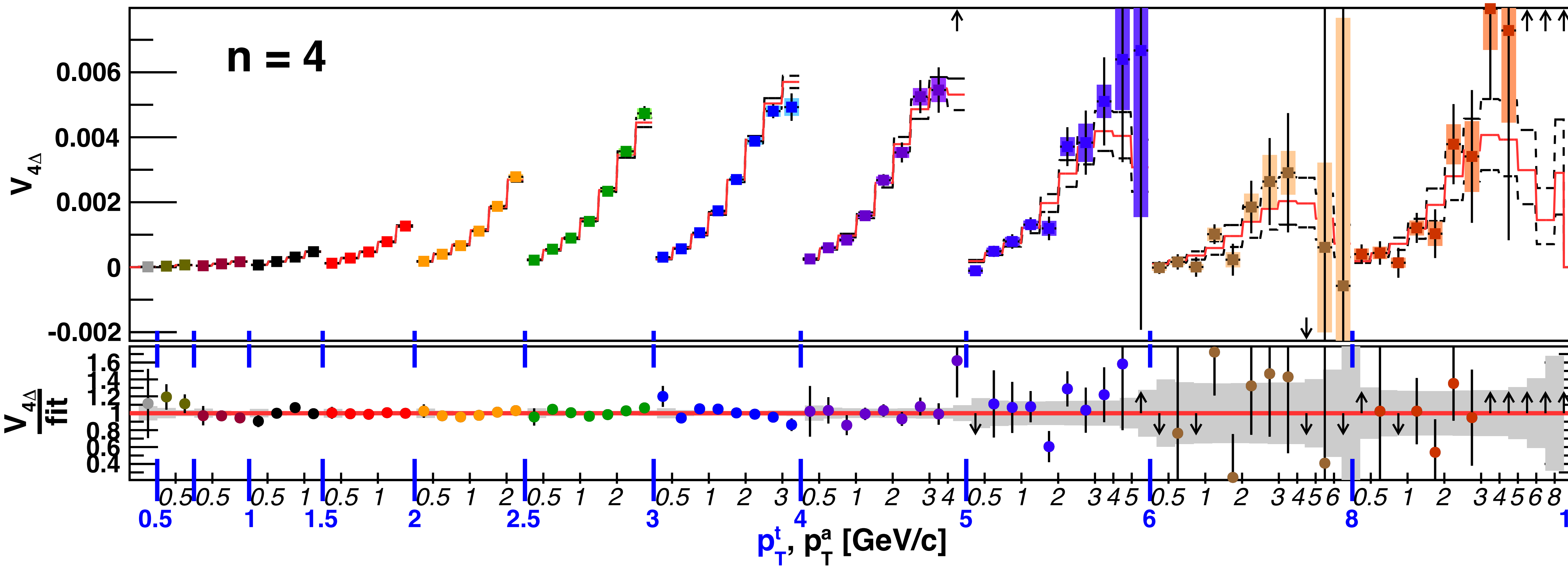

At each n:

- Fit supports factorization at low p_T^a

$\Rightarrow$ suggests flow correlations.

- Fit deviates from data in jet-dominated high p_T^a region

$\Rightarrow$ collective description less appropriate.

A. Adare (ALICE)

Testing factorization with a global fit

Improving on $V_{n\Delta} = v_n(p_T)^2$ with triggered correlations...

12 p_T^t bins, 12 p_T^a bins; $p_T^t \geq p_T^a$ $\Rightarrow$ 78 $V_{n\Delta}$ points.

Fit all simultaneously to find $v_n(p_T)$ curve with best-fit $v_n(p_T^t) \times v_n(p_T^a)$ product.

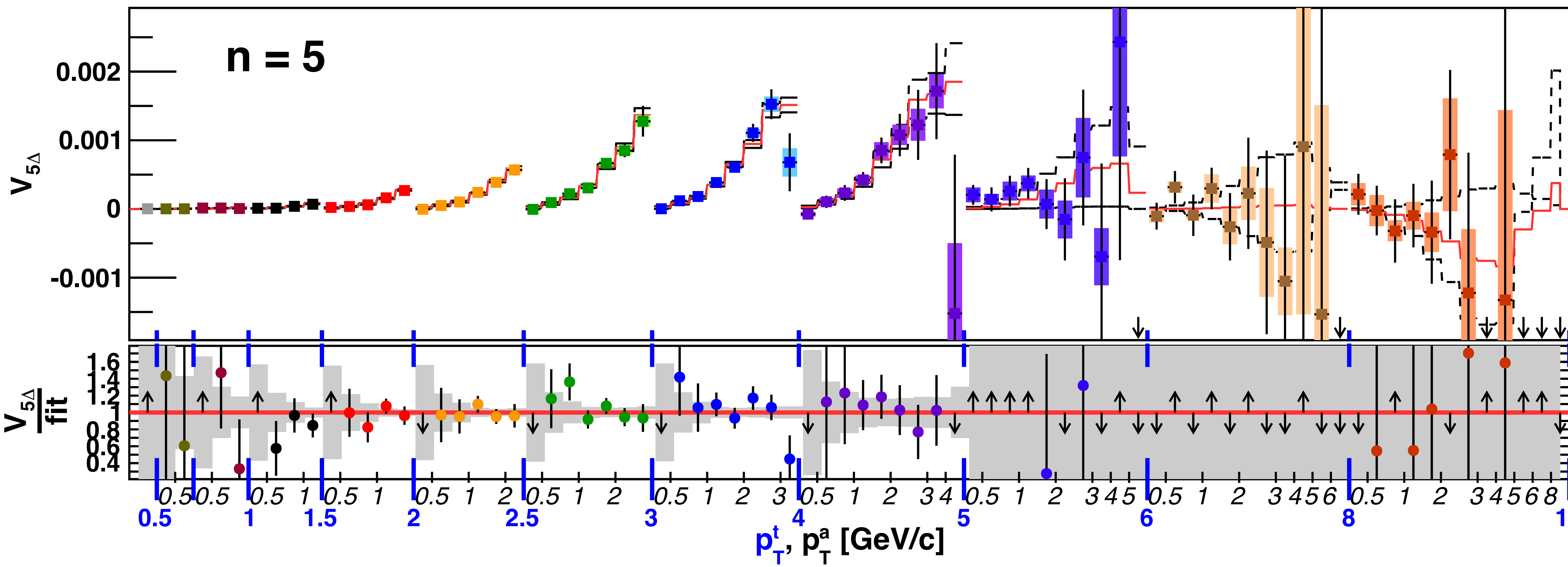

At each n:

- **Fit supports factorization at low p_T^a**

  $\Rightarrow$ suggests flow correlations.

- **Fit deviates from data in jet-dominated high p_T^a region**

  $\Rightarrow$ collective description less appropriate.

A. Adare (ALICE)

Testing factorization with a global fit

Improving on $V_{n\Delta} = v_n(p_T)^2$ with triggered correlations...

12 p_T^t bins, 12 p_T^a bins; $p_T^t \geq p_T^a$ ⇒ 78 $V_{n\Delta}$ points.

Fit all simultaneously to find $v_n(p_T)$ curve with best-fit $v_n(p_T^t)$ x $v_n(p_T^a)$ product.

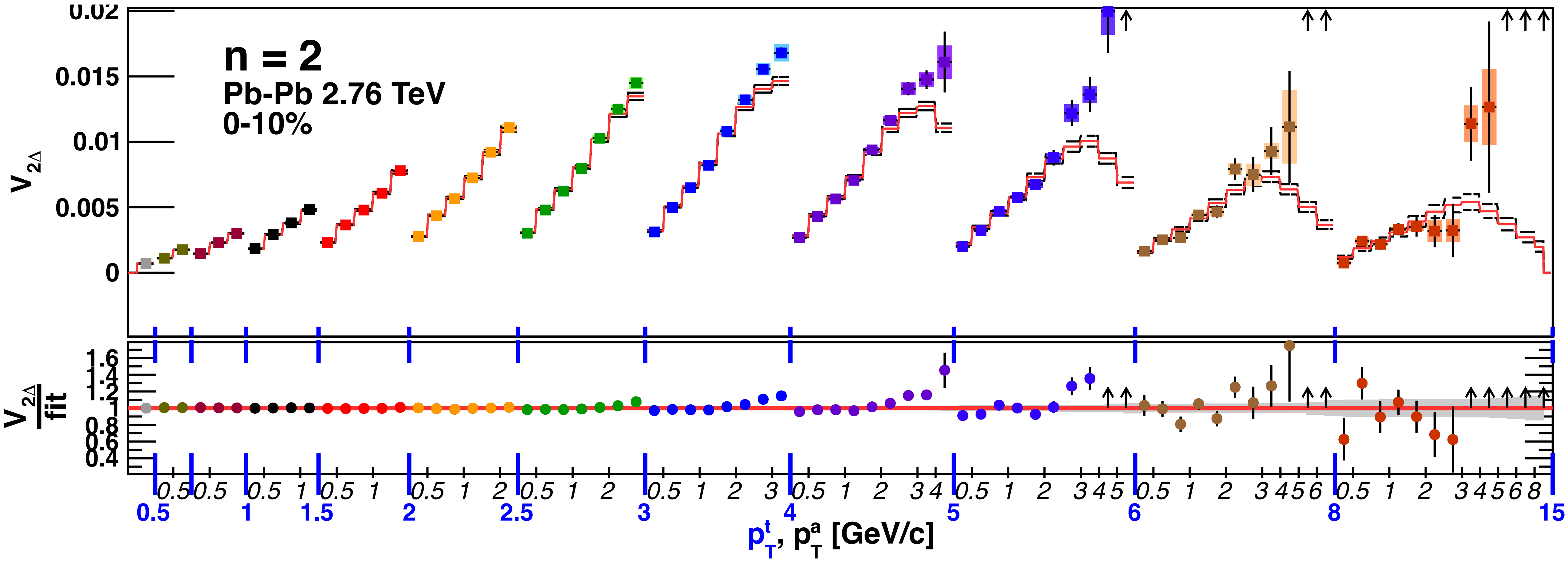

At each n:

- **Fit supports factorization at low p_T^a**

⇒ suggests flow correlations.

- **Fit deviates from data in jet-dominated high p_T^a region**

⇒ collective description less appropriate.

A. Adare (ALICE)

Best-fit $v_n\{GF\}(p_T)$

Global fit parameters are v_n coefficients

$2 \leq n \leq 5$ shown here (n=1 later)

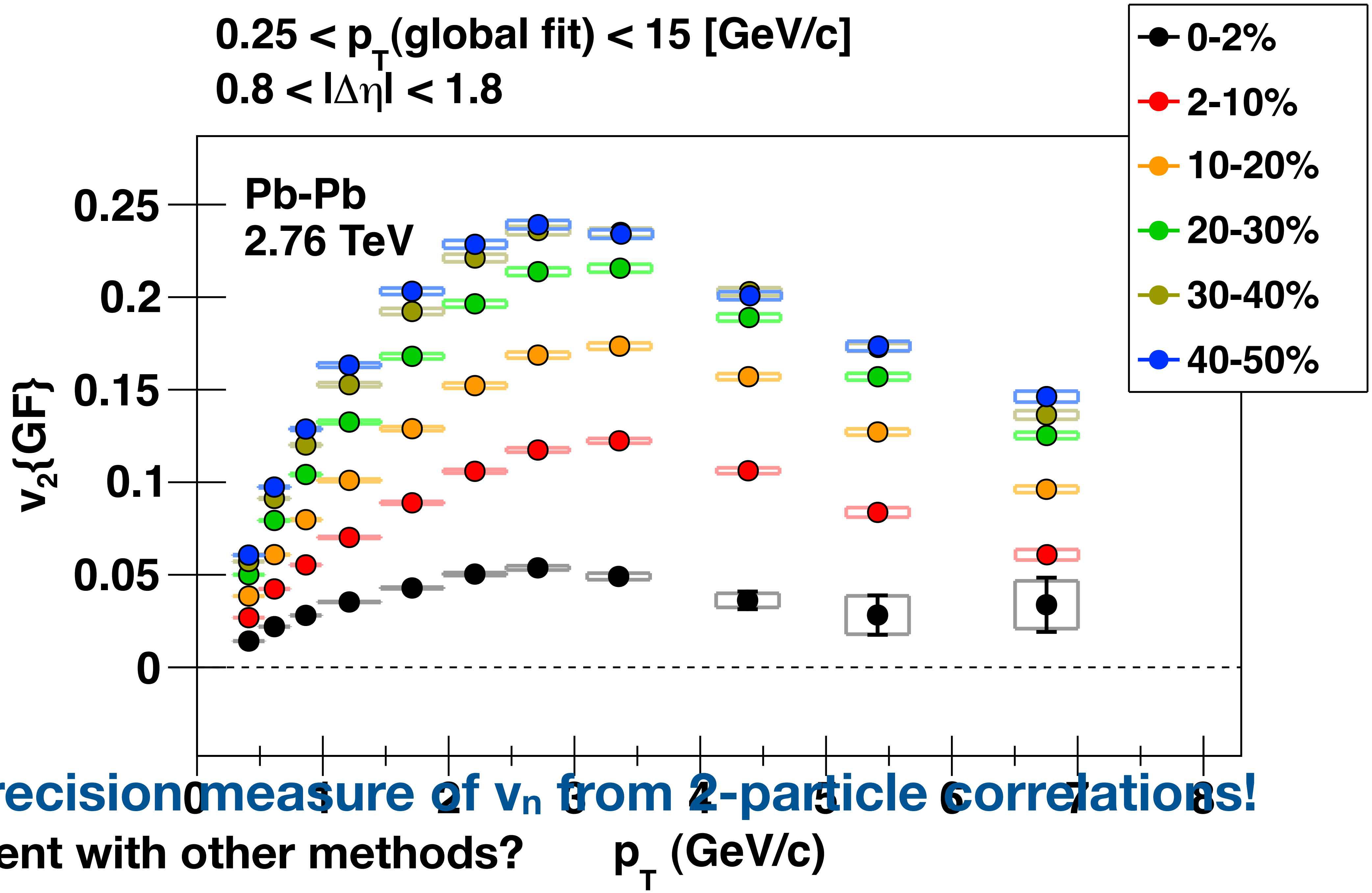

High-precision measure of v_n from 2-particle correlations!

Agreement with other methods?

Best-fit $v_n\{GF\}(p_T)$

Global fit parameters are v_n coefficients

$2 \leq n \leq 5$ shown here (n=1 later)

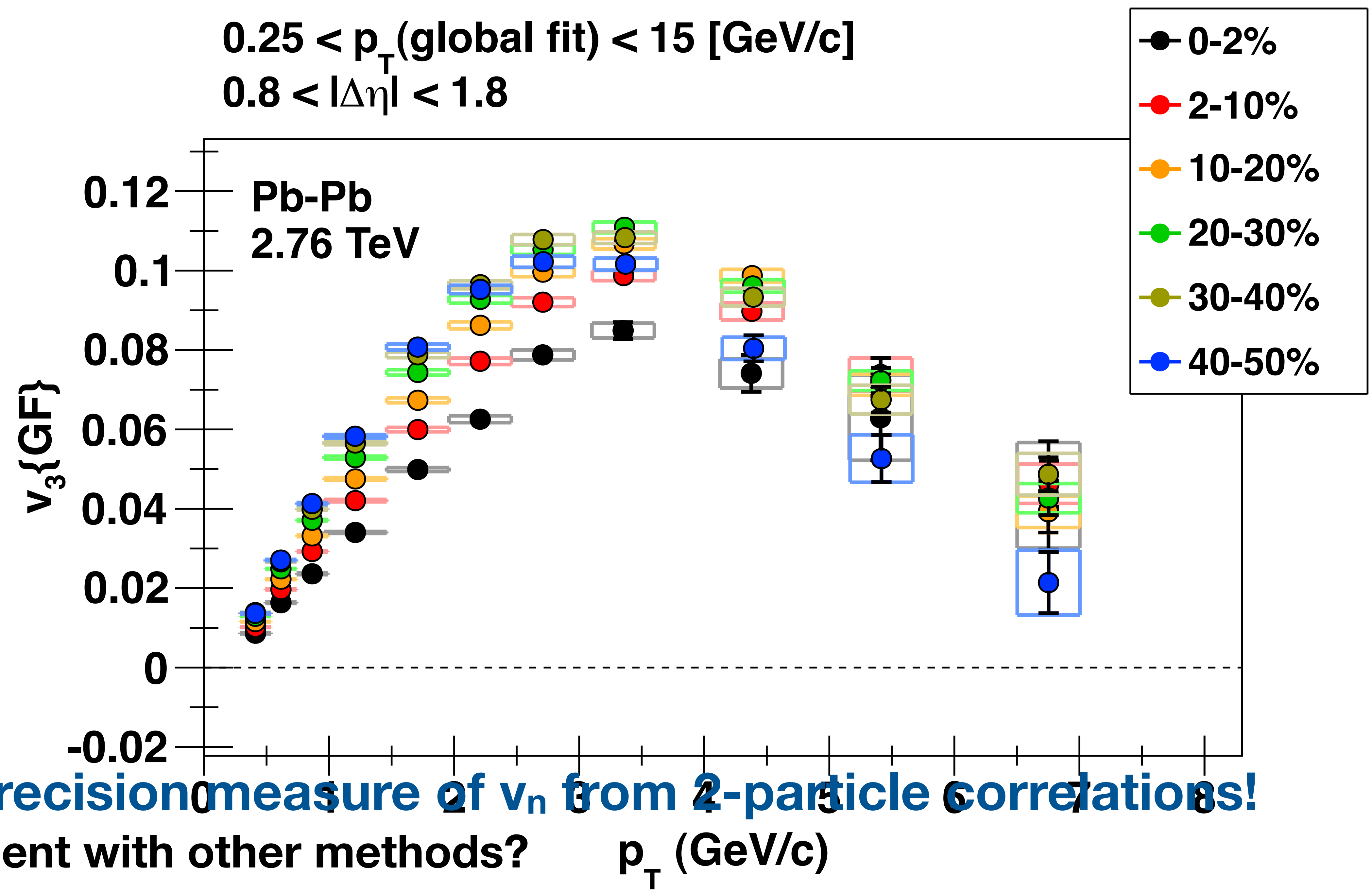

High-precision measure of v_n from 2-particle correlations!

Agreement with other methods?

Best-fit $v_n\{GF\}(p_T)$

Global fit parameters are v_n coefficients

$2 \leq n \leq 5$ shown here (n=1 later)

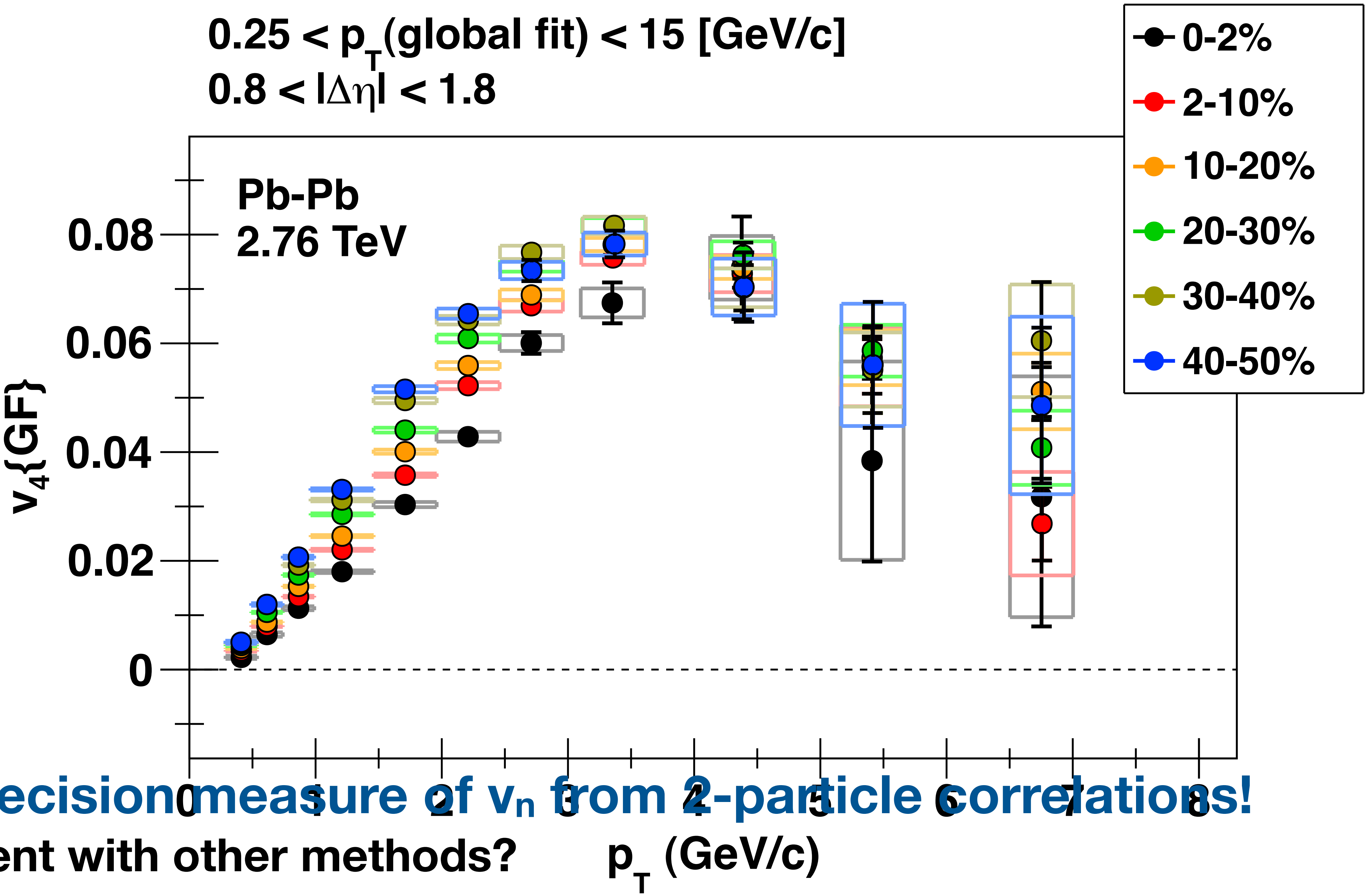

High-precision measure of v_n from 2-particle correlations!

Agreement with other methods?

Best-fit $v_n\{GF\}(p_T)$

Global fit parameters are v_n coefficients

$2 \leq n \leq 5$ shown here (n=1 later)

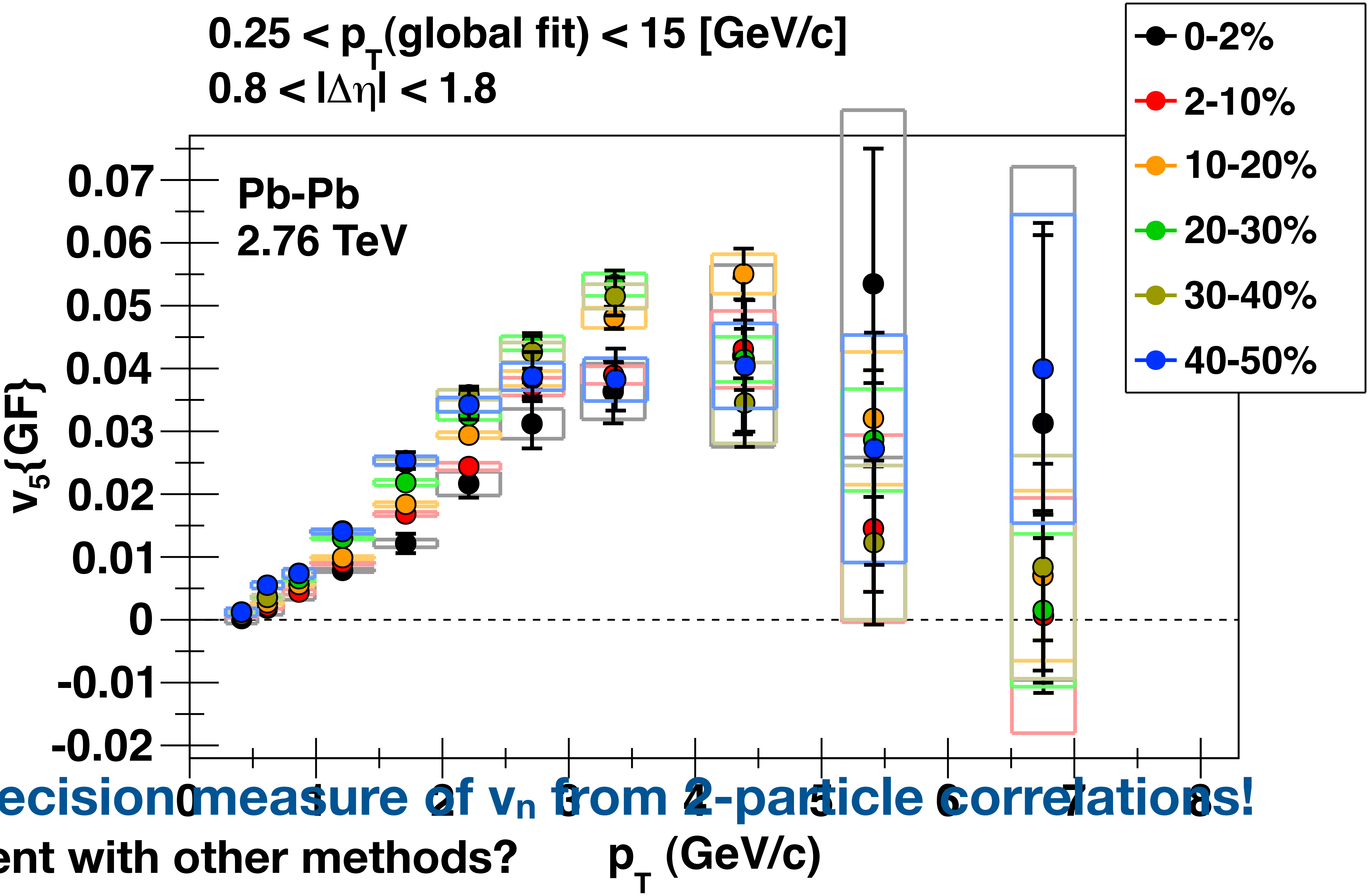

High-precision measure of v_n from 2-particle correlations!

Agreement with other methods?

Best-fit $v_n\{GF\}(p_T)$

Global fit parameters are v_n coefficients

$2 \leq n \leq 5$ shown here (n=1 later)

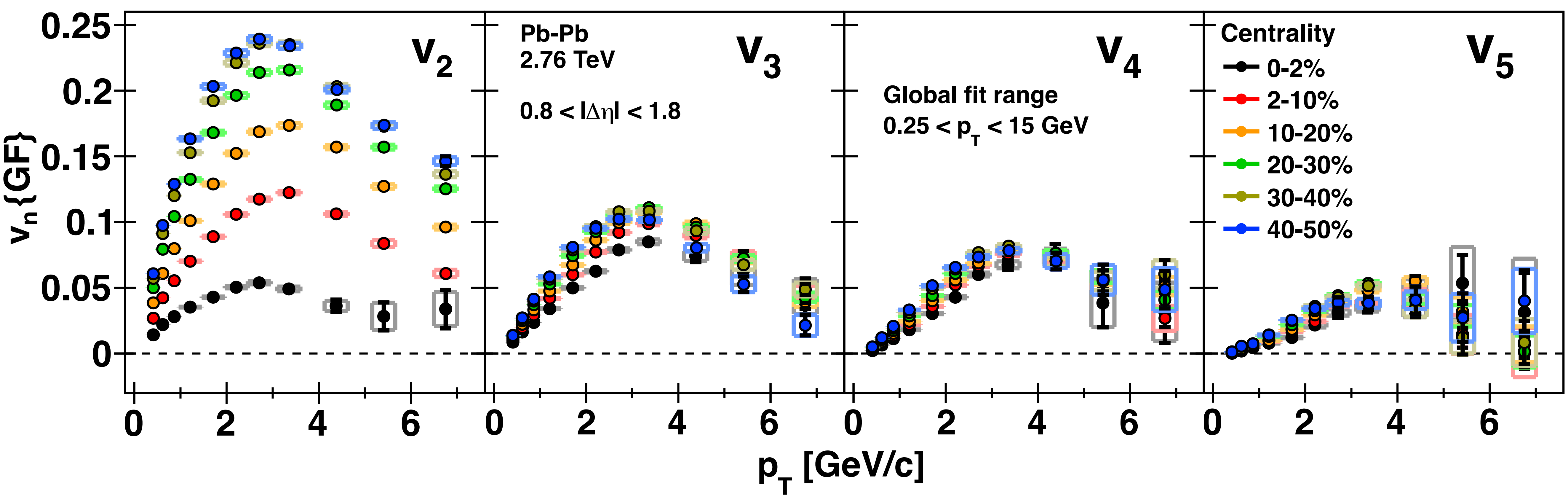

High-precision measure of v_n from 2-particle correlations!

Agreement with other methods?

Comparison with ALICE $v_n\{2\}$

Published ALICE $v_n\{2\}$

PRL 107 032301 (2011)

Scalar-product (SP) method

$|\Delta\eta| > 1.0$

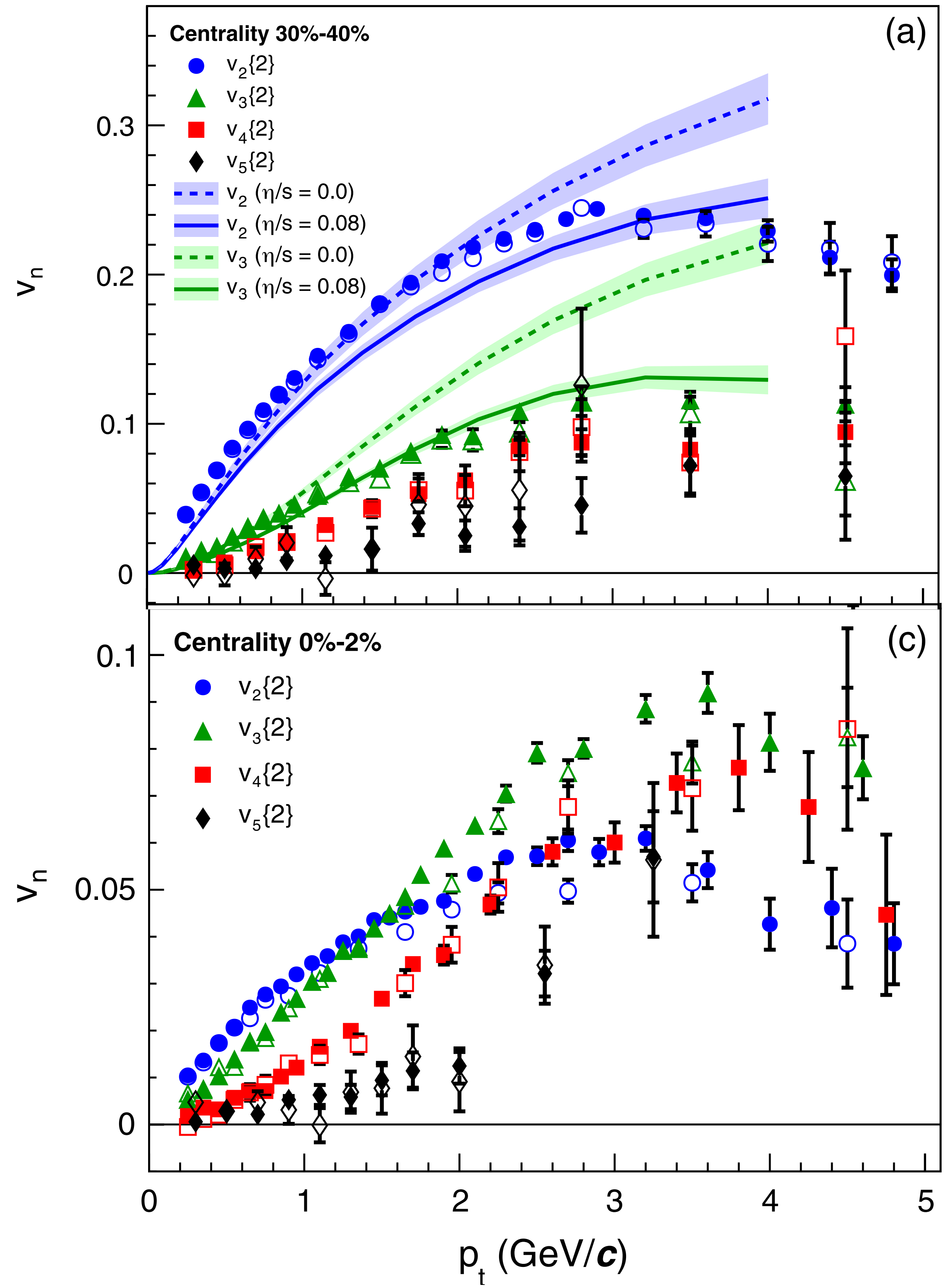

A. Adare (ALICE)

Comparison with ALICE $v_n\{2\}$

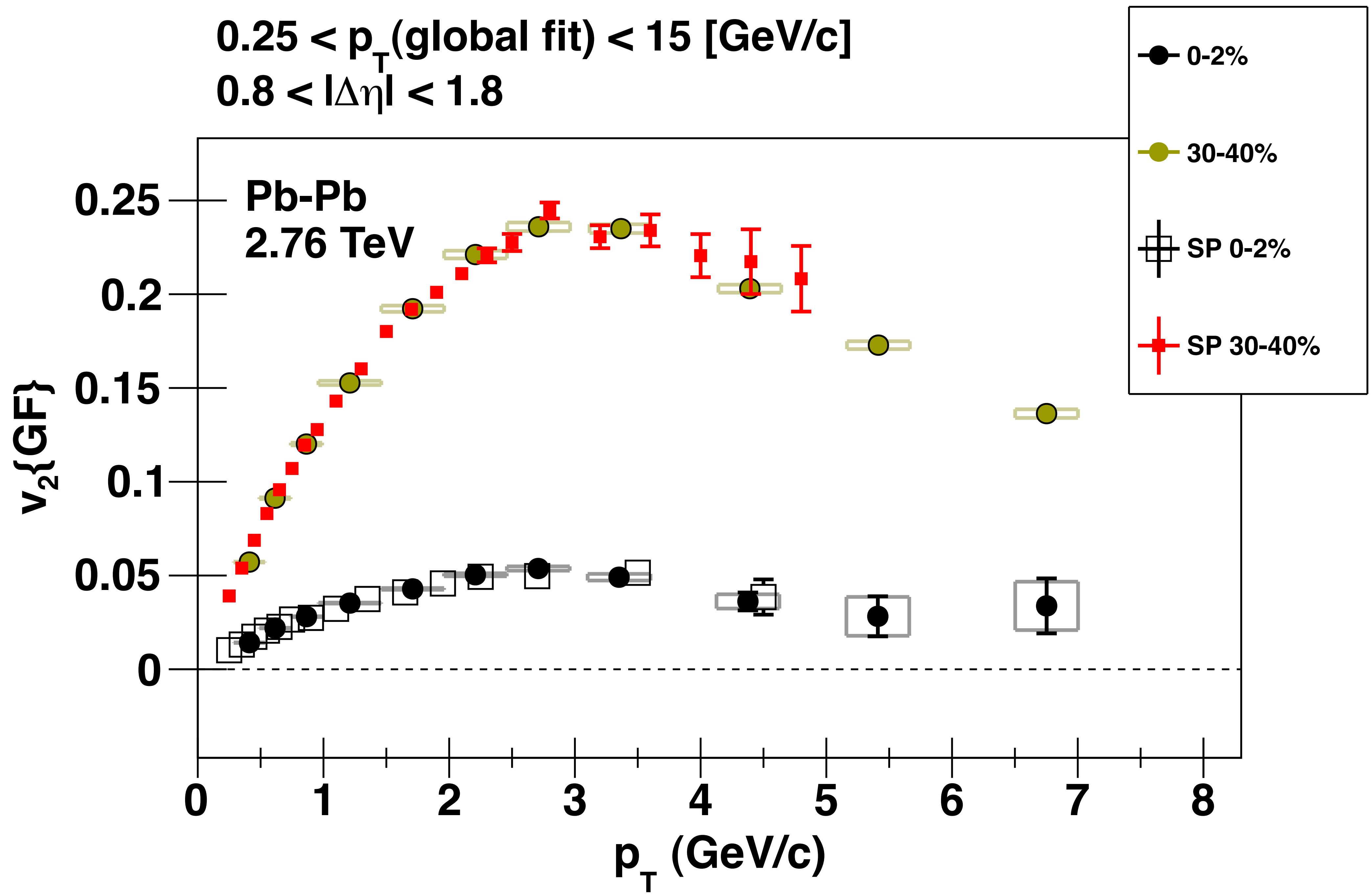

A. Adare (ALICE)

Comparison with ALICE $v_n\{2\}$

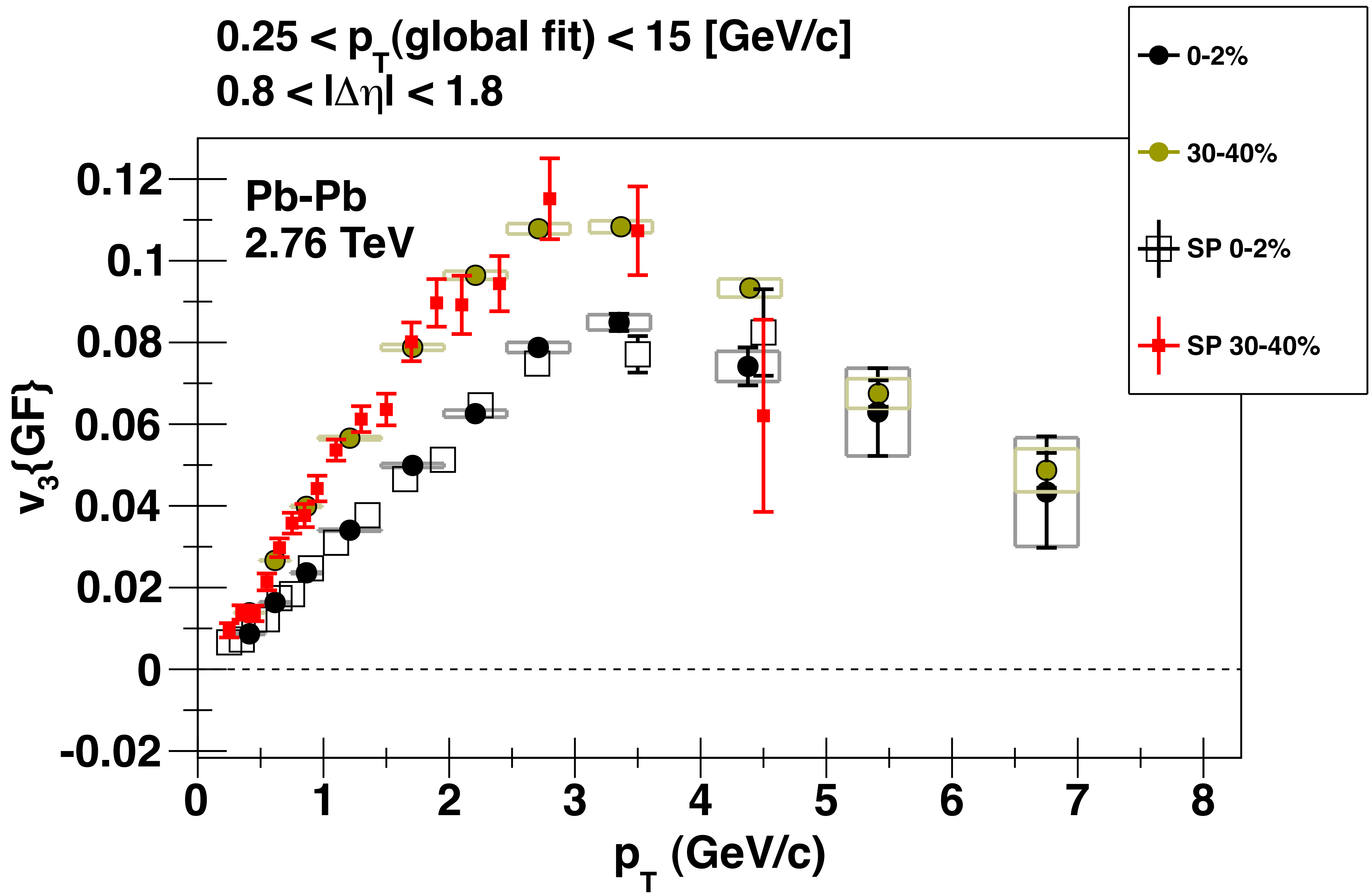

A. Adare (ALICE)

Comparison with ALICE $v_n\{2\}$

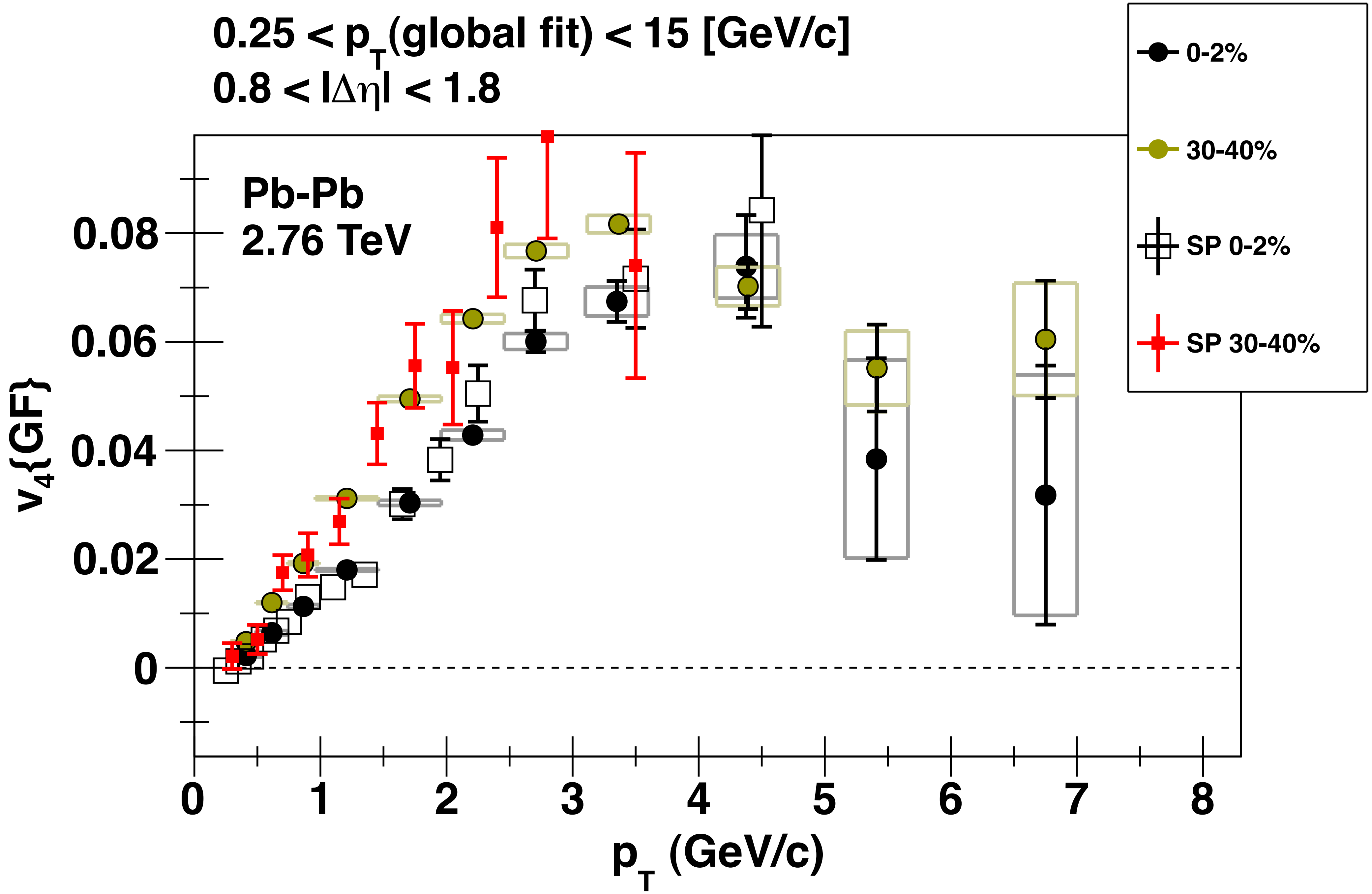

A. Adare (ALICE)

Comparison with ALICE $v_n\{2\}$

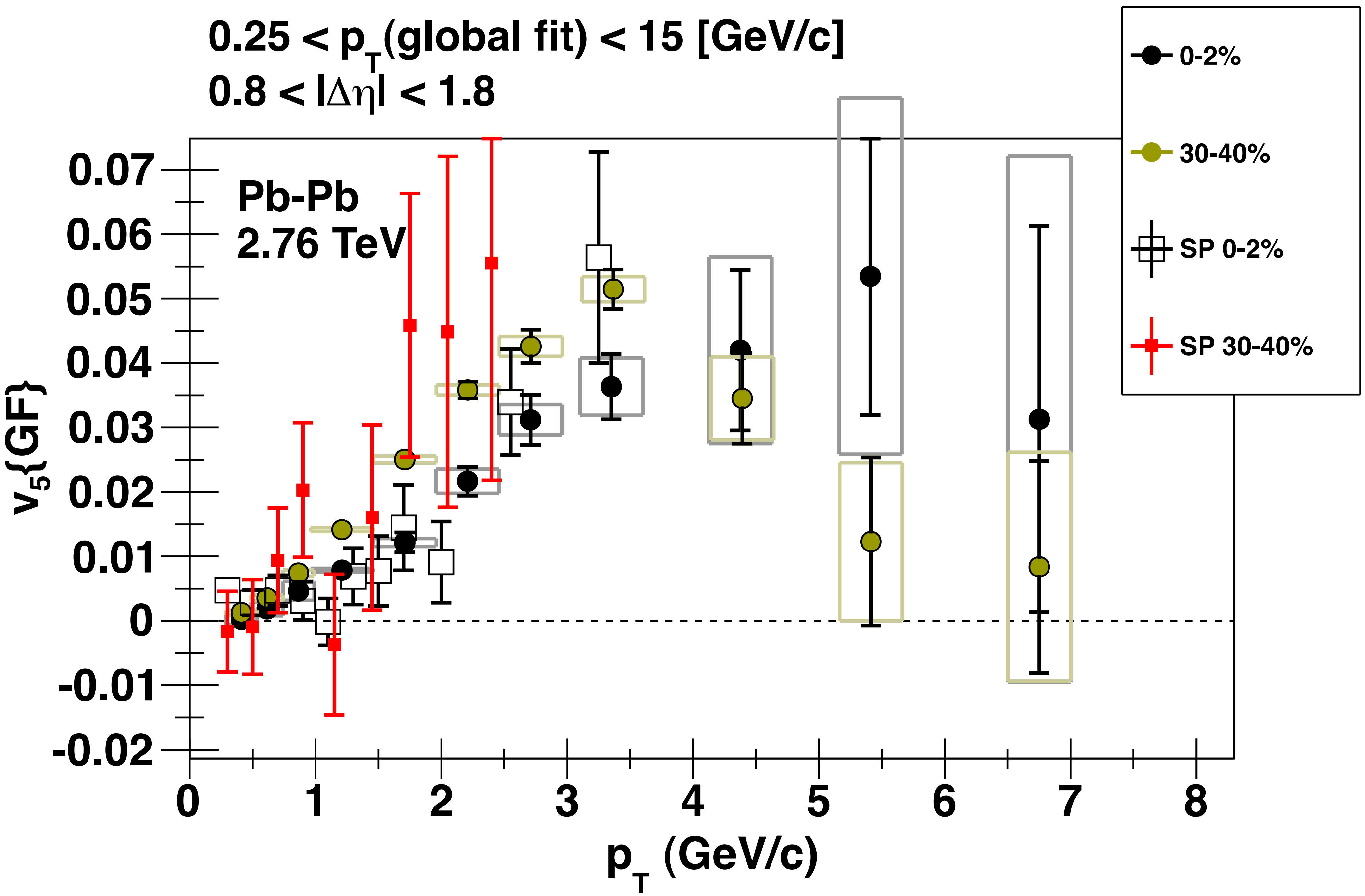

A. Adare (ALICE)

Comparison with ALICE $v_n\{2\}$

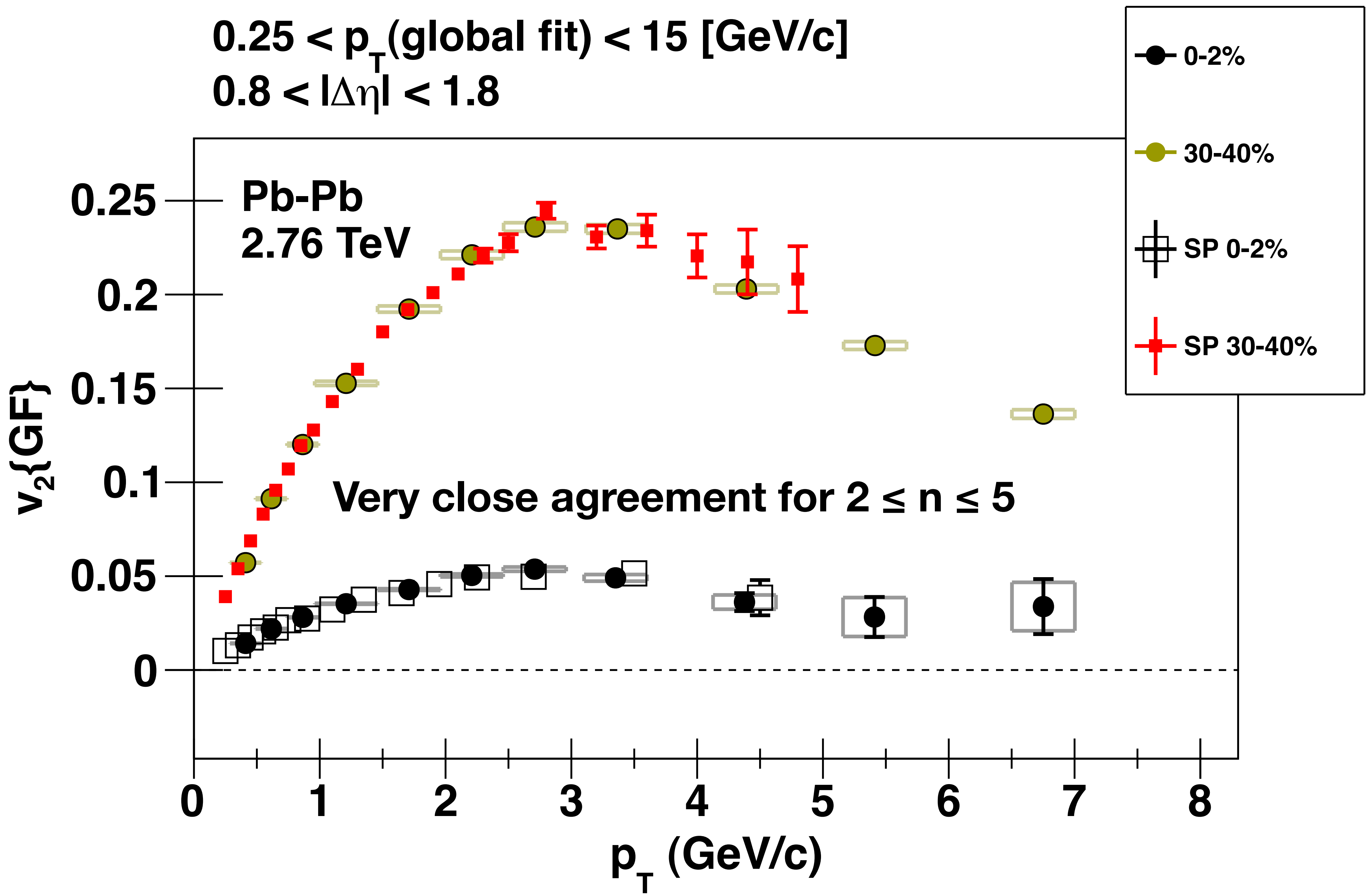

A. Adare (ALICE)

$V_{1\Delta}$ behaves exceptionally...

The n=1 harmonic doesn't factorize

Including the near-side peak enhances disagreement.

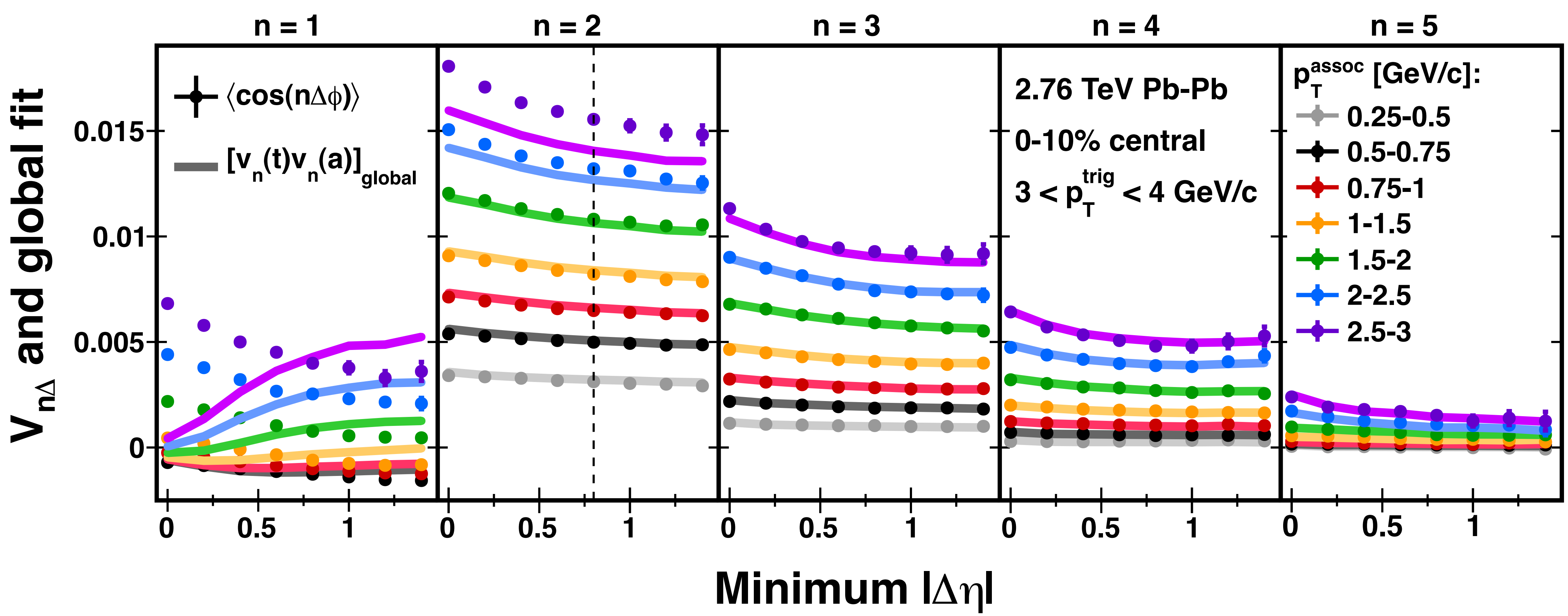

$V_{1\Delta}$ behaves exceptionally...

The n=1 harmonic doesn't factorize

Including the near-side peak enhances disagreement.

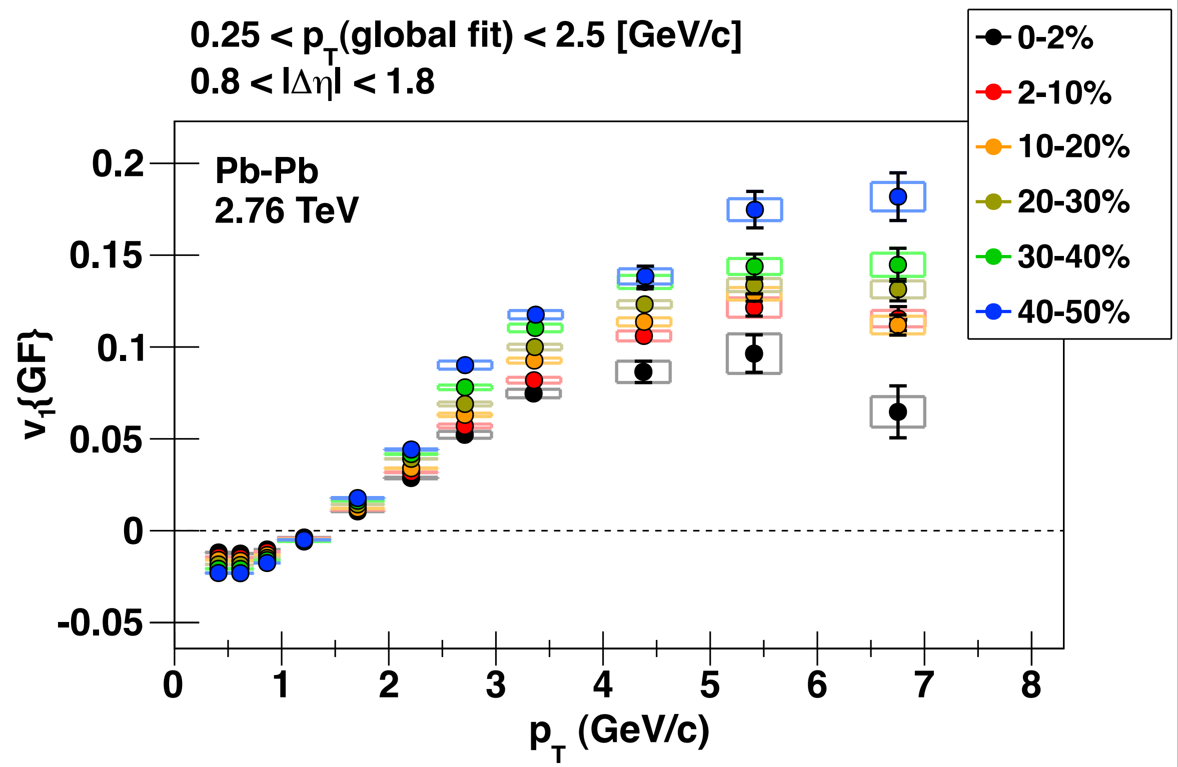

No good global fit over all momenta

However, v_1\{GF\} is qualitatively similar to viscous hydro predictions...under investigation.

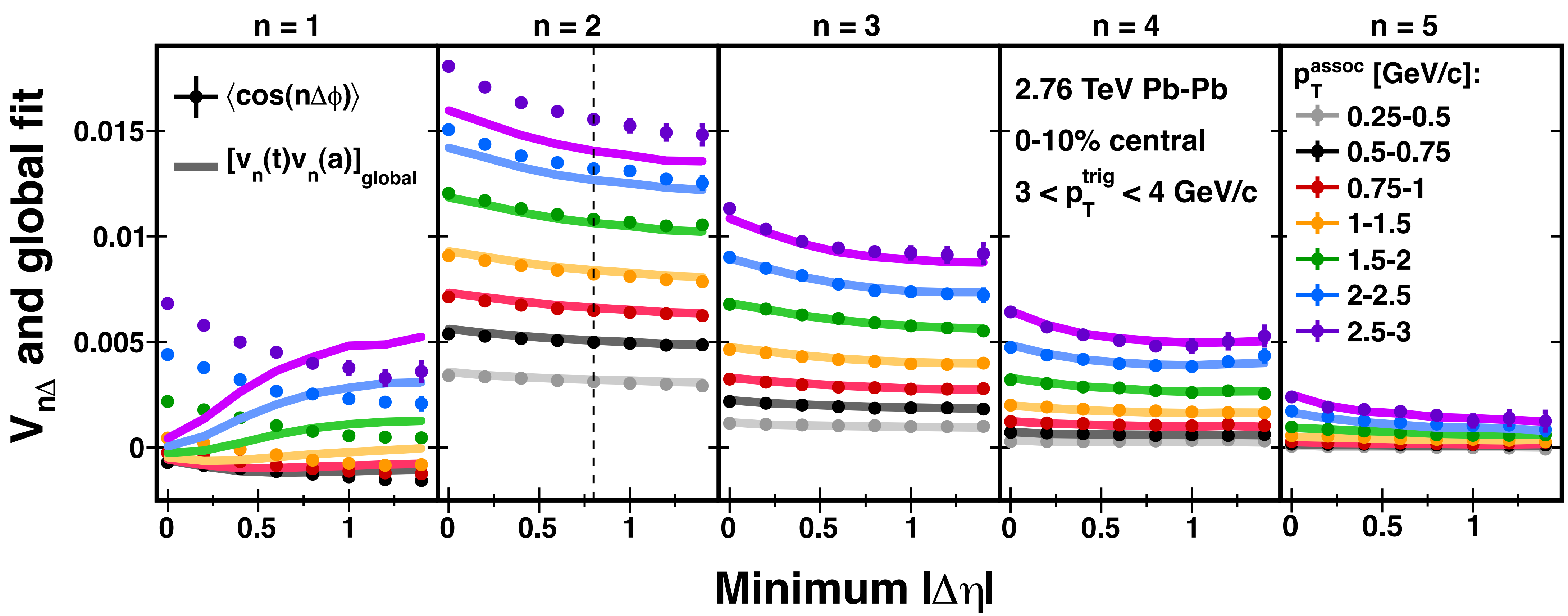

Summary

Factorization hypothesis and global fit:

Collective behavior (flow) describes bulk anisotropy (ridge, double-hump)

- No need to invoke Mach cone explanations.

Global fit coefficients (v_n{GF}) consistent with other measurements.

- Another method to measure flow coefficients

Bulk anisotropy factorizes, jet anisotropy does not.

- Bulk correlations related to global symmetries...
- But no such indication for shape of di-jet correlations.

Outlook:

Tackling open questions:

- Higher harmonics?
- Origin of $V_{1\Delta}$? Relation to v_1?

Second-year Pb-Pb data taking is just around the corner!

Looking ahead...

Open questions:

- Measured shapes are from I.S. + hydro evolution (+ hadronization). How would we distinguish between, e.g. very lumpy + viscous vs. smoother + more ideal hydro?

- Distinguishing hot-spot/string/sound perturbation pictures from superposition of event-by event density fluctuations?

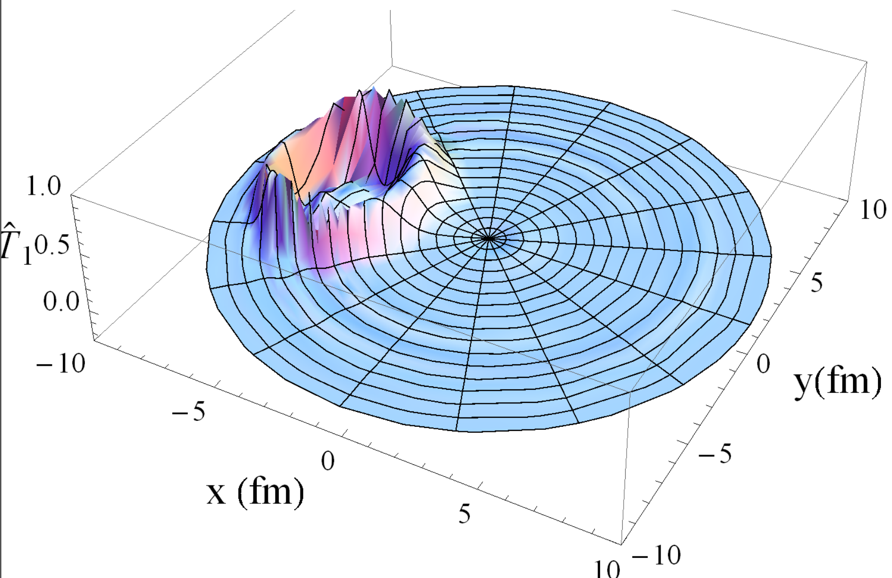

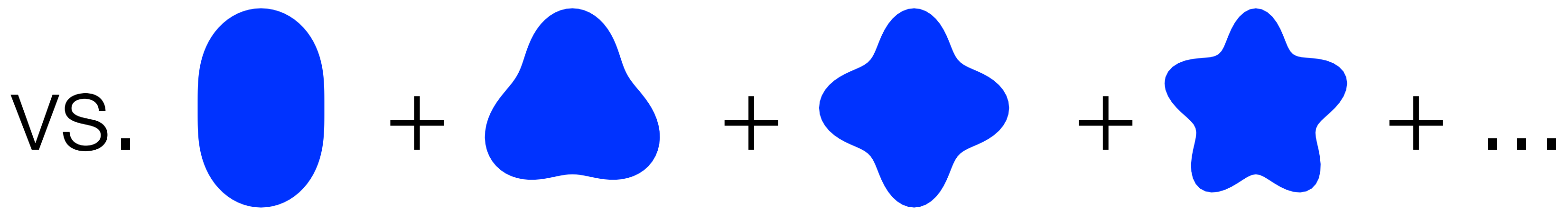

Sound perturbation animation

Hot spot / density perturbation produces coherent sound waves in hubble-expanding medium.

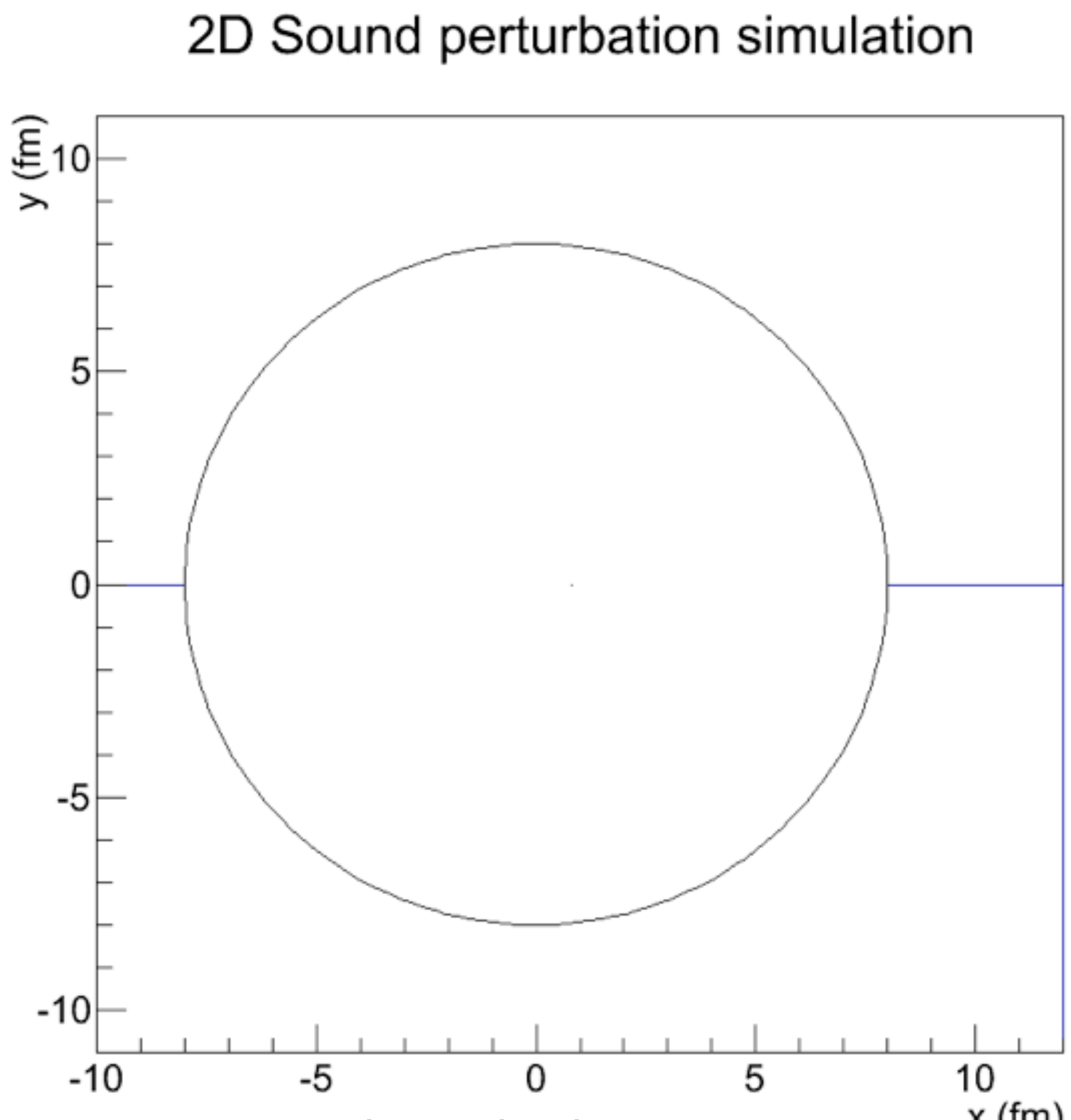

http://rhig.physics.yale.edu/~adare/sim/soundring.gif

Result from one event

Top

single particle distribution of particles having crossed freezout circle. Baseline was set at solid line to enhance effect (simulates combinatoric pedestal from averaging many events).

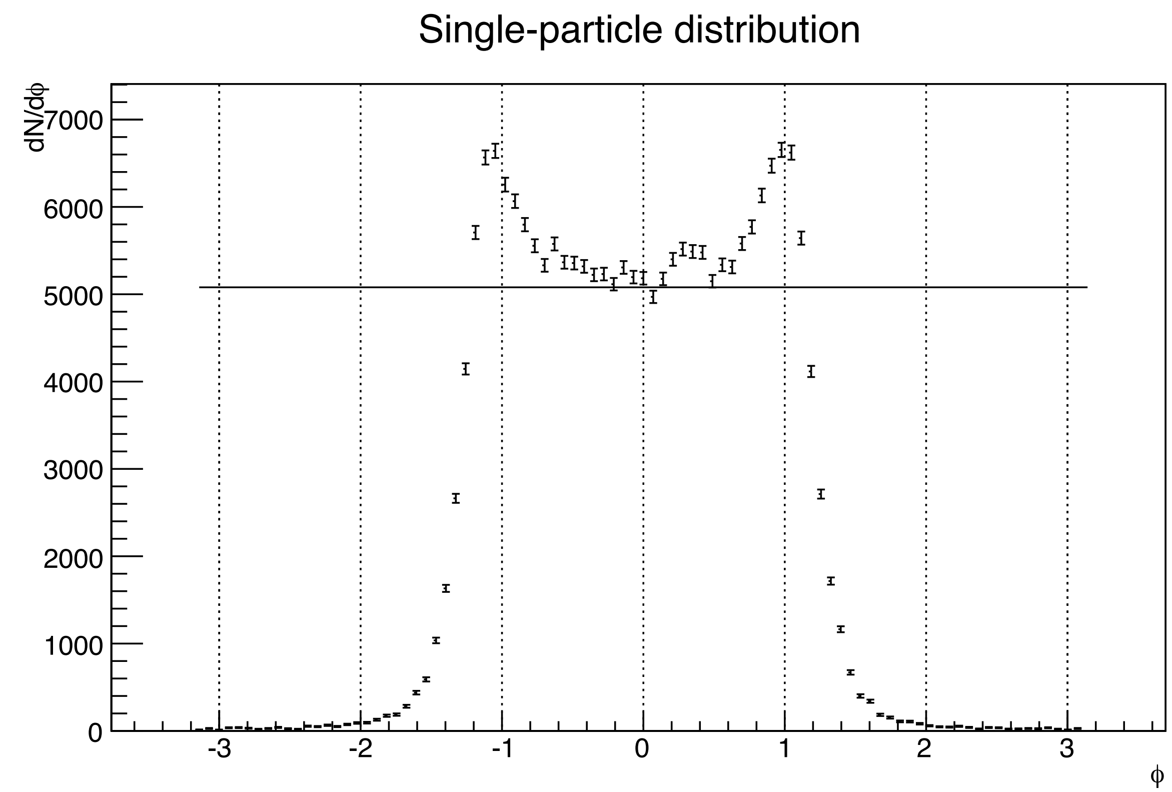

Bottom

Pair distribution showing 2-peak away side structure.

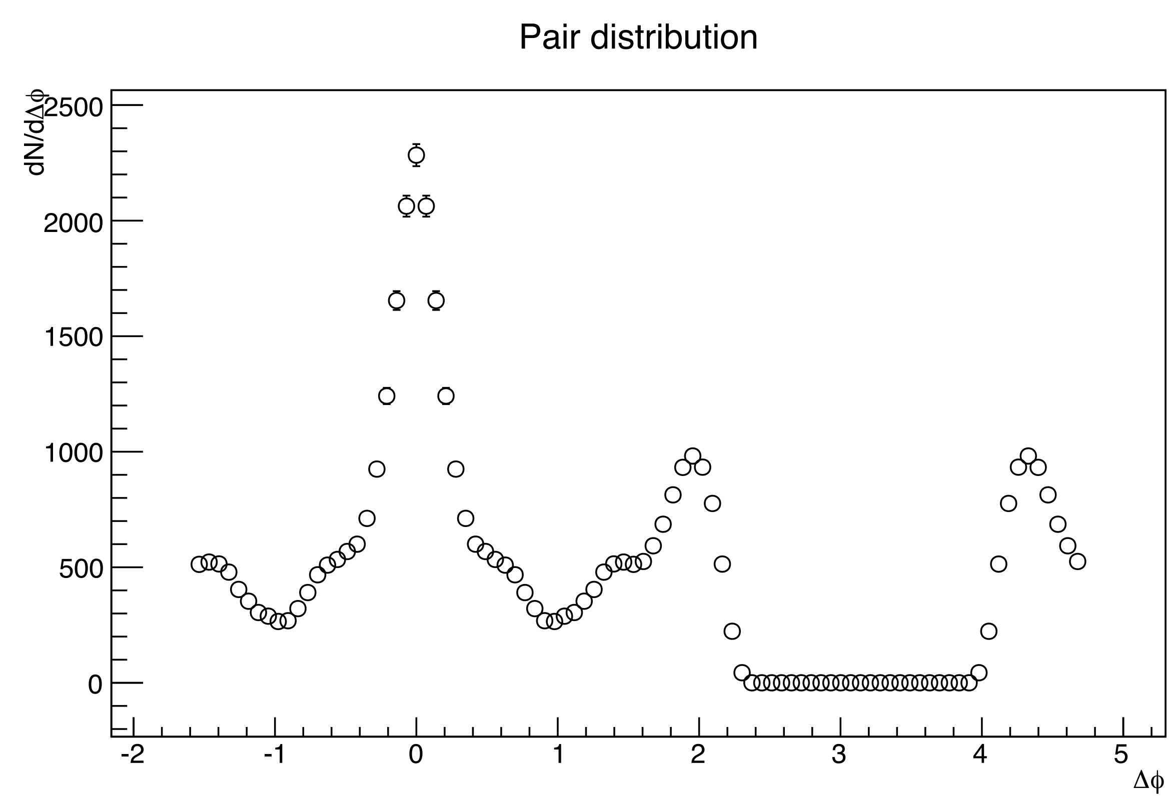

Cross-correlations and autocorrelations

For single-particle distributions x^a, x^b with length and period N

Pair cross-correlation*:

$$x_i^{ab} = \sum_{j=0}^{N-1} x_j^a x_{((i+j))_N}^b$$

$$((i))_N \equiv i \bmod N$$

$$0 \leq i \leq N-1$$

Three-particle cross-correlation:

$$x_{ij}^{ab} = \sum_{k=0}^{N-1} x_k^a \left(x_{((i+k))_N}^b + x_{((j+k))_N}^b \right)$$

Somewhat like a “really fast” MC technique for calculating difference between two periodic, random variables.

Linear cross correlations for nonperiodic variables (e.g. Δη correlations) are even simpler.

***Similar to convolution ($x^a \circ x^b$). (Cross-correlation uses i+j, while convolution sum uses i-j).**

Two peaks at +/- 1 rad

Top

Single-particle φ distribution with two Gaussian peaks.

$\sigma = \pi/3$ and $\mu = \pm 1$.

Bottom

Autocorrelation representing pair distribution

Observation

S.P. dists. with 120º peak separation lead to strong v3 correlated component, even if the event is not triangular.

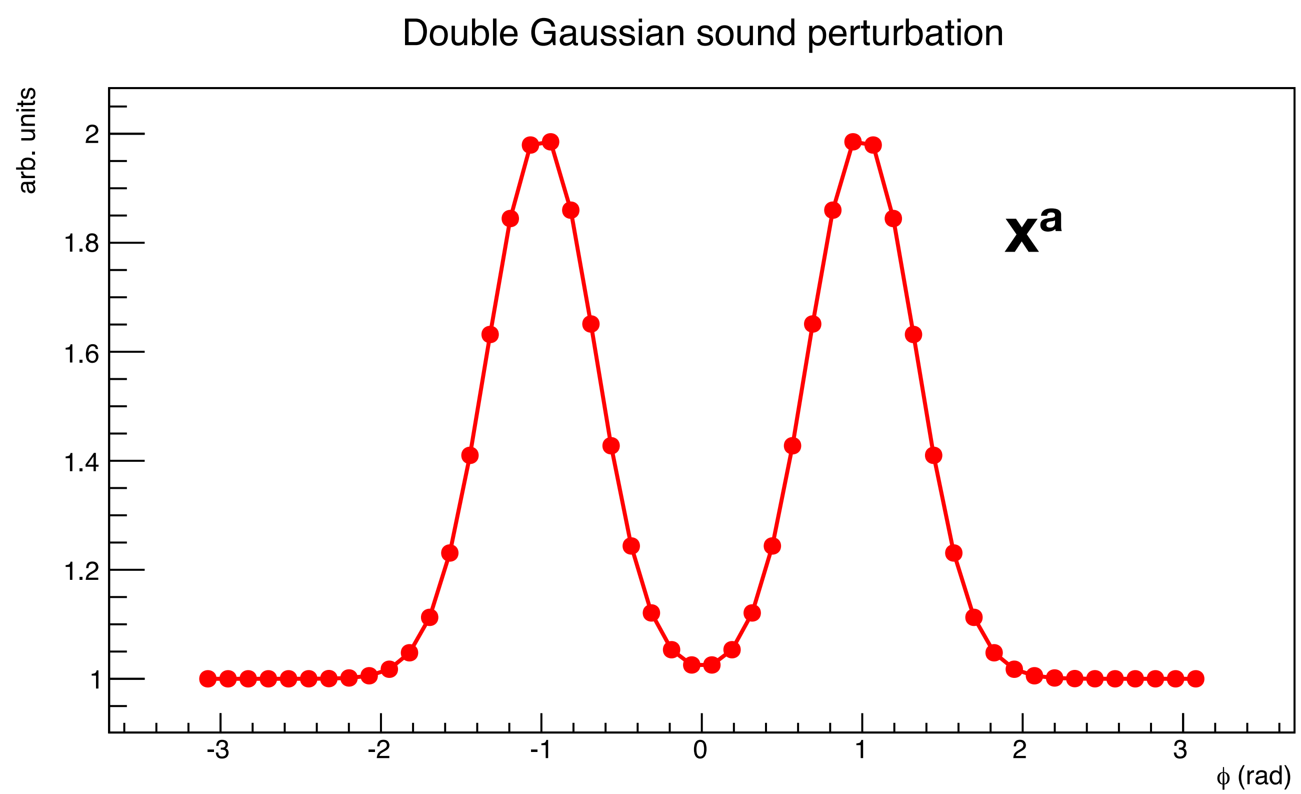

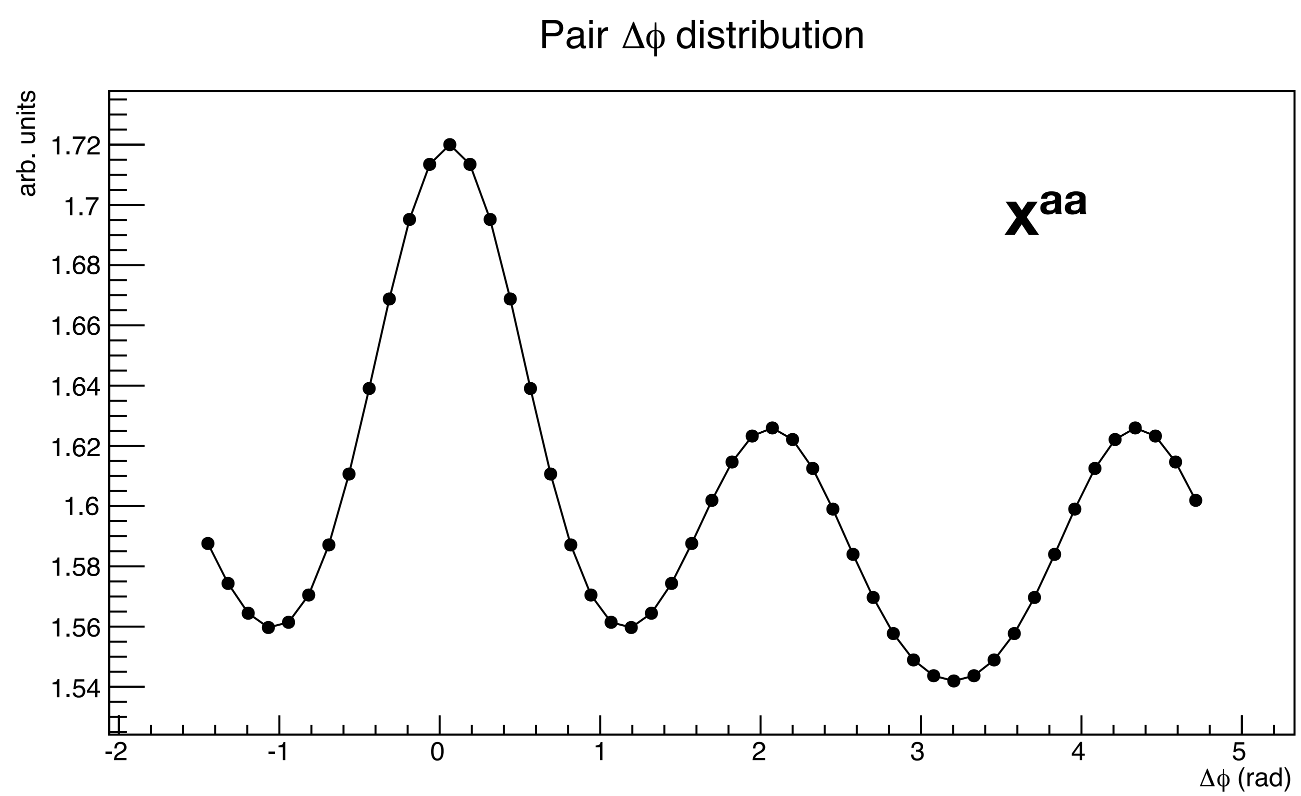

A. Adare (ALICE)

Different inputs, similar results

Left:

2-Gaussian superposition (Like Staig/Shuryak model)

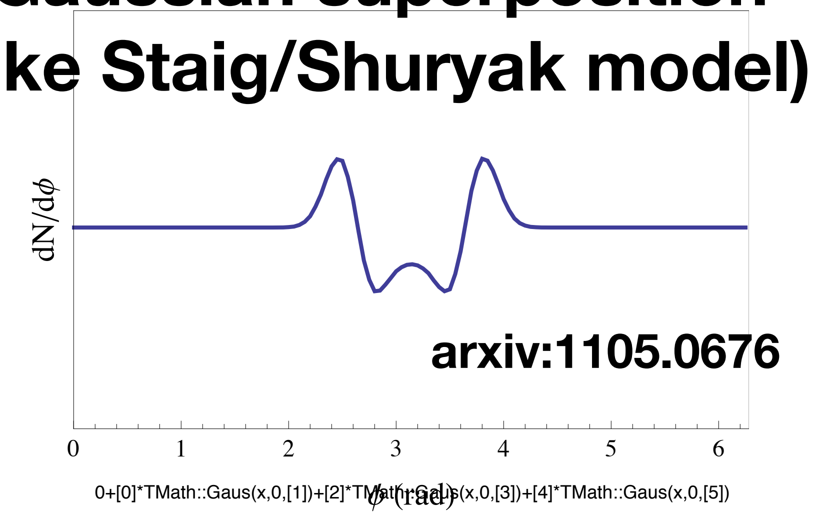

arxiv:1105.0676

Right:

v_1-v_4 sum {-0.05, 0.1, 0.1, 0.02}

Pair distribution qualitatively similar

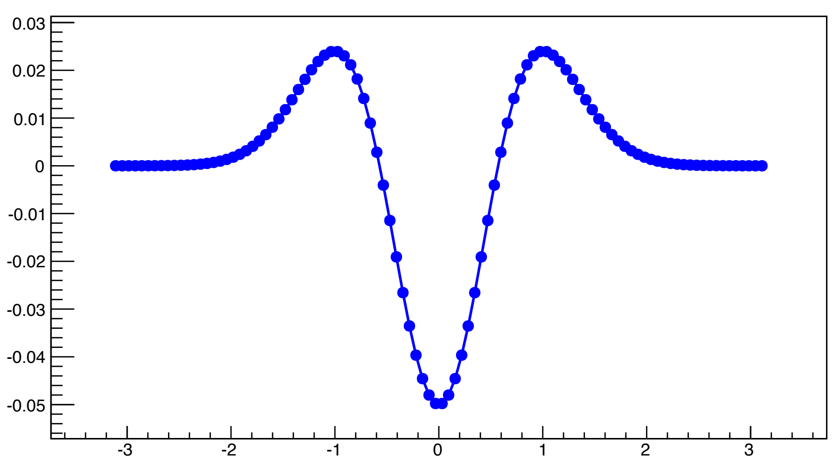

Single-particle φ distributions

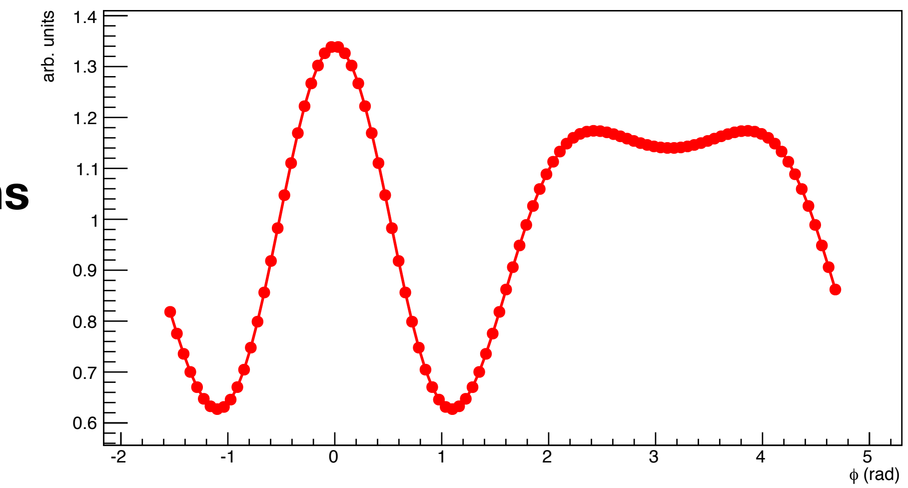

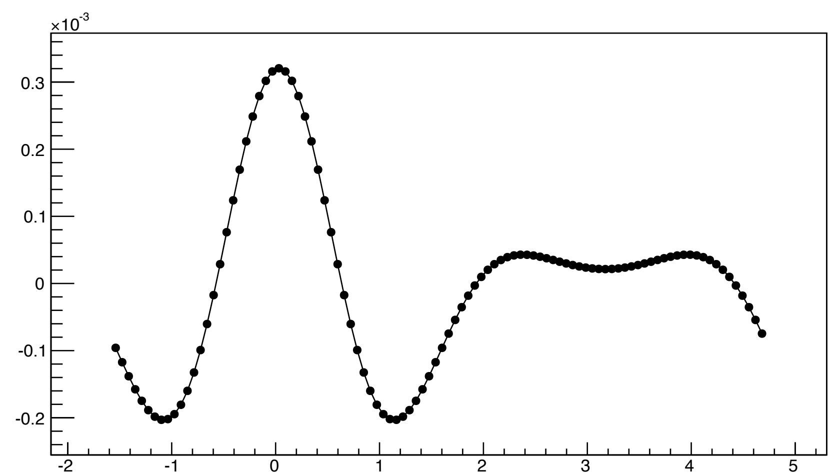

Pair Δφ distributions

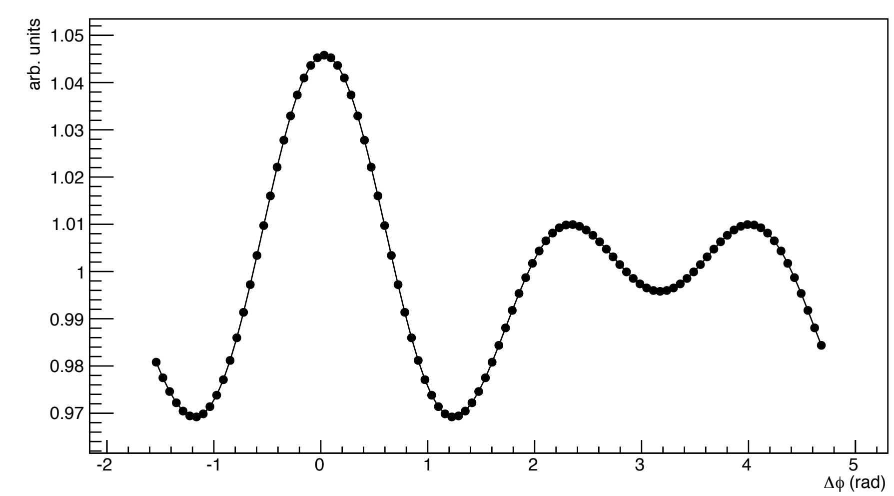

A. Adare (ALICE)

Top

Pure v_3 single-particle φ distribution.

Bottom

Again, autocorrelation (= pair distribution)

Observations

Pair distribution has same shape as S.P. distribution (true for all n)

Away-side correlation strength equal to near side

Allows distinction from flux-tube/ perturbation vs. triangular flow pictures?

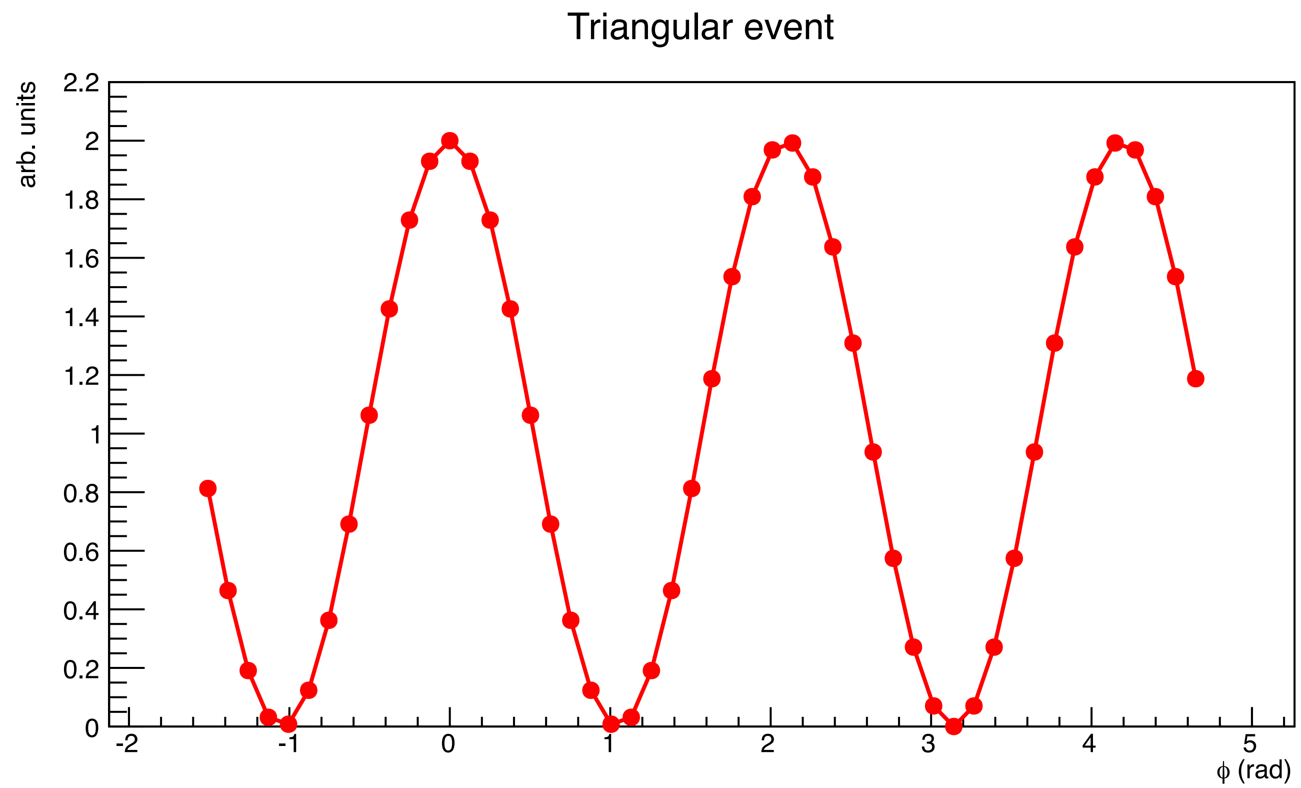

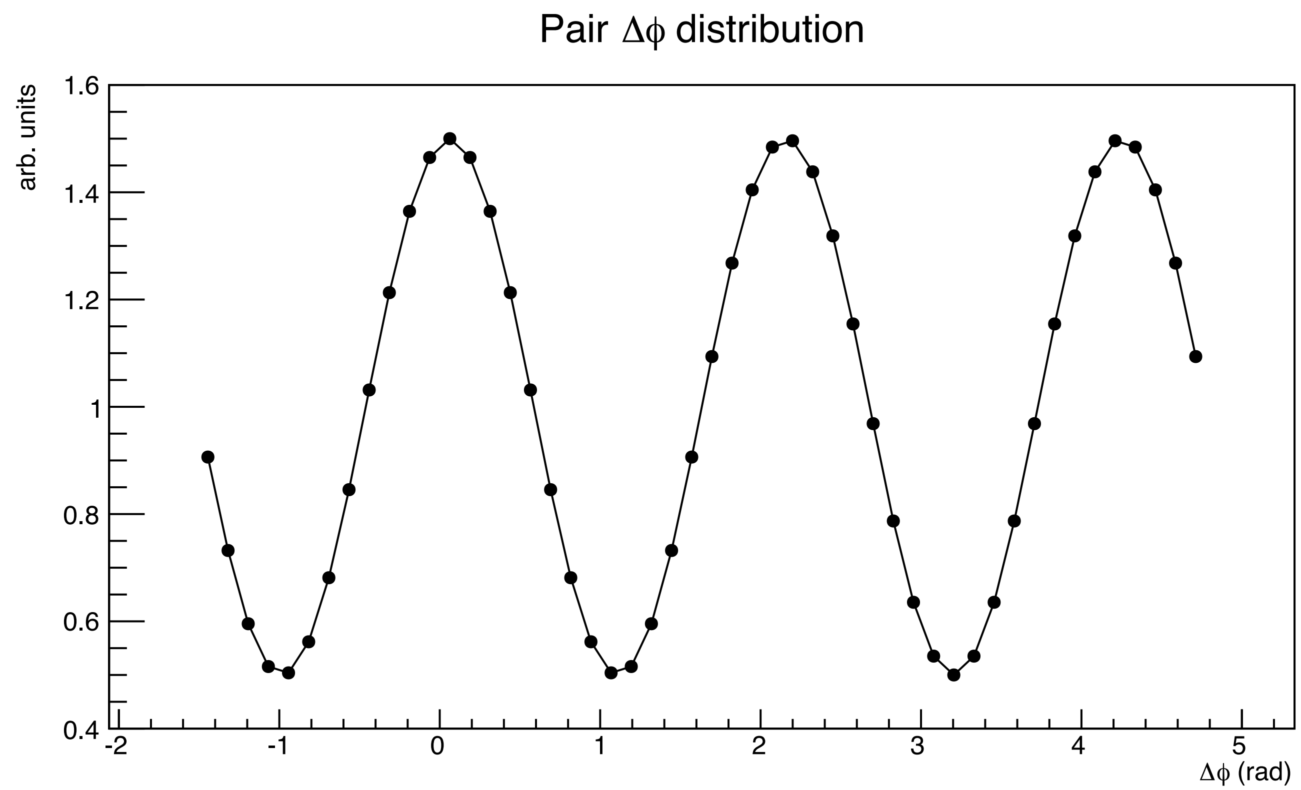

Three-particle shapes are very different between the two cases...

Even if reality is some admixture between these, experimental sensitivity may be sufficient.

But we should examine the unsubtracted, central data! No ZYAM!!

Double Gaussian autocorrelation

Triangular flow autocorrelation

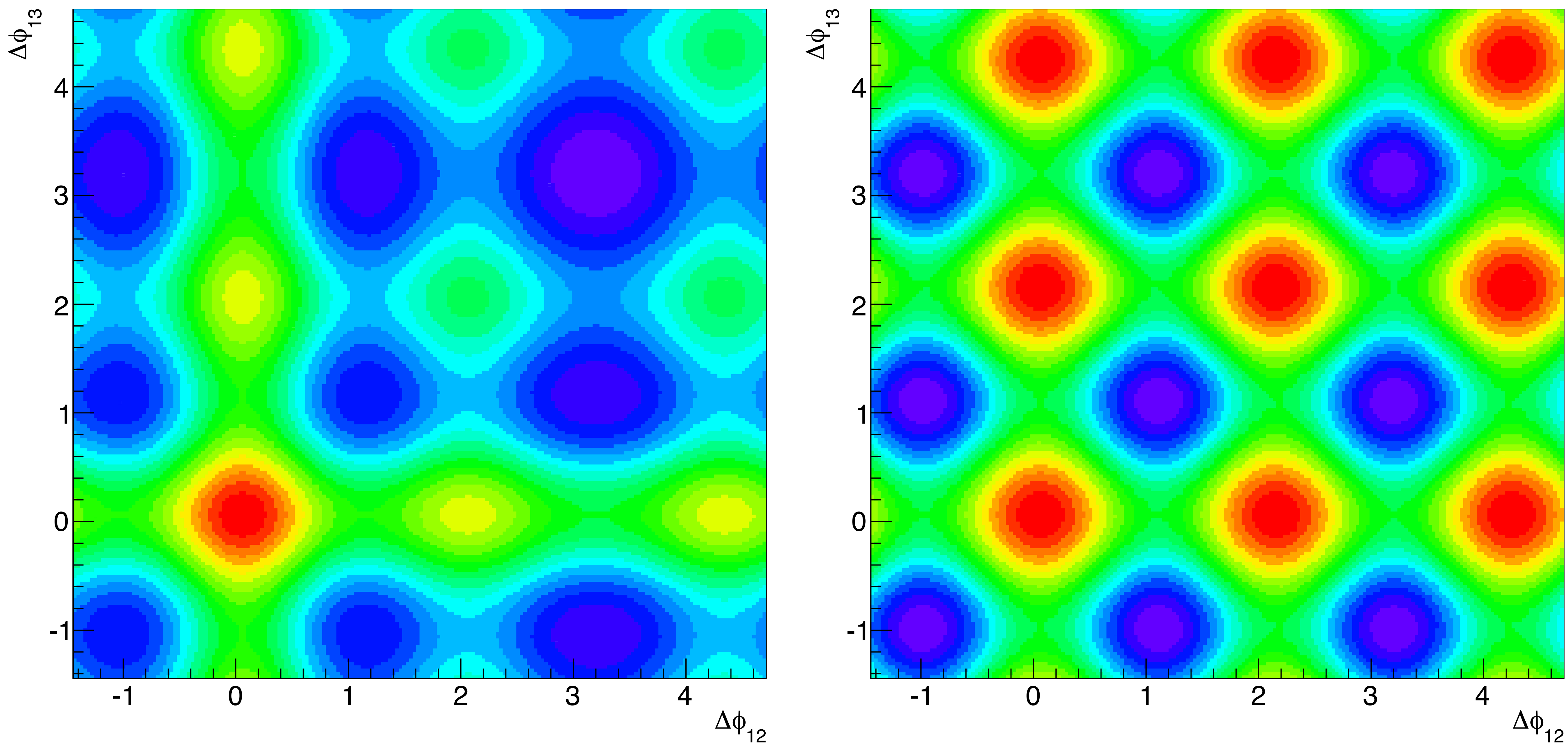

A. Adare (ALICE)

The end

High trigger, low associated p_T

High-p_T triggers from jet fragmentation

Expect anisotropy from pathlength-dependent quenching (PLDQ).

Low-p_T partners from bulk

Expect anisotropy from flow

Do correlations factorize for this case?

Yes, but not as cleanly as for low p_T^t, low p_T^a correlations.

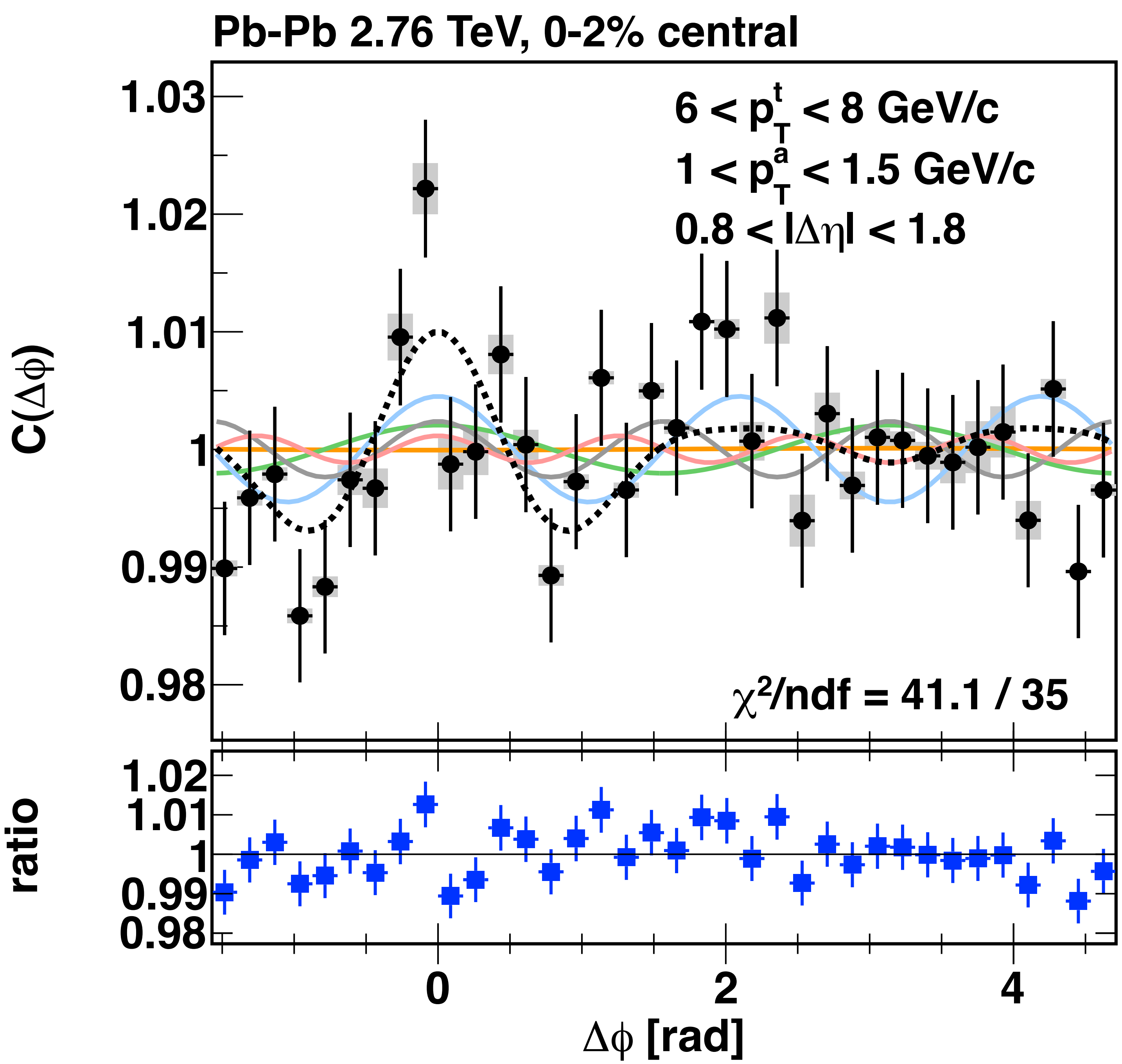

High-p_T triggers from jet fragmentation

Expect anisotropy from pathlength-dependent quenching (PLDQ).

Low-p_T partners from bulk

Expect anisotropy from flow

Do correlations factorize for this case?

Yes, but not as cleanly as for low p_T^t, low p_T^a correlations.

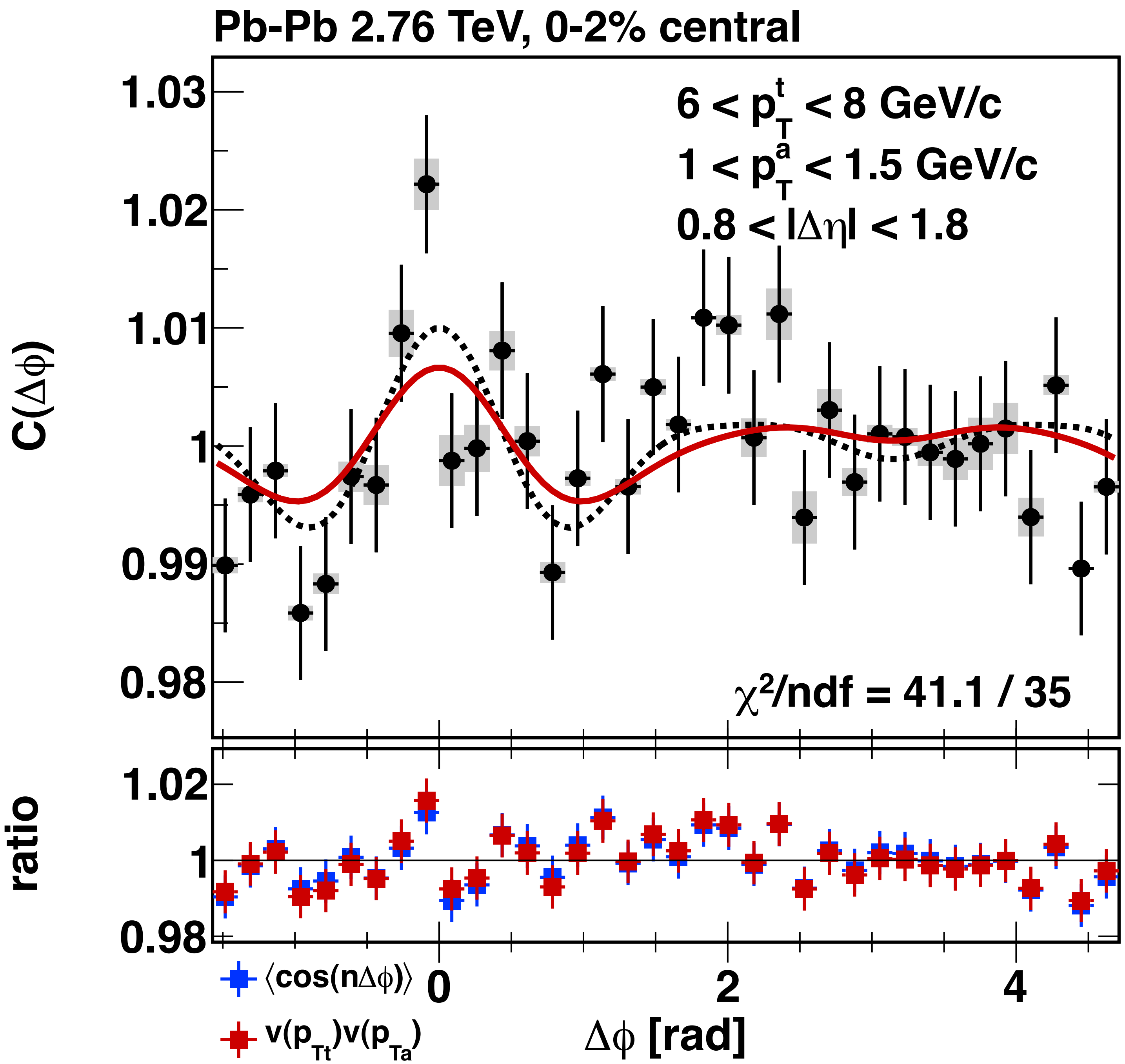

Hot-spot / flux-tube / sound models

Similar qualitative features

J. Phys. G: Nucl. Part. Phys. **37** (2010) 094043 R P G Andrade *et al*

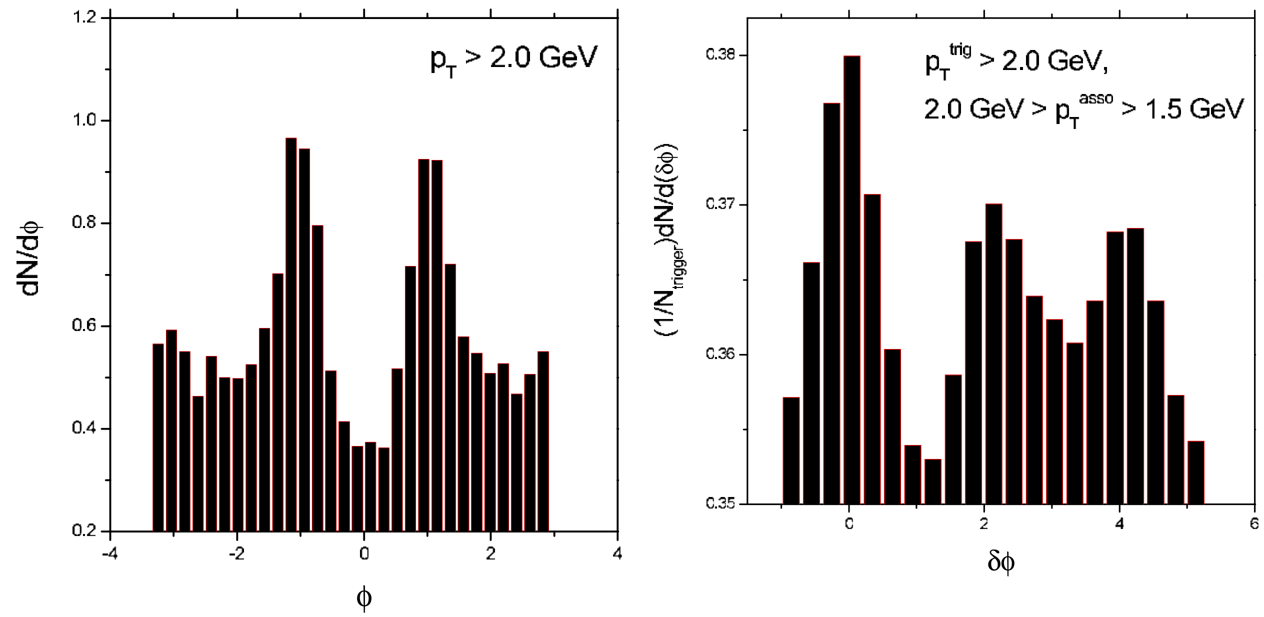

Figure 3. Single- (left) and two- (right) particle angular distributions in the simplified model.

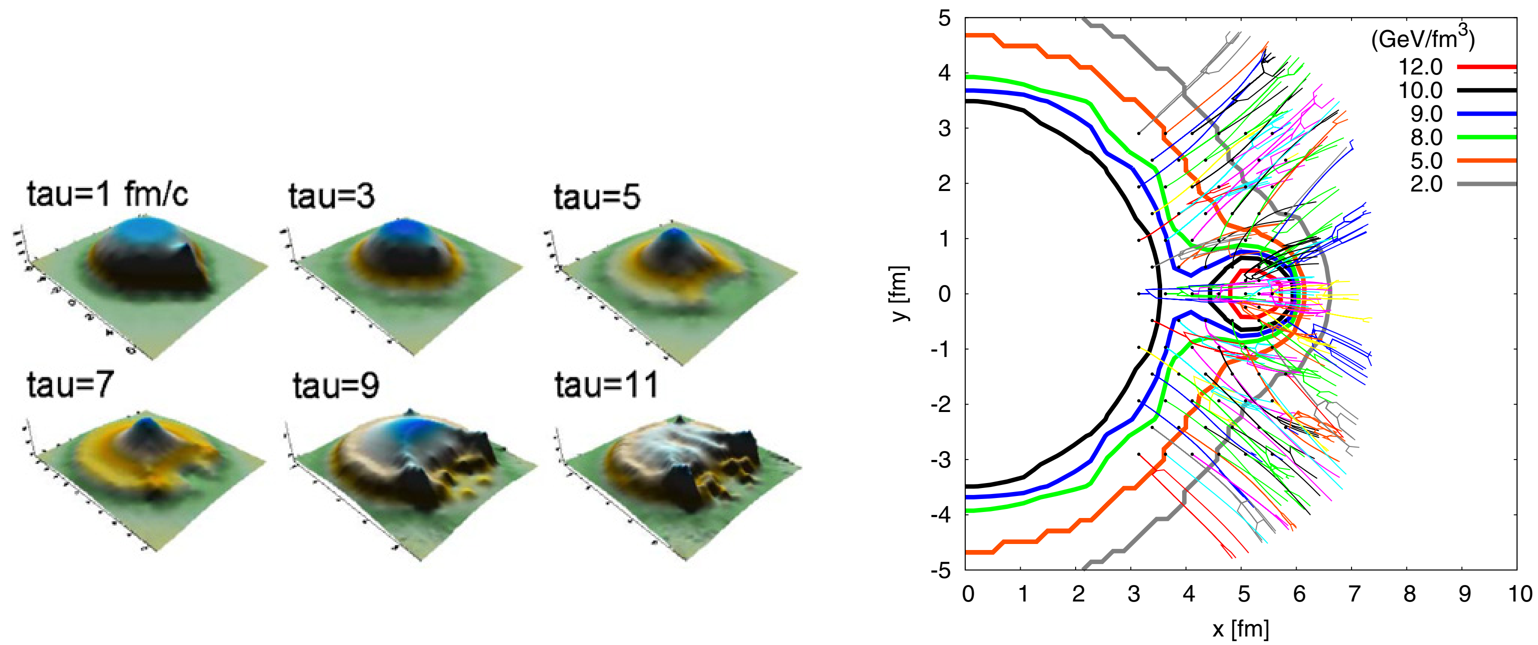

Figure 4. Temporal evolution of energy density for the simplified model (left). Trajectories of the fluid cells around the tube (right).

A. Adare (ALICE)